Investigation on the mechanistic roles of Tom1 and Dia2 in DNA replication and Cell cycle

A DISSERTATION
SUBMITTED TO THE FACULTY OF THE GRADUATE SCHOOL
OF THE UNIVERSITY OF MINNESOTA
BY

Dong-Hwan Kim

IN PARTIAL FULFILLMENT OF THE REQUIREMENTS
FOR THE DEGREE OF
DOCTOR OF PHILOSOPHY

Deanna M. Koepp, Ph.D.
Advisor

October 2012

ACKNOWLEDGEMENTS

I would like to thank my advisor Deanna Koepp for her great support and advice during my Ph.D. training. When I joined the lab five years ago, I did not have any experience about yeast experiments. Whenever I struggled with my research, she gave me wonderful advice so that I could solve problems and make my way toward a Ph.D.

I am also grateful to former graduate students Anderw Kile, Wei Zhang, and Chi Fong and a former technician Allison Ritter for their helpful discussion and technical advice.

I also thank C. Brandl (U. Western Ontario) for the gift of *tom1* strains, J. Li (UCSF) for the gift of the re-replication sensitive strains, J. Wade Harper (Harvard Medical School) for the anti-Skp1 antibodies, and members of D. Clarke and D. Kirkpatrick's laboratories for helpful discussions and sharing their experimental equipments.

Special thanks to my committee members David Kirkpatrick, Duncan Clarke, Kathleen Conklin, Anja Bielinsky, and Kylie Walters for their helpful inputs on my thesis research.

Finally, I am deeply indebted to my family for their invaluable support.

ABSTRACT

As cells duplicate and divide, the inheritance of accurate genetic information is critical to maintaining cell viability and preventing the generation of cancer-causing mutations. Thus, DNA replication is important and limited to once per cell cycle. The replication protein Cdc6 is required to assemble pre-replicative (pre-RC) complexes on origins of replication and is degraded after it has completed its function. The mechanisms of Cdc6 degradation in budding yeast are complex and not completely understood. I have identified a novel pathway that targets Cdc6 for degradation during G1 and at the G1 to S phase transition. The Hect E3 ligase Tom1 and the F-box protein Dia2 function co-operatively but independently of the SCF^{Cdc4} complex. When this pathway is disrupted, the assembly of Cdc6 and Mcm4 on chromatin and replication origins is aberrant. Strikingly, defects in Tom1 or Cdc4 lead to increased DNA content in cells sensitized to re-replication. Therefore, multiple degradation pathways that limit Cdc6 protein levels cooperate to regulate pre-RC assembly and may act to prevent DNA re-replication.

Preserving genomic stability is crucial to cell viability and proliferation. The budding yeast F-box protein Dia2 is required for genomic stability and is targeted for ubiquitin-dependent degradation in a cell cycle-dependent manner, but the identity of the ubiquitination pathway is unknown. I have uncovered that the Hect-domain E3 ligase Tom1 targets Dia2 for ubiqutin-dependent degradation during G1 and G2/M. Tom1 binding to Dia2 is switched during the cell cycle. Tom1 recognizes specific positively charged residues in a Dia2 degradation/NLS domain. Defects in Dia2 proteolysis such as the loss of positively charged residues and deletion of *TOM1* cause a delay in G1 to S-phase progression. Together, these results suggest that Tom1 is required for degradation of Dia2 during the cell cycle and that Dia2 protein degradation contributes to G1 to S-phase progression.

TABLE OF CONTENTS

LIST OF TABLES

LIST OF FIGURES

LIST OF EXPERIMENTAL CONTRIBUTIONS IN CHAPTER II AND III

CHAPTER II: Cdc6 degradation by a Tom1 and Dia2-dependent pathway regulates pre-RC assembly during the cell cycle

Dong-Hwan Kim: performed all experiments and generated figures and tables.
Wei Zhang: generated Cdc6, ΔN214 Dia2, and TPR Dia2 baculoviruses.
Deanna Koepp: generated fractionated yeast extracts

CHAPTER III: The Hect E3 ubiquitin ligase Tom1 controls Dia2 degradation during the cell cycle

Dong-Hwan Kim: performed all experiments and generated figures and tables.

CHAPTER I

INTRODUCTION

1. Ubiquitin-Proteasome System (UPS)

Ubiquitination

Ubiquitination plays a role in a variety of cellular processes including proliferation, cell cycle, signal transduction, transcription, DNA damage, and DNA repair (38, 41, 50, 65, 85). Ubiquitin is a small protein with 76 amino acids. Ubiquitination is a process in which the C-terminal glycine of ubiquitin is covalently attached onto a lysine of a substrate protein through a cascade of enzymatic reactions. Moreover, ubiquitins are themselves covalently linked to each other through one of seven lysines found on ubiquitin, leading to a chain. Ubiquitination determines the fate of substrate proteins, depending on the number of ubiquitin molecules or the type of ubiquitin-linked chains (49). Polyubiquitination (at least four ubiquitin molecules linked through the lysine 48) targets a protein for degradation via the 26S proteasome, whereas monoubiquitination or polyubiquitination through the lysine 63 or other lysines alters protein interaction, protein localization, intracellular trafficking, signal transduction, and DNA repair (38, 39, 41, 87).

Ubiquitination is a series of enzymatic reactions consisting of ubiquitin-activating enzyme (E1), ubiquitin-conjugating enzyme (E2), and ubiquitin ligase (E3) (77, 78). Ubiquitin is activated by an E1 enzyme through a thioester bond in an ATP-dependent manner and transferred to an E2 enzyme. When the E2 binds to an E3 ubiquitin ligase,

ubiquitin is directly or indirectly attached onto a lysine of a substrate, which further targets the substrate for degradation via the 26S proteasome (Figure 1). The substrate can be monoubiquitinated and dissociated from the E3 ligase or polyubiquitinated after multiple rounds of these reactions. The human genome encodes 2 potential E1s, about 30 E2s, and more than 600 E3s (78), suggesting that an enormous number of substrates are recognized and targeted by those E2 and E3 enzymes.

RING domain E3 ubiquitin ligases

There are two major groups of E3 ubiquitin ligases - The RING domain E3 ligases and the Hect domain E3 ligases. RING domain E3 ligase family constitutes a large proportion of E3 ligases found in humans. RING E3s are either a single polypeptide or multi-subunit complexes. These RING E3 ligases contain a ring domain characterized by a Cys-X2-Cys-X(9-39)-Cys-X(1-3)-His-X(2-3)-Cys-X2-Cys-X(4-48)-Cys-X2-Cys (where X is any amino acid) sequence (16). The SCF (Skp1/Cdc53/F-box proteins) complexes are modular E3 ubiquitin ligases and their structures have been extensively studied as a multi-subunit RING domain E3. The SCF complexes are also highly conserved from yeast to humans (16). Each component of the SCF complex has a specific role in ubiquitination of a substrate. For example, an F-box protein acts as an adaptor and binds to a substrate. There are approximately 70 different F-box proteins in humans and 20 F-box proteins in yeast (11, 98). In addition, Skp1 interacts with an F-box protein and tethers it to the rest of an SCF complex. Cul1, also known as Cdc53, is a scaffold protein and functions as a landing pad for the formation of an SCF complex. Rbx1 (Roc1) is a

RING domain protein and recruits an E2 enzyme charged with ubiquitin. When a substrate is bound to an SCF complex, the SCF complex brings the substrate in close proximity to the E2-ubiquitin and ubiquitin is directly transferred from E2 to the substrate (Figure 2).

Hect domain E3 ubiquitin ligases

The other type of E3 ligases is Hect (homologous to E6-AP carboxyTerminus) E3 ligases. Hect family E3 is a single polypeptide protein and contains a Hect domain of 350 amino acids found at the C-terminus of the protein. The Hect domain was first described from human papilloma virus (HPV) E6-associated protein (E6AP) (81). The Hect E3s contain at least one or more protein-protein interaction domains located at the N-terminus of the proteins. However, the important function of the E3s such as E2 binding and ubiquitin transfer resides in the Hect domain. Unlike the SCF complexes described above, the Hect domain E3s have a distinct mechanism in that ubiquitin is transiently transferred from E2 to a catalytic cysteine of the protein and subsequently attached to a lysine of a substrate (Figure 3).

How this function is regulated is an emerging research topic. Several reports suggest that an intramolecular interaction between protein-protein interaction domains located at the N-terminus of the protein prevents the Hect E3s from being autoubiquitinated. Moreover, the binding of an adaptor protein to the Hect E3s via the protein interaction domains at the N-terminus alters the localization of the Hect E3s (81). The detailed

mechanisms by which the activity or function of the Hect E3s is regulated remain to be understood.

26S proteasome

The 26S proteasome is the core of proteolytic machinery in which ubiquitinated proteins are degraded. The 26S proteasome that is highly conserved in eukaryotes consists of the 20S core particle and the 19S regulatory particle (46, 63).

The 20S core particle is a barrel-shaped cylindrical structure that contains two identical inner β-rings consisting of seven β-subunits and two outer α-rings carrying seven α-subunits. The protease sites are located in the surface of the inner rings (46, 63). Thus, ubiquitinated proteins should enter the core particle to be degraded by the proteases.

By contrast, the 19S regulatory particle is divided into lid and base complexes. The base is composed of six different ATPase subunits and a few non-ATPase subunits, whereas the lid contains more than 10 Rpn subunits (46, 63). The role of the 19S regulatory particle is to recognize and guide ubiquitinated proteins to the 20S core particle of the 26S proteasome. When a ubiquitinated protein binds to the regulatory subunit, it is deubiquitinated, unfolded, and translocated into the core particle where it is degraded by the action of proteases (46, 63).

2. Cell cycle

Cells divide and undergo the cell cycle in response to external stimuli including nutrients, growth factors, and mitogens. In order to faithfully replicate DNA once per cell cycle, cell cycle is largely divided into the mitotic phase and interphase which includes G1, S, and G2. In late G1, a cell senses the availability of nutrients and growth factors and decides whether or not to enter the S phase. If the environmental stimuli signal to the cell not to go into the S phase, it maintains the quiescent state until it is ready to resume cell division. Once the cell enters the S phase, it will complete the cell cycle. During the S phase, DNA replication occurs and chromosomes are duplicated. After the S phase, the cell enters the G2 phase of the cell cycle and prepares for the mitosis. During the mitotic phase, duplicated chromosomes are segregated into two daughter cells and the cell cycle is completed. When errors and mistakes are generated as a cell replicates DNA and chromosomes are attached to the microtubules, the cell cycle is halted and various checkpoints and repair proteins fix these problems before the cell cycle is resumed or completed.

Cell cycle control by ubiquitin-dependent degradation

The degradation of cell cycle regulators by the ubiquitin-proteasome system is important to control the cell cycle. The cell cycle is tightly controlled by cell cycle regulators such as cyclins and Cdk-inhibitors (CKIs) (10, 25, 74). Cyclin-dependent kinase (Cdk) is a major engine for the cell cycle and its activity is periodically regulated throughout the cell cycle not only by the fluctuation of cyclin synthesis but also by ubiquitin-dependent degradation of cyclins or CKIs. For instance, Sic1, a CKI, inhibits

the activity of the S phase Clb-Cdks to maintain the Cdk activity low during G1. In late G1, Sic1 is phosphorylated by Cln-Cdk complex and targeted for ubiquitin-dependent degradation by the SCF^{Cdc4} E3 ligase complex (25). This allows a cell to enter the S phase from the G1 of the cell cycle (Figure 4).

In addition, the degradation of Pds1, also known as securin, (15) and mitotic cyclin (96) by the APC E3 ligase during the mitotic phase is required for the proper segregation of chromosomes and mitotic exit. During the metaphase, duplicated chromosomes are aligned and held together by cohesins. When sister chromatids are accurately attached to the microtubules through the kinetochores and bi-oriented, Cdc14 dephosphorylates the Pds1 and the dephosphorylated Pds1 is subsequently recognized by the APC^{Cdc20} E3 ligase for ubiquitin-mediated degradation. This leads to the activation of Esp1, separase, and separation of sister chromatids during the anaphase (15, 93). In order for a cell to exit mitosis, the activity of mitotic Clb-Cdks needs to be inhibited. Mitotic exit is also triggered by the action of the APC^{Cdc20} E3 ligase that targets mitotic Clb for ubiquitin-mediated degradation (Figure 4) (96).

S-phase checkpoint

The regulation of the cell cycle is critical to maintaining cell viability and genome stability. The integrity of cell cycle progression is monitored by multiple checkpoints including the S phase checkpoint and spindle checkpoint.

When a cell encounters DNA lesions or stalled replication forks in response to replication stress, the S phase checkpoint is activated and DNA replication is halted until

the obstacles are fixed or overcome. Two major kinases that govern the S phase checkpoint are the ATM/Tel1 and ATR/Mec1. The ATM/Tel1 kinase is primarily activated by DNA double-strand breaks (DSBs), whereas the activity of the ATR/Mec1 kinase is triggered by various DNA damage including replication stress, base adducts, UV-induced damage, and DSBs (26, 58). The uncoupling of helicase complexes and polymerases generates a region of single-strand DNA (ssDNA) which is further coated by replication protein A (RPA), resulting in the recruitment and activation of Mec1. In addition, the 9-1-1 checkpoint clamp consisting of Rad17-Mec3-Ddc1, a heterotrimer structure related to PCNA, also senses the RPA-coated ssDNA and activates the Mec1 kinase. The activated Mec1 kinase phosphorylates downstream kinases such as Mrc1 and Rad9, which subsequently activate the effector kinases, Rad53 and Chk1. This signal cascade leads to the inhibition of the S phase progression, prevention of late origin firing, stabilization of replication fork, upregulation of repair genes, and transcriptional repression of cyclins (Figure 5) (26, 34, 58, 66).

Spindle checkpoint

The spindle checkpoint ensures that duplicated chromosomes are correctly attached to the mitotic spindles via the kinetochores at the metaphase. Failure to attach the microtubules to the kinetochores on each sister chromatid or bi-orient chromosomes prevents the onset of anaphase until all sister chromatids are properly attached to the microtubules.

The mitotic checkpoint complex (MCC) consisting of Mad2, BubR1, Bub3, and Cdc20 monitors the attachment between the kinetochores and microtubules (64). The unattached kinetochores cause the MCC complex to inhibit Cdc20 so that the APC^{Cdc20} E3 ligase activity is blocked, resulting in the inhibition of sister chromatid separation (Figure 6). The spindle assembly checkpoint (SAC) also plays an important role in maintaining kinetochore attachment (64). Mad2 senses the lack of tension and unattached kinetochores. Mad2 is highly concentrated at the kinetochores and its level is reduced as the kinetochores are correctly attached to the microtubules and tension is created between two sister chromatids. Aurora-B/Ipl1 also functions to correct improper attachments such as merotelic attachments in which one sister kinetochore is attached to the microtubules from opposite spindle poles (64). When the microtubules are precisely attached to the kinetochores of sister chromatids and chromosomes are bi-oriented by proper tension, Cdc20 is released from the MCC and forms the active APC^{Cdc20} complex, which further targets Pds1 for degradation, resulting in separation of sister chromatids (Figure 6). In addition, the SAC activity is also extinguished to allow the metaphase-anaphase transition to occur.

3. DNA Replication

Pre-replicative complex (pre-RC) assembly

Accurate duplication of chromosomes is essential for cell proliferation and genomic stability. There are about 400 replication origins in budding yeast. Those origins are fired during S phase of the cell cycle and all of chromosomes are precisely duplicated. In order

to initiate DNA replication, sites at which DNA replication takes place called origins need to be specified during the G1 phase of the cell cycle.

The autonomously replicating sequence (ARS) was originally identified in budding yeast, *Saccharomyces cerevisiae*. This block of the genome contains the A, B1, B2, and B3 elements. The A element carries the 11 bp AT-rich ARS consensus sequence (ACS) conserved in budding yeast chromosomes (44, 84). This conserved sequence (A element) and B1 element are the site recognized by the origin recognition complex (ORC) which is composed of ORC1-6 (43, 44). Once the ORC complex binds to origins of replication, it recruits additional pre-RC components, Cdc6 and Cdt1 and this process requires ATP hydrolysis.

Cdc6 is a member of AAA+ ATPases and required for DNA replication initiation (43, 44). In support of this, overexpression of Cdc18, a homolog of fission yeast, leads to re-replication (8, 70). However, overexpression of Cdc6 does not result in overduplication of genome in budding yeast (8), suggesting that other inhibitory mechanisms such as Cdk-mediated Mcm export and Orc inhibition are critical to prevent re-replication in budding yeast.

Cdt1 is also an important initiation protein that recruits the Mcm complex to the origins of replication. Recent study showed that two Cdt1 proteins bind to Orc6 via the two Cdt1 binding sites on Orc6 and bring a double hexamer of MCM complexes to the origins (Figure 7) (13).

Mcm2-7 complex, a helicase, plays an essential role in DNA replication initiation. In most eukaryotic organisms, Mcm2-7 complex is localized in the nucleus throughout the

cell cycle (44). Mcm2-7 complex associates with origins in G1 but dissociates from the origins as cells enter the S phase (44). Unlike the Mcm2-7 complexes in eukaryotic organisms, budding yeast Mcm2-7 complex is localized in the nucleus in G1 and exported to the cytoplasm during S and G2/M (8, 44, 67). This different localization of the Mcm2-7 complex in budding yeast helps to prevent origins from being fired more than once in a single cell cycle. When the Mcm2-7 complex is loaded onto origins, initiator proteins Cdt1 and Cdc6, are dissociated from the origins and not reassembled into the origins until the next G1 phase of the cell cycle.

DNA replication initiation

After the Mcm2-7 double hexamer is loaded onto origins of replication, Cdc45 helicase-activating protein and Sld3 are recruited to the Mcm2-7 complex by Dbf4-dependent Cdc7 kinase (DDK)-mediated Mcm2-7 phosphorylation (35). Then, the S phase cyclin-dependent kinase (S-Cdk) phosphorylates Sld2 and Sld3 and the phosphorylated Sld2 binds to Dpb11 which contains two tandem phosphopeptide-binding domains, also known as BRCT domains (28). The N-terminal BRCT domain recruits phosphorylated Sld3, whereas the C-terminal pair of the BRCT domains binds to phosphorylated Sld2. When phosphorylated Sld2 interacts with Dpb11, Sld2-Dpb11 complex interacts with polymerase ε-GINS complex. In this complex, polymerase ε mediates the interaction between GINS and Sld2 since GINS alone does not have a high affinity for Sld2 binding in vitro (2).

Once the pre-loading complex (pre-LC) including Sld2, Dpb11, GINS, and polymerase ε is formed, the pre-LC is subsequently recruited to the Mcm2-7, Sld3, and Cdc45 complex via the interaction between phosphorylated Sld3 and Dpb11. Thus, the function of the pre-LC complex is to bring the polymerase ε-GINS to the pre-RC complex to form the Cdc45-Mcm-GINS (CMG) complex, an active helicase. This leads to the formation of DNA replication initiation complex (Figure 8, DNA replication initiation I).

After pre-LC complex binds to the pre-RC complex to form the CMG complex, Dpb11, Sld2, and Sld3 are released from the complex. Then, the CMG complex containing polymerase ε unwinds the origin DNA and moves along the replication fork as DNA is synthesized (Figure 9, DNA replication initiation II).

There are multiple early origins that need to be fired during the S phase of the cell cycle. Therefore, the role of Sld3 turnover is critical to initiate the firing of other early origins. When the pre-LC is loaded onto the first replication origin, Sld3 is dissociated and binds to the second origin located next to the first origin. This also forms a complex with new Cdc45 onto the second origin and prepares for subsequent loading of the pre-LC complex to form the CMG complex (2).

DNA replication elongation

Eukaryotic organisms require three DNA polymerases including polymerase α, δ, and ε for DNA replication (2, 51). Polymerase α forms a complex with primase which synthesizes a short RNA primer. The polymerase α extends the DNA using this RNA

primer. The RFC, clamp loader, recognizes the 3'end of the DNA and brings the PCNA sliding clamp onto the double-strand DNA. This short stretched DNA is further extended by either polymerase δ or polymerase ε. The polymerase δ primarily extends the lagging strand, whereas polymerase ε synthesizes the DNA on the leading strand.

Polymerase ε is made of four subunits, Pol2, Dpb2, Dpb3, and Dpb4 (2). The N-terminal half of Pol2 has the catalytic activity and is dispensable for cell viability. However, the C-terminal half of Pol2 is necessary for cell growth.

On the lagging strand, the okazaki fragments formed by Pol α/primase and Pol δ are further processed by the action of Pol δ and flap endonuclease FEN1 to remove and replace the RNA primer with DNA (4, 42). The gaps made by this process are sealed and joined together by DNA ligase.

4. Biological roles of Tom1, Dia2, and Cdc6

Hect E3 ligase Tom1

Tom1 is a Hect family E3 ubiquitin ligase in budding yeast. It contains a conserved Hect domain at the C-terminus, two E3 ubiquitin ligase domains of which function is not known and a potential protein-protein interaction domain at the N-terminus of the protein. Tom1 plays a role in a wide variety of cellular processes including transcriptional activation, mRNA export, and DNA damage response (32, 40, 82, 86). In particular, Tom1 targets histone H3 for ubiquitin-dependent degradation in response to activation of the S-phase checkpoint via Rad53-mediated histone H3 phosphorylation (86). In addition, DNA replication initiator protein Cdc6 is also targeted for degradation by Tom1 in

response to DNA damage (32). These reports indicate that Tom1 has a role in DNA damage response, although more potential Tom1 substrates involved in this process remain to be identified.

Huwe1, a human homolog of Tom1, has been shown to be important for cell proliferation and growth suppression. Under normal cell growth conditions, Huwe1 polyubiquitinates c-Myc via the lysine 63-linked chains, leading to transcriptional activation of downstream target genes. Huwe1 also targets p53 for ubiquitin-dependent degradation (1, 12) during cell proliferation. By contrast, Huwe1 switches its targets during DNA damage. For example, replication initiator Cdc6 and anti-apoptotic protein Mcl-1 are targeted for degradation to inhibit the assembly of pre-RC complex and promote apoptosis in response to DNA damage, respectively (32, 100). These findings suggest that some aspect of Huwe1 function appears to be conserved in budding yeast, *Saccharomyces cerevisiae*.

In addition to its role in DNA damage response, Tom1 also plays a role in mRNA export. Yra1/REF, a component of mRNA ribonucleoprotein (mRNP) complex, is ubiquitinated by Tom1 and dissociated from mRNP complex before mRNA export (40). Intriguingly, Yra1 has also been known to interact with and recruit Dia2 to replication origins (90), implying that Tom1 may also directly or indirectly bind Dia2.

F-box protein Dia2

The budding yeast F-box protein Dia2 assembles a functional SCF complex with Cdc53, Skp1, and Rbx1 and recruits a substrate to the SCF complex for ubiquitin-

mediated degradation (36, 47, 48, 52). Dia2 also has a role in maintaining genomic stability and DNA replication. For example, the deletion of *DIA2* renders cells sensitive to DNA damage, increases chromosome loss and rearrangement, and accumulates DNA damage foci (5, 47, 71). In addition, our previous work showed that Dia2 is a chromatin bound protein and associates with origins of DNA replication (47). In support of the idea that Dia2 plays a role in DNA replication, Dia2 has been shown to assemble with replisome components and control the progression of replication forks (60, 62). Moreover, Dia2 protein is stabilized during S phase or in response to activation of the S-phase checkpoint (45), suggesting that stabilized Dia2 may form the SCF^{Dia2} complex to target S-phase or replication proteins for degradation. Two potential Dia2 substrates, Mrc1 and Ctf4, that travel along with replication fork have been identified, although the biological significance of their ubiquitination remains to be understood (60).

The rate of Dia2 degradation varies during the cell cycle. Dia2 is unstable during G1 and G2/M phases but stable in S phase. There are two conflicting reports about the pathway responsible for Dia2 degradation. One report suggests that Dia2 is degraded via an auto-ubiquitination mechanism (60), as shown in other F-box proteins (27, 101). In contrast, our previous work shows that Dia2 degradation is not dependent on an auto-ubiquitination mechanism (45), as deletion of the F-box domain required for assembly of an SCF complex does not stabilize Dia2, indicating that a non-SCF E3 ligase might control Dia2 degradation. However, the identity of E3 ligase responsible for this pathway is not known.

Cdc6 degradation and its role in re-replication control

Cdc6 is a replication initiation protein required for assembly of pre-RC complex during the G1 phase of the cell cycle. Cdc6 is targeted for ubiquitin-dependent degradation during the cell cycle and is subject to multiple modes of degradation in budding yeast (20, 21, 73, 75).

Mode 1 represents the degradation of Cdc6 during G1 phase and does not require either the anaphase-promoting complex (APC/C) or SCF E3 ligase complex. Mode 1 Cdc6 degradation is relatively rapid and independent of Cdk-mediated phosphorylation (20). More importantly, the E3 ubiquitin ligase responsible for this pathway is not known.

Mode 2 Cdc6 degradation is dependent on the SCF^{Cdc4} E3 ligase complex at the G1 to S-phase transition. The turnover of Cdc6 protein at this stage is extremely rapid and requires Cdk-mediated phosphorylation for the SCF^{Cdc4} complex to recognize Cdc6 for ubiquitin-dependent degradation. This phosphorylation event is dependent on G1-cyclins but not S-cyclins. Cdc6 contains eight Cdk consensus sites and the phosphorylation of the first four consensus sites located at the N-terminus of the protein is important for Mode 2 degradation (20, 21, 73).

During G2/M phases of the cell cycle, Cdc6 is subject to Mode 3 degradation. This pathway is also governed by activity of the SCF^{Cdc4} complex and requires phosphorylation of two Cdk consensus sites found at the C-terminus of Cdc6 (73).

As described above, Cdc6 turnover rate varies during the cell cycle and only a single E3 ubiquitin ligase for Cdc6 degradation has been identified, the SCF^{Cdc4} complex.

Moreover, the turnover rate of Cdc6 at the G1 to S phase transition (Mode 2) is very rapid compared to those of Mode 1 and 3, suggesting that multiple E3 ligases may be required for Mode 2 Cdc6 degradation.

Cdc6 degradation is an important pathway to inhibit DNA re-replication. In budding yeast, multiple regulatory mechanisms including Cdc6 degradation, nuclear export of Mcm2-7 complex, and ORC inhibition are critical to prevent the re-assembly of pre-RC complex after S phase until the G1 phase of the next cell cycle (3, 6, 68). First, Cdk-dependent Cdc6 phosphorylation marks it for ubiquitination by the SCF^{Cdc4} complex, resulting in degradation via the 26S proteasome. In addition, phosphorylation of Cdc6 at the N-terminal domain (amino acids 2-47) also induces its association with Clb2-Cdk complex such that Cdc6 activity for pre-RC assembly is blocked (61). Second, Cdk inhibits the activity of ORC through phosphorylation of Orc2 and Orc6, leading to inhibition of Cdt1/Mcm2-7 complex loading onto origins. Moreover, binding of S-phase cyclin Clb5 to Orc6 also inhibits the recruitment of Cdt1/Mcm2-7 complex to ORC (13). Third, Mcm2-7 complex is exported to the cytoplasm to avoid re-loading of Mcm2-7 complex onto origins during S or G2/M phases (67). When these multiple inhibitory mechanisms are compromised, re-replication is observed in budding yeast (3, 68). For example, mutations of Orc2 and Orc6 phosphorylation sites along with constitutively nuclear localization of Mcm2-7 complex and overexpression of stable Cdc6ΔN mutant are simultaneously required to induce re-replication in budding yeast.

To precisely duplicate the genome, origins in eukaryotic cells are fired during S phase only once per cell cycle. However, disruption of the above regulatory mechanisms in

budding yeast causes some origins to be fired more than once during S or G2/M phases, resulting in over-duplication of portions of the genome (Figure 10). Thus, failure to control re-replication leads to genomic instability such as gene amplification, chromosome loss and rearrangement. Although multiple overlapping mechanisms are required to control re-replication in budding yeast, overexpression of Cdc18, a fission yeast homolog of Cdc6, is sufficient to induce re-replication in fission yeast (70). In addition, human Cdc6 is often overexpressed in various cancers (8), suggesting that regulation of Cdc6 expression is crucial to prevent genomic instability and tumorigenesis.

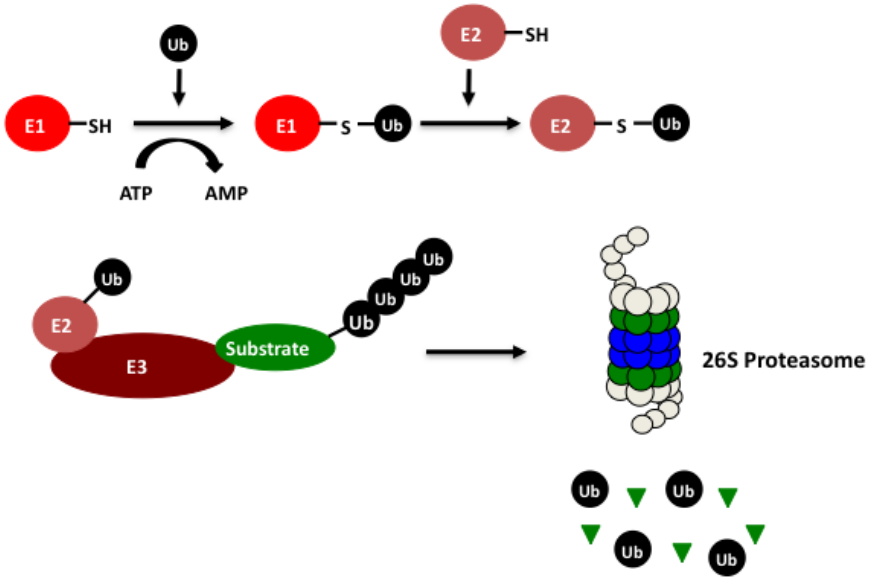

Figure 1. Ubiquitin-proteasome system.

E1 ubiquitin-activating enzyme is charged with ubiquitin in an ATP-dependent manner. Ubiquitin is then transferred to E2 ubiqutin-conjugating enzyme through a thioester bond. With the help of E3 ubiquitin ligase, ubiquitin is directly or indirectly attached onto a lysine of a substrate. After multiple rounds of this reaction, polyubiquitinated substrate is targeted for degradation via the 26S proteasome.

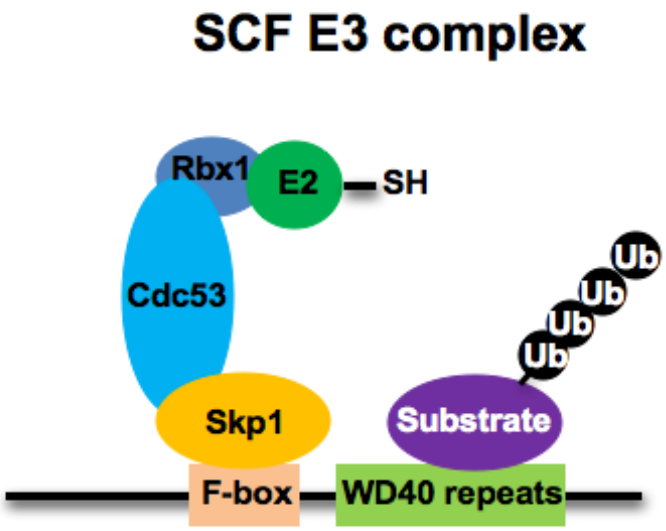

Figure 2. SCF E3 ligase complex.

Multi-subunit SCF E3 ligase complexes consist of Cdc53 (Cul1), Rbx1(Roc1), Skp1, and F-box protein. When an F-box protein binds a substrate, ubiquitin is directly transferred from an E2 to a lysine of the substrate. Rbx1 interacts with the E2 through the RING domain. The F-box protein interacts with the substrate via the WD40 repeats located at the C-terminus of the protein. The SCF^{Cdc4} E3 ligase complex is shown here as an example.

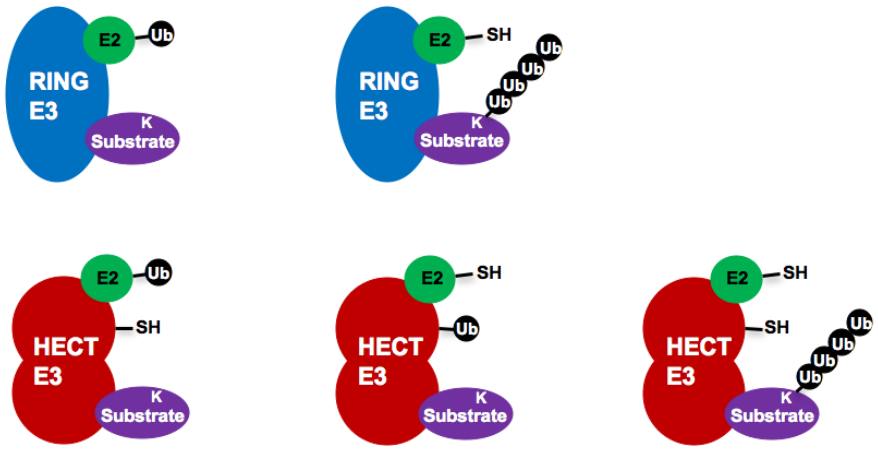

Figure 3. Major E3 ligase types.

RING E3 ligases contain the RING and substrate binding domains. When a RING E3 binds an E2 and a substrate, ubiquitin is directly transferred from the E2 to a lysine of the substrate. By contrast, a HECT E3 ligase transiently accepts ubiquitin from an E2 via a catalytic cysteine in the HECT domain. Ubiquitin is then subsequently attached onto a lysine of the substrate.

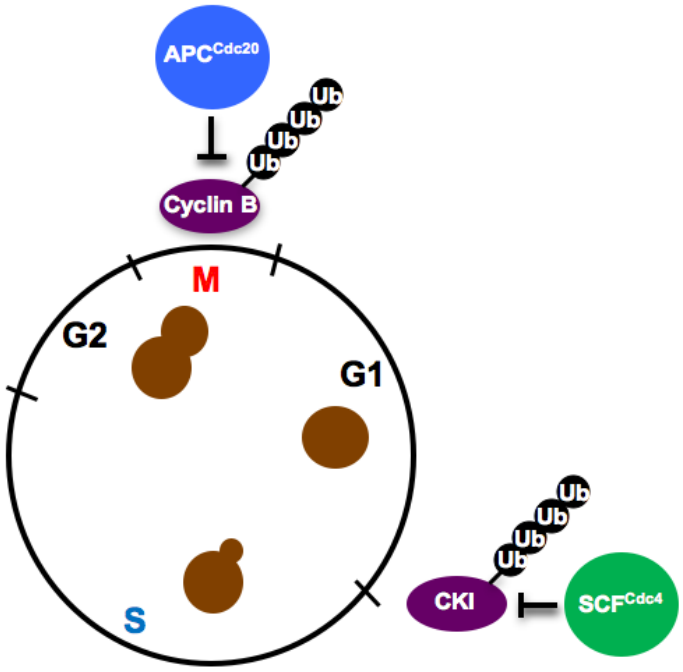

Figure 4. Ubiquitin-mediated degradation controls the cell cycle.

In late G1, Cdk inhibitor (CKI) such as Sic1is targeted for ubiquitin-mediated degradation by the SCF^{Cdc4} complex to promote the G1 to S phase transition. During mitosis, the APC^{Cdc20} complex targets mitotic cyclin for ubiquitin-dependent degradation to allow a cell to exit mitosis.

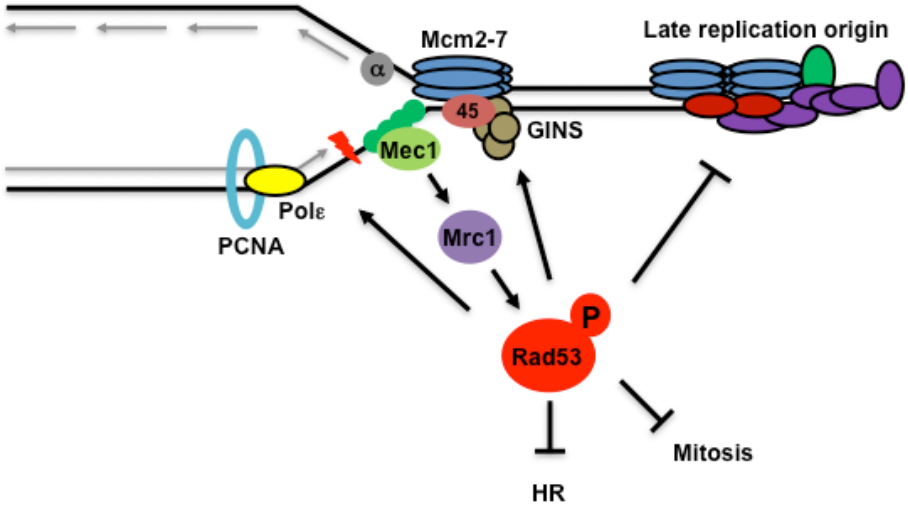

Figure 5. Activation of the S-phase checkpoint.

Upon DNA damage or replication stress (i.e. DNA lesion shown here), Mec1is recruited to RPA (shown in green) and activated. This leads to activation of downstream effector kinase Rad53 via phosphorylation of Mrc1. Activation of Rad53 inhibits S-phase progression, stabilizes the replication fork, and inhibits late origin firing. In addition, activated Rad53 also blocks homologous recombination and mitosis.

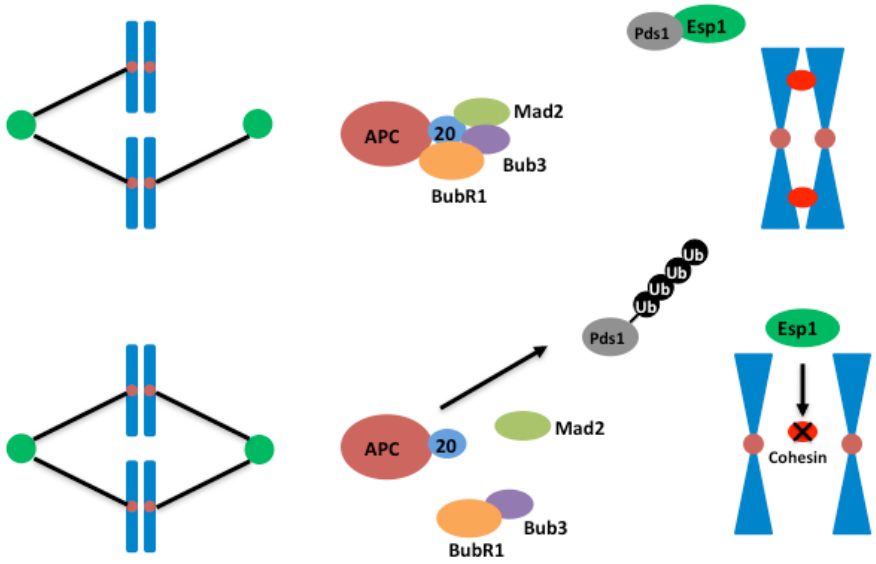

Figure 6. Role of the Spindle checkpoint in chromosome separation.

The inaccurate attachment of microtubules from spindle poles (shown in green circle) to the kinetochore (i.e. monotelic attachment) is monitored by the MCC complex and leads to the inhibition of the APC^{Cdc20} complex. When sister chromatids are correctly attached to the microtubules, this results in activation of the APC^{Cdc20} complex which in turn targets Pds1 for ubiquitin-dependent degradation. Esp1, separase, is then released from Pds1 and cleaves the cohesin to separate sister chromatids.

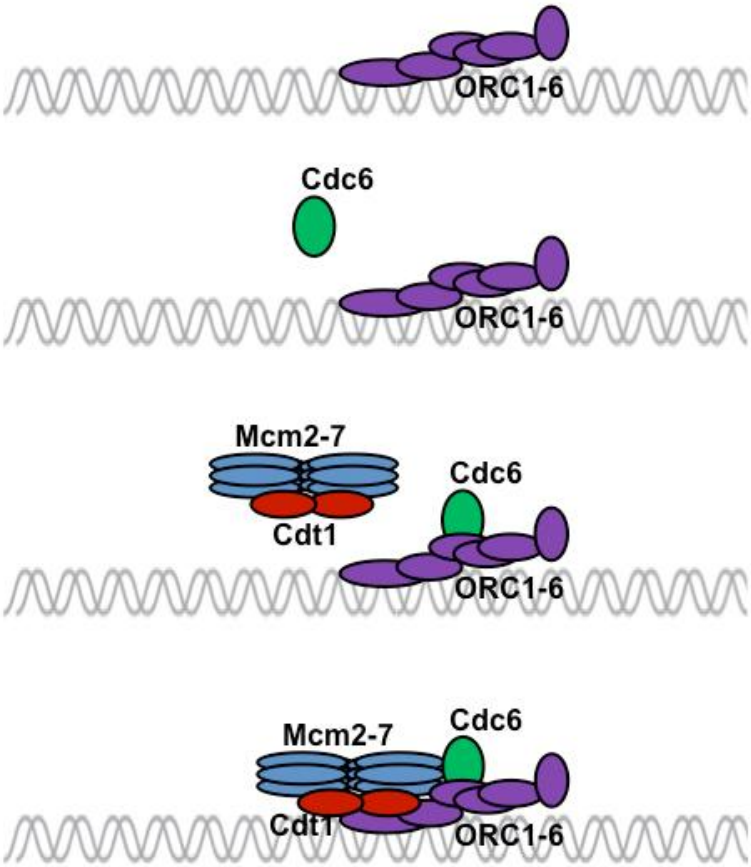

Figure 7. pre-RC assembly in G1.

ORC complex binds to replication origin and recruits Cdc6 which further brings Cdt1/Mcm2-7 complex to the origin of replication to assemble the pre-RC complex.

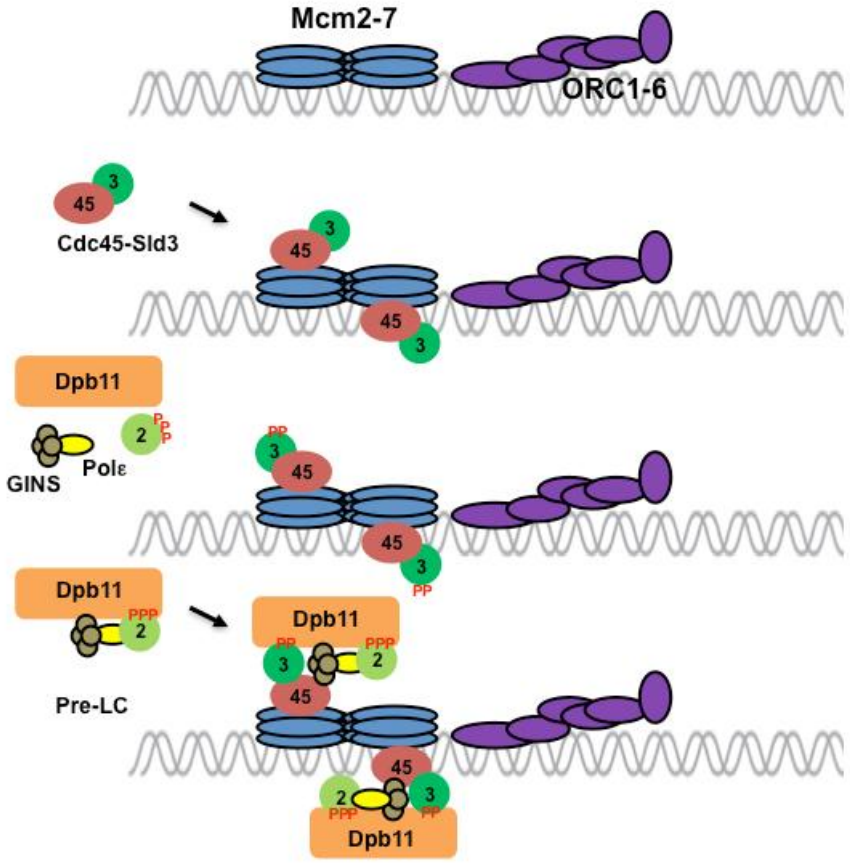

Figure 8. DNA replication initiation I.

Dbf4-dependent Cdc7 Kinase (DDK)-mediated Mcm2-7 phosphorylation (not shown here) causes Cdc45 and Sld3 to bind to the Mcm2-7 complex. S-phase Cyclin-dependent Kinase (S-Cdk) then phosphorylates Sld2 and Sld3. Once phosphorylated Sld2 binds to Dpb11, GINS-polymerase ε complex is also recruited to the Sld2-Dpb11 complex to form the pre-loading complex (pre-LC), which subsequently interacts with the pre-RC complex via the interaction between Sld3 and Dpb11.

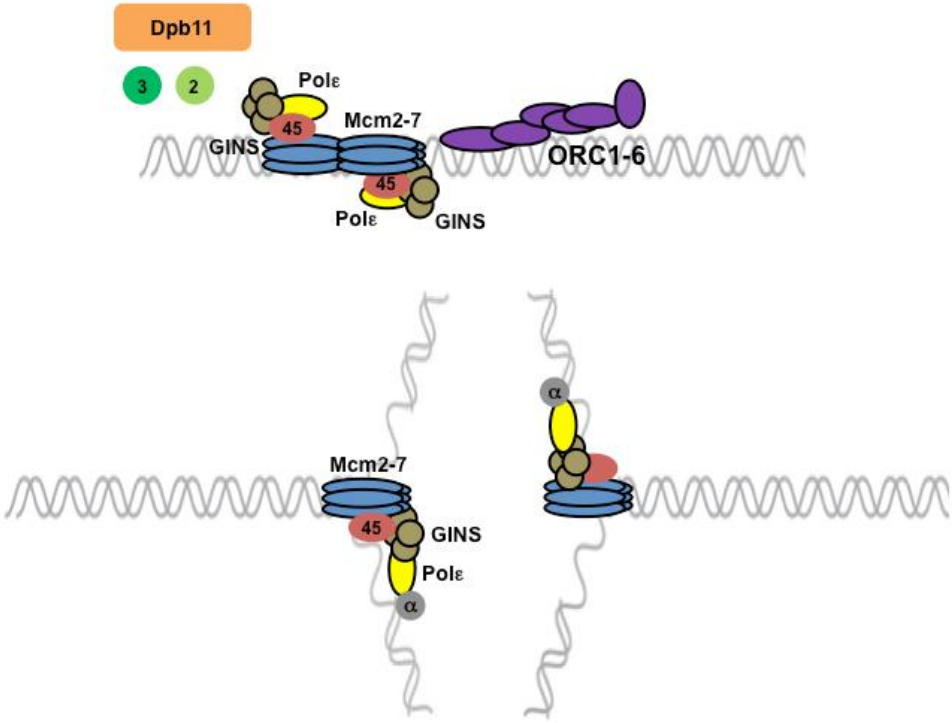

Figure 9. DNA replication initiation II.

When the Cdc45-Mcm-GINS (CMG) complex is formed next to the origin, Sld2, Sld3, and Dpb11 are dissociated from the complex. The active CMG complex containing polymerase ε then unwinds DNA and establishes replication forks. Polymerase α/primase complex (Primase is not depicted here) later joins the CMG complex to initiate DNA replication on both strands. Polymerase ε and polymerase δ (not shown in the diagram) then elongate the leading and lagging strands, respectively. DNA elongation process is not shown in the diagram.

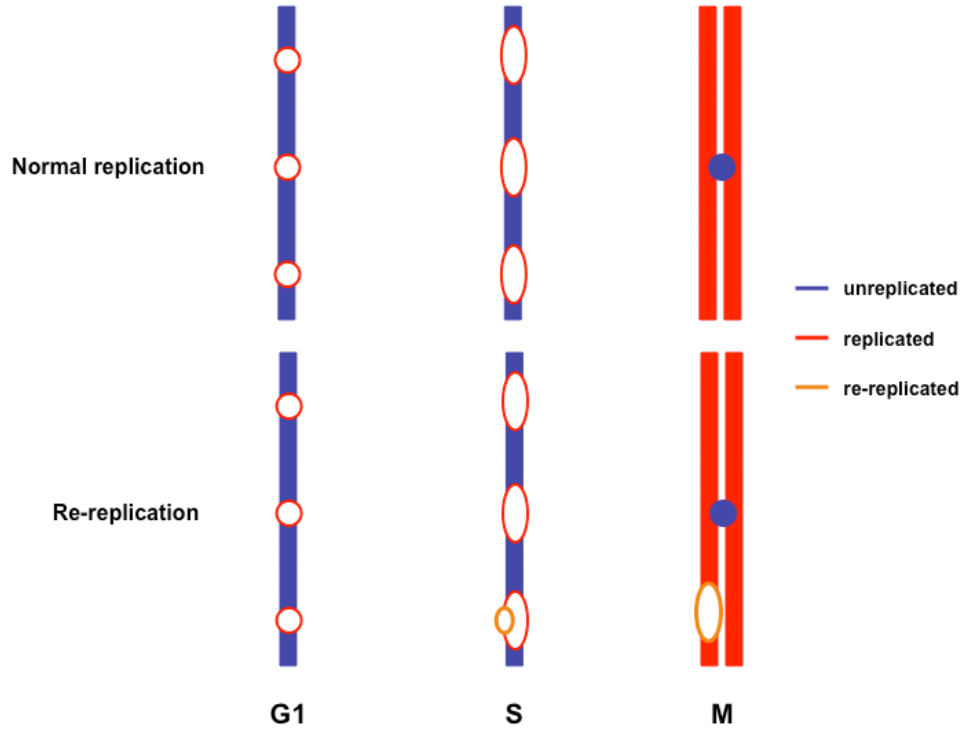

Figure 10. Re-replication.

Multiple inhibitory mechanisms including Cdc6 degradation, Mcm2-7 export, and ORC inhibition play a crucial role in preventing origins from being fired more than once within a single cell cycle in budding yeast, *Saccharomyces Cerevisiae*. In re-replication condition, one of the origins is re-fired during S or G2 phase, leading to the portion of chromosome over-duplicated.

CHAPTER II

Cdc6 degradation by a Tom1 and Dia2-dependent pathway regulates pre-RC assembly during the cell cycle

Cdc6 functions in the assembly of pre-replicative complexes at replication origins. This activity is controlled to limit DNA replication to once per cell cycle. Cdc6 is targeted for protein degradation by multiple mechanisms in *Saccharomyces cerevisiae,* although only a single pathway and E3 ubiquitin ligase for Cdc6 has been identified, the SCF^{Cdc4} complex. Using a genetic approach, I identified two additional E3 ubiquitin ligase components required for Cdc6 degradation, the F-box protein Dia2 and the Hect-domain E3 Tom1. Both Dia2 and Tom1 control Cdc6 turnover during G1, a cell cycle stage when Cdc4 does not recognize Cdc6. Surprisingly, Dia2 and Tom1 also contribute to Cdc6 protein turnover at the G1/S transition when SCF^{Cdc4} acts. Genetic epistasis analysis indicates that Dia2 and Tom1 function cooperatively but act separately from SCF^{Cdc4}. A mutant defective in all three ubiquitin ligase activities exhibits exacerbated Cdc6 protein stabilization and sensitivity to replication stress. Cdc6 and Mcm4 chromatin association is aberrant in *tom1Δ* and *dia2Δ* cells after S phase has been completed. Strikingly, defects in Tom1 or Cdc4 lead to increased DNA content in cells sensitized to re-replication. Thus, multiple degradation pathways that limit Cdc6 protein levels cooperate to regulate pre-RC assembly and may act to prevent DNA re-replication.

Introduction

DNA replication is a highly coordinated process to precisely duplicate chromosomes during S phase of the cell cycle. Initiation of DNA synthesis requires assembly of pre-replicative complexes (pre-RCs) at replication origins (reviewed in (84)). Regulation of pre-RC assembly is critical to prevent over duplication of genetic material. Pre-RC assembly occurs during the G1 phase of the cell cycle and re-assembly is blocked for the remainder of the cycle (reviewed in (7)).

Cdc6 is an AAA+-ATPase required for pre-RC assembly (14, 54, 72, 97). Cdc6 binds to the Origin Recognition Complex (ORC) along with another pre-RC protein, Cdt1, to recruit the MCM2-7 replicative helicase complex to replication origins (17, 18, 57, 69, 92). Budding yeast Cdc6 is a highly unstable protein subject to multiple modes of degradation (20, 21, 75). In the best-understood degradation pathway, cyclin-dependent kinase (Cdk) phosphorylation targets Cdc6 for ubiquitination and degradation via the ubiquitin ligase complex SCF^{Cdc4} at the G1/S phase transition and during G2/M (20-22, 73, 83). However, Cdc6 is also unstable during G1 and the degradation pathway responsible has not been identified (21). Moreover, the rate of Cdc6 degradation fluctuates during the cell cycle (21), an observation not fully explained by the activity of a single ubiquitin ligase.

To identify other pathways that might target Cdc6 for ubiquitination and degradation, I assayed other E3 ubiquitin ligases that function in DNA replication or during S phase. Tom1 is a Hect-domain E3 ubiquitin ligase that targets excess histone H3 for DNA replication checkpoint-dependent degradation (86). The human homolog of Tom1,

Huwe1, targets human Cdc6 for degradation during the DNA damage checkpoint response (32, 33). This function appears to be conserved in *S. cerevisiae* (32), although the contribution of Tom1 to Cdc6 degradation in an unperturbed cell cycle has not been investigated. The SCF^{Dia2} ubiquitin ligase complex regulates DNA replication and is required for genomic stability (5, 47, 62, 71). Potential targets of SCF^{Dia2} include two proteins that travel with replication complexes at the replication fork, Mrc1 and Ctf4, although the physiological role of their degradation is unclear (60).

Here, I show that both Tom1 and Dia2 contribute to Cdc6 degradation during G1 and surprisingly, also during the G1 to S phase transition. This work describes new degradation pathways for Cdc6 and identifies a novel target for both the Tom1 and Dia2 ubiquitin ligase components.

Tom1 and Dia2 target Cdc6 for degradation

To determine whether other ubiquitin ligases might have a role in Cdc6 protein turnover, I examined whether overexpression of *CDC6* caused a growth defect in ligase mutants that had known roles in DNA replication or cell cycle. Two ligases that fit this profile include the F-box protein Dia2 and the Hect-domain E3 Tom1 (5, 33, 47, 71). Previous work has shown that Tom1 can target Cdc6 for degradation in response to DNA damage (33), but a role for Tom1 in Cdc6 turnover in an unperturbed cell cycle has not been examined. Overexpression of *CDC6* causes a growth defect in wildtype yeast cells (9, 23), but I observed an exacerbated growth phenotype in both *dia2Δ* and *tom1Δ* cells (Figure 11A).

I then performed a protein stability assay using HA-tagged Cdc6 expressed from the endogenous locus in wildtype, *tom1Δ* and *dia2Δ* cells. Log phase cultures were treated with cycloheximide to inhibit protein synthesis and Cdc6 protein levels examined over time. As shown in Figure 11B, Cdc6 was partially stabilized in both *dia2Δ* and *tom1Δ* cells. Another unstable cell cycle protein, Clb5, was not stabilized in *dia2Δ* or *tom1Δ* cells, indicating that the results with Cdc6 were not due to non-specific defects in protein degradation (Figure 12). In addition, no changes in *CDC6* RNA abundance was detected in these strains (Figure 11C), consistent with the possibility that Dia2 and Tom1 might control Cdc6 ubiquitination.

Cdc6 binds Dia2 and Tom1

I examined whether Dia2 and Tom1 interact with Cdc6 using two different approaches. First, I tested whether GST-Cdc6 co-purified with either Myc-tagged Dia2 or the Flag-tagged Hect domain of Tom1 when expressed in baculovirus-infected insect cells (Figure 13). When either Myc-tagged Dia2 or the Flag-tagged Hect domain of Tom1 was immunoprecipitated, I observed substantial co-purification of GST-Cdc6 (Figure 13A). I also observed reciprocal co-purification when GST-Cdc6 was purified from the same cells (Figure 13B). Next, I tested whether endogenously expressed HA-tagged Cdc6 can co-immunoprecipitate endogenously expressed Myc-tagged Dia2 or Flag-tagged Tom1 (Figure 13C). Immunoprecipitation of Cdc6 resulted in Tom1 and Dia2 co-purification, indicating that these proteins interact under physiological conditions. GST-tagged Cdc6 purified from baculovirus-infected insect cells also

interacted with endogenously expressed Flag-tagged Tom1 and Myc-tagged Dia2 in yeast extracts (data not shown). Since Dia2 is a chromatin-bound protein, I considered the possibility that Dia2 interacted with Cdc6 indirectly by virtue of both proteins binding to chromatin, but I still observed co-precipitation when lysates were treated with DNase I (Figure 14A). I also observe no change in Cdc6 association with either Tom1 or Dia2 when the other is missing, indicating that both Tom1 and Dia2 can bind Cdc6 independently of each other (Figure 14B). I conclude that both Tom1 and Dia2 form a complex with Cdc6, although I cannot determine whether all three proteins assemble into the same complex from these results.

Tom1 is a large protein with multiple domains, including the conserved Hect domain found in the C-terminus of the protein that contains the catalytic cysteine (82). My results with insect cell-expressed protein indicate that the Tom1 Hect domain interacts with Cdc6 (Figure 13A, B). Dia2 is an F-box protein that contains TPR repeats in the N-terminus and an LRR domain in the C-terminus (5, 47). Since F-box proteins typically associate with substrate proteins via their C-terminal repeat domains, I asked whether a truncated Dia2 protein lacking the N-terminus still bound Cdc6. I co-expressed ΔN214 Dia2, which lacks the N-terminal TPR repeats but still contains the F-box domain and LRR region, with GST-Cdc6 in insect cells. GST-Cdc6 co-purified ΔN214 Dia2 under these conditions (Figure 13D). Together, these results suggest that the N-termini of Tom1 and Dia2 are dispensable for binding Cdc6.

Tom1 and Dia2 mediate degradation of Cdc6 at the G1/S transition

Cdc6 protein turnover is regulated throughout the cell cycle (20, 75). Thus, I investigated whether Tom1- and Dia2-dependent turnover of Cdc6 changed during the cell cycle. I first examined the abundance of the Cdc6 protein as cells progressed from a late G1 arrest into G2. Cells were arrested with alpha factor and then released into media containing nocodazole. In wildtype cells, there is a burst of Cdc6 expression in late G1 (9, 20, 75), but the protein disappears as cells enter and proceed through S phase (Figure 15A). In both *tom1Δ* and *dia2Δ*, Cdc6 protein abundance decreases as cells enter S phase but does not disappear altogether as it does in wildtype cells. These results were somewhat surprising, as it has previously been shown that SCF^{Cdc4} targets Cdc6 at the G1/S transition (20, 21). My results suggest that Tom1 and Dia2 may also control Cdc6 degradation at the G1/S transition. To test protein turnover in early S phase, I performed cycloheximide protein stability assays on cells that had been arrested in G1 with alpha factor and then released into hydroxyurea-containing media. In wildtype cells, Cdc6 has a half-life of less than 5 minutes and in *cdc4-1* cells, the protein is partially, but significantly, stabilized as previously reported (20). Importantly, I also observed significant stabilization of Cdc6 in both *tom1Δ* and *dia2Δ* cells in early S phase (Figure 15B).

I next asked whether Tom1 and Dia2 function in the same pathway as Cdc4 in the turnover of Cdc6. I generated *cdc4-1 tom1Δ, cdc4-1 dia2Δ* and *tom1Δ dia2Δ* double mutants and assessed the stability of Cdc6 in early S phase. Strikingly, Cdc6 was strongly stabilized in both the *cdc4-1 tom1Δ* and *cdc4-1 dia2Δ* strains relative to the

single mutants (Figure 15B), indicating that the Cdc4 pathway functions independently of Tom1 and Dia2. However, stabilization of Cdc6 in the *tom1Δ dia2Δ* mutant was not significantly different than in the *dia2Δ* and *tom1Δ* single mutants (Figure 15B, C). Similar results were observed in cells arrested directly with hydroxyurea (data not shown). To examine this further, I compared the growth phenotypes of the single and double ligase mutants on rich media in the presence and absence of hydroxyurea or MMS to induce replication stress (Figure 16A). The *cdc4-1 tom1Δ* and *cdc4-1 dia2Δ* mutant exhibited enhanced growth defects compared to the respective single mutants. Strikingly, the *tom1Δ dia2Δ* mutant phenotype was very mild relative to the other double mutants. These results suggest either that Dia2 and Tom1 function in the same pathway or that they mutually reinforce each other's activity. Nevertheless, these data indicate that Cdc4 acts independently of Dia2 and Tom1.

If Dia2 and Tom1 were in the same pathway, I would expect the triple ligase mutant to show the equivalent growth phenotype to either of the *cdc4-1 dia2Δ* or *cdc4-1 tom1Δ* double mutants. However, in all conditions the *cdc4-1 tom1Δ dia2Δ* triple mutant showed the most severe phenotype, although the difference between the triple mutant and the *cdc4-1 tom1Δ* and *cdc4-1 dia2Δ* double mutants was subtle. I also compared the stability of Cdc6 in the double mutants to the triple mutant using a longer time course (Figure 16B). Here, I observed that the triple ligase mutant exhibited substantially greater stabilization of Cdc6 than the double mutants.

Thus, the genetic relationship among these three ligases is more complex than initially suggested.

Is the Tom1/Dia2 pathway responsible for Cdc6 degradation Mode 1?

Previous work from the Diffley laboratory has shown that there are three modes of Cdc6 degradation (21). Mode 1 functions prior to Start during G1 and is Cdk-independent, whereas Modes 2 and 3 are Cdk- and Cdc4-dependent and function in early S and G2/M, respectively (21). The identity of the E3 ligase in Mode 1 was not determined, although genetic evidence suggested that neither the APC nor SCF complexes were responsible (21). I tested whether Tom1 or Dia2 might contribute to the turnover of Cdc6 in G1 using the cycloheximide stability assay in cells arrested with alpha factor. As has been previously shown (21), Cdc6 is still unstable in *cdc4-1* cells under these conditions (Figure 17). Strikingly, I found that Cdc6 was stabilized in both *tom1Δ* and *dia2Δ* strains (Figure 17). The observation that Dia2 is involved in Cdc6 turnover in G1 was surprising, as Cdc6 is not stabilized in *scf* mutants in G1 (21). I next asked whether Tom1 and Dia2 function in the same pathway in G1 by examining Cdc6 turnover in the *tom1Δ dia2Δ* double mutant arrested in G1 with alpha factor. I found that the rate of turnover in the double mutant was equivalent to the turnover in *tom1Δ* (Figure 17), indicating that Tom1 and Dia2 contribute to Cdc6 degradation in G1, again either in the same pathway or acting cooperatively.

Tom1 and Dia2 are required for Cdc6 ubiquitination

The most straightforward explanation for these results is that Cdc6 may be a direct ubiquitination target of both Tom1 and Dia2. To test this hypothesis, I examined whether the ubiquitin ligase activity of Tom1 or Dia2 was required for Cdc6 protein turnover. Tom1 is a member of the Hect-domain E3 ubiquitin ligase family and so uses a catalytic cysteine in the transfer of ubiquitin to substrate proteins (82). Cdc6 was stabilized in a *tom1* mutant that had this cysteine replaced with alanine (Figure 18A). These assays were performed in G1-arrested cells, but similar results were observed in S-phase arrested cells (data not shown). Likewise, Dia2 contains an F-box domain required for assembly with the other SCF components to form a functional E3 ligase complex (5, 47). Cdc6 is stabilized in a *dia2 ΔF-box* mutant in cells arrested in G1 (Figure 18A) or early S phase (data not shown). This result suggests a requirement for the F-box domain of Dia2, but it is at odds with previous work indicating that *scf* mutants do not stabilize Cdc6 in G1 (21). I verified that *skp1-11, cdc53-1* and *cdc34-2* mutants do not stabilize Cdc6 in G1-arrested cells (Figure 19A). Moreover, I did not observe any Skp1 associated with Cdc6 in G1 cells (Figure 19B). However, when I examined Cdc6 turnover in a Dia2 mutant lacking both the F-box domain and the C-terminal LRR region (TPR mutant), I also observed Cdc6 stabilization (Figure 18B). These results suggest that Dia2 contributes to Cdc6 turnover in an F-box dependent manner but that this function may be independent of a traditional SCF complex.

I next asked whether Tom1 and Dia2 are required for Cdc6 ubiquitination. I immunoprecipitated HA-tagged Cdc6 from wildtype, *tom1Δ* and *dia2Δ* cells that had

been incubated with the proteasome inhibitor MG132. I probed the immunoprecipitates with anti-ubiquitin antibodies. Under these conditions, I observed modified forms of Cdc6 in proteasome-inhibited cells, but these forms were moderately reduced in both *tom1Δ* and *dia2Δ* cells, even in the presence of MG132 (Figure 18C). In addition, I developed an *in vitro* ubiquitination assay using GST-Cdc6 purified from baculovirus-infected insect cells. When GST-Cdc6 was incubated with fractionated yeast extracts, E1, E2, ubiquitin and an ATP regeneration system, I observed Cdc6 ubiquitin conjugates (Figure 18D, lanes 1-4). As a negative control, I performed the same assay using fractionated yeast extracts from the *cdc4-1* strain and observed a significant decrease in ubiquitination of Cdc6 (Figure 18D, lanes 5 & 6). I repeated these assays using extracts from *tom1Δ* and *dia2Δ* strains and also observed decreased ubiquitination with these extracts (Figure 18D, lanes 7-14). The loss of ubiquitinated Cdc6 appeared more complete in *tom1Δ* extracts than in *dia2Δ* extracts. Together, these results indicate that Cdc6 ubiquitination and protein stability are dependent on both Tom1 and Dia2.

Tom1 and Dia2 still recognize a Cdc6 N-terminal mutant

Deletion of an N-terminal region in Cdc6 has been shown to lead to a stabilized protein (20). The region encompassing amino acids 2-47 contains 4 CDK consensus sites that are important for SCF^{Cdc4}-mediated degradation of Cdc6 at the G1 to S phase transition. However, this N-terminal truncation mutant of Cdc6 (Cdc6ΔN) is also stabilized in G1 cells, a time when Cdc4 does not control Cdc6 proteolysis (20, 21). Thus, I sought to determine whether the Tom1 and Dia2-dependent pathway was

responsible for stabilization of this mutant in G1. I generated strains that endogenously expressed HA-tagged Cdc6ΔN in wildtype, *tom1Δ* and *dia2Δ* backgrounds and performed protein stability assays. As previously reported, Cdc6ΔN is partially stabilized in G1-arrested cells (20). Surprisingly, Cdc6ΔN stability is increased in *tom1Δ* and *dia2Δ* cells, indicating that Tom1 and Dia2 likely interact with a different region of the Cdc6 protein (Figure 20A). Similar results are observed when the stability assay is performed in cells arrested in early S phase (Figure 20B). To test whether Tom1 and Dia2 associate with a Cdc6 protein lacking the N-terminus, I co-incubated GST-tagged Cdc6ΔN, Flag-tagged Tom1 Hect domain and Myc-tagged Dia2 expressed from baculovirus-infected insect cells and performed immunoprecipitation assays. When either the Tom1 Hect domain or Dia2 was immunoprecipitated, Cdc6ΔN co-purified (Figure 20C), indicating that these proteins are able to form a complex. I conclude that Dia2 and Tom1 recognize a domain in Cdc6 downstream of amino acid 47.

Cdc6 remains associated with chromatin in ubiquitin ligase mutants

Cdc6 associates with chromatin in late M and early G1 to facilitate origin licensing and pre-RC formation (14, 18, 54). The degradation of Cdc6 as cells finish G1 and enter S phase is thought to contribute to preventing origins from firing more than once per cell cycle (37, 68). Cdc6 mutants that exhibit impaired degradation have been linked to inappropriate re-loading of Cdc6 on chromatin during G2/M and even re-replication under specific conditions (19, 37, 68). I examined the chromatin association of Cdc6 during S and G2/M in *tom1Δ* and *dia2Δ* cells. I used wildtype cells as a negative control

and the *cdc4-1 sic1Δ* strain as a positive control. Cells were arrested in G1 with alpha factor and then released into media containing nocodazole to arrest in M phase. Samples were collected at 0, 45, and 90 minutes after release from G1 for chromatin fractionation. The abundance of Cdc6 is significantly increased in the whole cell extracts from *tom1Δ*, *dia2Δ* and *cdc4-1 sic1Δ* cells relative to wildtype, consistent with impaired degradation in these strains (Figure 21A). Wildtype cells exhibited Cdc6 chromatin association at time 0 that subsequently dropped and stayed low throughout the time course. In the *cdc4-1 sic1Δ* positive control, Cdc6 chromatin association was somewhat reduced relative to wildtype cells at time 0 but showed considerable chromatin association throughout the time course. The chromatin association of Cdc6 in the *dia2Δ* and *tom1Δ* strains was higher at time 0 than wildtype and remained higher at 45 minutes for both strains, with association decreasing in *tom1Δ* cells at 90 minutes but remaining higher in *dia2Δ* cells at 90 minutes. The *dia2Δ* and *tom1Δ* strains did not achieve a complete G1 arrest, which may have contributed to greater Cdc6 chromatin association early in the time course, although cell cycle profiles later in the time course were comparable to wildtype. Overall, these results suggest that a fraction of Cdc6 remains associated with chromatin from late G1 through S phase and into G2/M in *dia2Δ* and *tom1Δ* cells as ubiquitination of Cdc6 is impaired.

To examine whether the aberrant Cdc6 chromatin association led to increased association of the MCM2-7 complex with replication origins, I used chromatin immunoprecipitation. Wildtype, *tom1Δ* and *dia2Δ* cells expressing HA-tagged Mcm4 were arrested in G1 and then released into nocodazole. Mcm4 chromatin association at

two early firing origins (*ARS1* and *ARS305*) and one non-origin region (*ACF2*) was assayed at 30-minute intervals (Figure 21B). All strains exhibited only negligible Mcm4-binding at the non-origin region *ACF2* throughout the time course. For both origins, the association of Mcm4 dropped to low levels at the 60 and 90-minute timepoints in wildtype cells. By contrast, Mcm4 association at *ARS1* and *ARS305* remained higher than wildtype in *tom1Δ* cells throughout the experiment and was especially pronounced at the 60 and 90-minute timepoints. In *dia2Δ* cells, Mcm4 was strongly associated with *ARS1* during the entire time course, but the effect at *ARS305* was less obvious. Mcm4 association with *ARS305* was reduced in *dia2Δ* cells relative to wildtype at the 30-minute timepoint, but remained at this level at the 60 and 90-minute timepoints as the association in wildtype cells dropped. Overall, the trend suggests that increased Cdc6 abundance and chromatin association in both the *tom1Δ* and *dia2Δ* strains may lead to increased association of Mcm proteins at origins.

Failure to clear Cdc6 from chromatin has the potential to lead to firing origins more than once per cell cycle. In budding yeast, there are three key pathways that prevent re-replication: destruction of Cdc6, nuclear export of the Mcm2-7 complex, and inactivation of ORC by phosphorylation (3, 6, 68). When all three of these pathways are compromised, re-replication can be observed in a single cell cycle (68). To investigate whether the degradation of Cdc6 dependent on Tom1 and Dia2 may contribute to re-replication control, I generated *dia2Δ*, *tom1Δ*, *cdc4-1* mutants in a strain background sensitized to re-replication, *orc2-6A orc6-4A mcm7-2NLS* (hereafter referred to as *orc* mcm**) (68). I used the *cdc6ΔN* allele as a positive control. Cells were arrested with 2C

DNA content using nocodazole and then shifted to 37°C, as *cdc4-1* and *tom1Δ* are sensitive to high temperature. The *dia2Δ* strain was tested at both 25°C and 37°C, as this strain is sensitive to low temperatures, but no discernible differences were observed. I used flow cytometry to measure DNA content in each strain prior to nocodazole arrest (asy), after nocodazole arrest (time 0) and 1, 2 and 3 hours after arrest at the elevated temperature. The percentage of cells above 2C DNA content in the *orc* mcm** control strain remained relatively constant throughout the experiment. By contrast, a large fraction of the *cdc6ΔN orc* mcm** population shifted above 2C DNA content at the 1, 2 and 3 h timepoints, suggesting increased DNA levels (Figure 22). Strikingly, the *tom1Δ orc* mcm**and *cdc4-1 orc* mcm**mutants also had large populations above 2C DNA content, whereas the *dia2Δ orc* mcm** mutant resembled the negative control *orc*mcm** strain. To determine whether the observed increase in DNA content was the result of nuclear DNA replication and not mitochondrial DNA replication, I generated rho^0 versions of all strains and repeated the re-replication assays (76). Even in the absence of mitochondrial DNA, I observed a significant increase in the population of cells exhibiting greater than 2C DNA content in the *cdc4-1*, *tom1Δ* and *cdc6ΔN* strains (data not shown). I note that all of the strains, with the exception of *cdc4-1 orc* mcm**, did not achieve a complete nocodazole arrest at the start of the experiment, suggesting that some cells were in G1 or S-phase at the time of the shift to 37°C. Increased Cdc6 protein levels in these stages could conceivably lead to increased loading of Mcm complexes that contribute to DNA over-replication. However, the *orc* mcm** control strain did not exhibit significant increases in >2C DNA content despite an incomplete nocodazole arrest.

Discussion

Altogether these data suggest a model in which the Hect-domain E3 ligase Tom1 and the F-box protein Dia2 cooperate to target Cdc6 for ubiquitin-mediated destruction during G1 and the G1/S transition. The activity of Tom1 and Dia2 is distinct from SCF^{Cdc4} during the G1/S transition. Failure to target Cdc6 for destruction via Tom1 leads to accumulation of chromatin-bound Cdc6 and Mcm4 during S and G2/M. These pathways may contribute to the control of DNA replication as increased nuclear DNA was observed when regulation of ORC and the MCM complex are also compromised.

Based on the genetic data, the relationship between Dia2 and Tom1 is complex and is not fully explained by the suggestion that they function in the same pathway. One explanation that accounts for all observed phenotypes is that Dia2 and Tom1 cooperate to target Cdc6 and that the Cdc4 pathway inhibits the activity of Dia2/Tom1. In this scenario, Dia2 and Tom1 might function in the same pathway, although they could not be strictly dependent on each other because defects in Cdc6 turnover are observed in the single mutants. Alternatively, Dia2 and Tom1 might function separately but promote each other's activity. For example, Dia2 may enhance the function of Tom1, as the Cdc6 degradation and ubiquitin phenotypes are more severe in the *tom1Δ* mutant than *dia2Δ.* Alternatively, it is possible that Tom1 and Dia2 form a larger complex, which is required for efficient association with Cdc6. It is not clear how Cdc4 inhibition of Dia2 or Tom1 might be manifested. It is apparent that Dia2 functions outside the context of an SCF complex in this pathway, as Skp1 is not associated with Cdc6 during G1or Cdc6 is still turned over in *scf* mutants in G1, similar to previous studies (20, 21). A non-SCF role for

Dia2 has not been previously described, but other F-box proteins have been shown to function outside of traditional SCF complexes (24, 29, 91, 99).

It is surprising that three E3 ubiquitin ligases are required to target a single protein for degradation at the same point in the cell cycle. However, previous work has shown that the half-life of Cdc6 is significantly longer in G1 and G2/M than it is at the G1 to S transition (20, 21). It may be that the convergence of three ubiquitin ligase activities at this point in the cell cycle is responsible for the accelerated turnover rate. This leads to the obvious question of how specificity is achieved. My results suggest that Tom1 and Dia2 can bind to a region of Cdc6 that also contains one of the Cdc4-interacting domains, but it seems unlikely that the domain recognized by Cdc4 will precisely match the region recognized by Tom1 and Dia2. Cdc4 has been shown to recognize particular Cdk phosphorylation sites on Cdc6 (21), but it is not clear whether Cdk phosphorylation is important to Cdc6 protein turnover mediated by Tom1 and Dia2. Indeed, it seems unlikely that Cdk phosphorylation will be critical in this pathway, as the degradation also occurs during G1 when Cdk activity levels are low. I look forward to future studies that address the nature of specificity for these ubiquitin ligases.

My results support the idea that the Tom1 and Dia2 might also account for a fraction of the G1-specific degradation of Cdc6. The observation that they act separately from the Cdc4 pathway is consistent with Mode 1 degradation, but investigation of whether Cdk activity affects the activity of Tom1 or Dia2 will be necessary to resolve this question. One possibility is that Cdc6 is targeted for degradation after DNA damage, as Tom1 has been shown to have a role in such a pathway (32) and *dia2Δ* cells exhibit endogenous

DNA damage (5, 47, 71). However, I think this is unlikely during G1 phase, as *dia2Δ* cells only accumulate DNA damage foci during S and G2/M (5, 47). Alternatively, it is possible that Tom1 and Dia2 might represent a novel mode of Cdc6 degradation. Indeed, the observation that Cdc6ΔN stability is enhanced in G1 in the absence of Tom1 and Dia2 suggests that there may be still another degradation pathway for Cdc6 in G1.

Failure to clear Cdc6 from origins as cells progress into S phase is likely to have deleterious consequences. *In vitro* studies have shown that the extent of Mcm2-7 loading onto origins is linked to the amount of Cdc6 present (79). I also observe increased Mcm4 association with two early firing origins in mutants that partially stabilize Cdc6. In addition, inappropriate re-loading of Cdc6 onto origins in G2/M correlates with re-replication when the DNA replication initiation factor Dpb11 is also overexpressed (37), suggesting that origins may be firing more than once per cell cycle. Recent *in vitro* studies suggest that Cdc6 dissociates from origins in a late pre-RC assembly step that requires ATP hydrolysis (94). My *in vivo* studies cannot distinguish between the possibility that Cdc6 is rapidly dissociating and re-associating with chromatin in the ubiquitin ligase mutants versus a constant amount of Cdc6 remaining associated with chromatin during S and G2. The Cdc4 and Tom1/Dia2 pathways may provide redundancy to ensure that Cdc6 protein levels are reduced sufficiently to prevent replication defects. Consistent with this, the *cdc4-1* and *tom1Δ* mutants exhibit increased nuclear DNA synthesis in a strain background sensitized to re-replication. It is not clear why the *dia2Δ* mutant does not exhibit any significant increase in the percentage of cells with greater than 2C DNA content in these assays, but I note that the *dia2Δ* mutant

exhibits much weaker defects in Cdc6 ubiquitination, degradation and chromatin association than either *tom1Δ* or *cdc4-1*. Thus, there may be a threshold level of Cdc6 chromatin association required to observe increased DNA synthesis. Alternatively, *dia2Δ* mutants may exhibit only limited DNA synthesis at a subset of origins, which is difficult to detect by measuring bulk DNA content by flow cytometry.

Future directions

I have identified two E3 ubiquitin ligase components required for Cdc6 degradation during G1 and at the G1 to S phase transition, the Hect E3 ligase Tom1 and the F-box protein Dia2. The observation that Cdc6 is stabilized in *dia2 Δ F-box* mutant but not in *scf* mutants in G1 suggests that the F-box protein Dia2 might form a non-traditional SCF complex via the F-box domain. Consistent with this idea, I also observed that Dia2 does not bind to Skp1 in G1. Budding yeast has three Cullins (Cdc53 (Cul1), Rtt101 (Cul8), and Cul3). Of these Cullin proteins, both Rtt101 and Cul3 do not require Skp1 as an F-box protein to form a functional SCF complex (59, 80). Interestingly, *rtt101Δ* mutant has similar phenotypes to *dia2Δ* mutant such as the sensitivity of DNA damaging agents or replication stress, suggesting that Rtt101 might be a promising candidate. To test the possibility that Dia2 forms an SCF complex with Rtt101, a co-immunoprecipitation assay would be required to determine whether Rtt101 interacts with Dia2 during G1. In addition, Cdc6 stability also needs to be examined in *rtt101Δ* mutant in G1.

I showed that both Tom1 and Dia2 regulate Cdc6 turnover at the G1 to S phase transition independently of the SCF^{Cdc4} complex. When hydroxyurea is used to arrest

cells in early S phase, it also activates the S-phase checkpoint since hydroxyurea treatment lowers dNTP pools, which induces replication stress. To rule out the possibility that Tom1 and Dia2 target Cdc6 for degradation in response to activation of the S-phase checkpoint, I examined Cdc6 abundance in *tom1Δ* and *dia2Δ* mutants when cells were released from a G1 arrest into medium. These results show that Cdc6 abundance is increased in *tom1Δ* and *dia2Δ* mutants as cells enter the S phase from the G1 phase of the cell cycle. To further confirm that Tom1- and Dia2-mediated Cdc6 degradation is distinct from the SCF^{Cdc4} pathway at the G1 to S phase transition, Cdc6 abundance also needs to be observed in *cdc4-1tom1Δ* and *cdc4-1dia2Δ* mutants when cells are released from a G1-arrest to rich medium.

My data suggest that both Tom1 and Dia2 bind a domain in Cdc6 downstream of amino acid 47. This domain contains two Cdk-phosphorylation sites that are recognized by the SCF^{Cdc4} complex. In order to map the binding sites of Tom1 and Dia2 on Cdc6, a series of Cdc6 truncation mutants need to be generated and tested to identify the minimum domain required for Tom1 and Dia2 binding using in vitro binding assays.

An important question that needs to be answered in the future is to determine the specificity of three E3 ubiquitin ligases for Cdc6 degradation. I do not know whether Tom1 and Dia2 require Cdk-dependent phosphorylation for Cdc6 degradation or not. However, it is unlikely that Cdk phosphorylation is required for this pathway as Tom1 and Dia2 also control Cdc6 degradation during G1 when Cdk activity is low. Nevertheless, the requirement of Cdk phosphorylation for Tom1- and Dia2- mediated pathway needs to be determined by examining the stability of *cdc6* phosphorylation

mutants carrying various Cdk consensus site mutations in *tom1Δ* and *dia2Δ* strains. Moreover, in vitro binding assays would also be necessary to determine whether Tom1 and Dia2 still bind to Cdc6 phosphorylation mutants.

Finally, I have found that Tom-mediated Cdc6 degradation pathway is important to control re-replication in a strain background sensitized to re-replication. To support this result, 2-D gel and microarray comparative genomic hybridization (CGH) analyses would be required to confirm the re-replication and determine what percentage of early origins are re-fired after the S phase within a single cell cycle in *tom1Δ* mutant sensitized to re-replication.

Figure 11

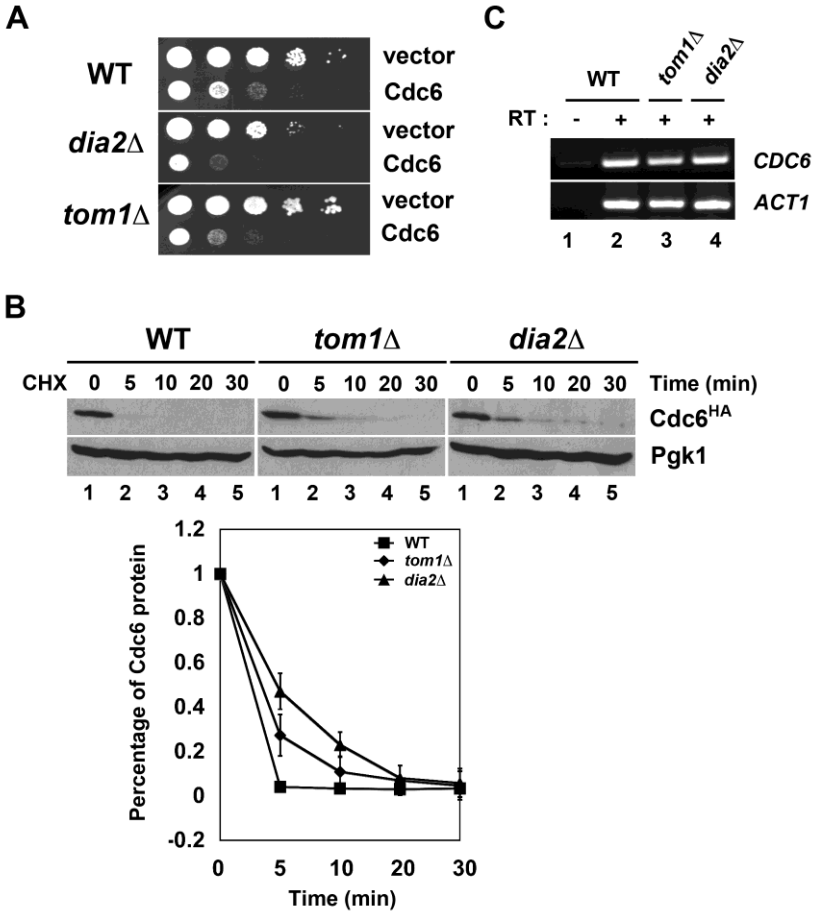
A
WT
vector
Cdc6
dia2Δ
vector
Cdc6
tom1Δ
vector
Cdc6
C
WT
tom1Δ
dia2Δ
RT : - + + +
CDC6
ACT1
1 2 3 4
B
WT
tom1Δ
dia2Δ
CHX 0 5 10 20 30 0 5 10 20 30 0 5 10 20 30
Time (min)
Cdc6HA
Pgk1
1 2 3 4 5 1 2 3 4 5 1 2 3 4 5
Percentage of Cdc6 protein
1.2
1
0.8
0.6
0.4
0.2
0
-0.2
WT
tom1Δ
dia2Δ
0 5 10 20 30
Time (min)

Figure 11. Tom1 and Dia2 control Cdc6 proteolysis. (A) Over-expression of Cdc6 results in an exacerbated growth defect in both *dia2Δ* and *tom1Δ* strains. The 10-fold serial dilutions of wild-type, *dia2Δ*, and *tom1Δ* cells carrying empty vector or *CDC6* under the control of *GAL1,10* promoter were spotted onto minimal plates with 2% galactose. Plates were incubated at room temperature for 2-3 days. (B) Cdc6 is partially stabilized in *tom1Δ* and *dia2Δ* mutants. Wildtype, *tom1Δ*, and *dia2Δ* strains were grown to mid-log phase at 30°C. After cycloheximide treatment (100 μg/ml), samples were taken at the indicated times and immunoblotted with anti-HA and -Pgk1 antibodies. Pgk1 was used as a loading control. (C) Cdc6 mRNA level is not changed in both *tom1Δ* and *dia2Δ* mutants. RT-PCR assay was conducted to examine the level of Cdc6 transcript in wildtype, *dia2Δ,* and *tom1Δ* strains. *ACT1* was used as a loading control. RT, reverse transcriptase.

Figure 12

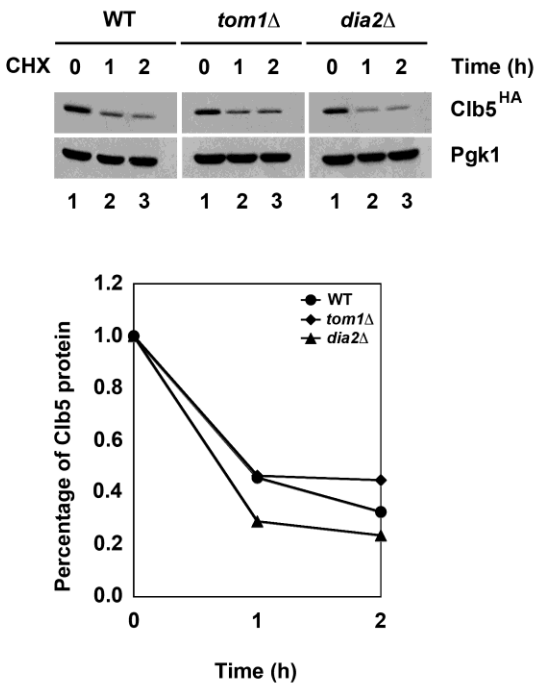
WT
tom1Δ
dia2Δ
CHX 0 1 2 0 1 2 0 1 2 Time (h)
Clb5HA
Pgk1
1 2 3 1 2 3 1 2 3
Percentage of Clb5 protein
1.2
1.0
0.8
0.6
0.4
0.2
0.0
0 1 2
Time (h)
WT
tom1Δ
dia2Δ

Figure 12. Clb5 stability is not affected in *tom1Δ* and *dia2Δ* mutants. Wildtype, *tom1Δ*, and *dia2Δ* cells were grown to mid-log phase in minimal medium supplemented with 2% raffinose. Clb5 transcription was induced by addition of galactose for 1h and repressed by adding glucose in the medium. 100 μg/ml cycloheximide was also added to block protein translation. Samples were taken at the indicated times. The turnover of Clb5 protein was analyzed by performing stability assays.

Figure 13

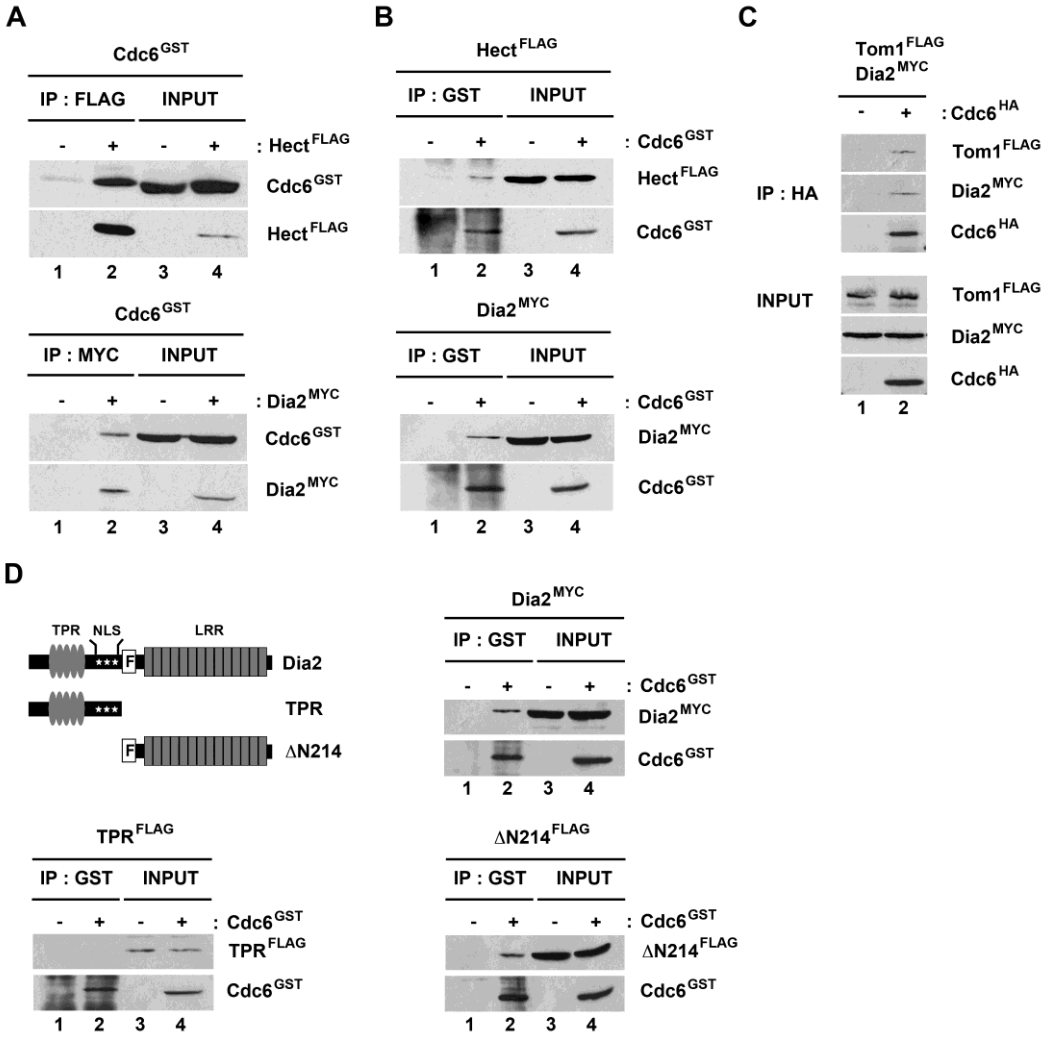
A
Cdc6GST
IP : FLAG
INPUT
- + - +
: HectFLAG
Cdc6GST
HectFLAG
1 2 3 4
Cdc6GST
IP : MYC
INPUT
- + - +
: Dia2MYC
Cdc6GST
Dia2MYC
1 2 3 4
B
HectFLAG
IP : GST
INPUT
- + - +
: Cdc6GST
HectFLAG
Cdc6GST
1 2 3 4
Dia2MYC
IP : GST
INPUT
- + - +
: Cdc6GST
Dia2MYC
Cdc6GST
1 2 3 4
C
Tom1FLAG
Dia2MYC
- +
: Cdc6HA
IP : HA
Tom1FLAG
Dia2MYC
Cdc6HA
INPUT
Tom1FLAG
Dia2MYC
Cdc6HA
1 2
D
TPR NLS LRR
F
Dia2
TPR
ΔN214
TPRFLAG
IP : GST
INPUT
- + - +
: Cdc6GST
TPRFLAG
Cdc6GST
1 2 3 4
Dia2MYC
IP : GST
INPUT
- + - +
: Cdc6GST
Dia2MYC
Cdc6GST
1 2 3 4
ΔN214FLAG
IP : GST
INPUT
- + - +
: Cdc6GST
ΔN214FLAG
Cdc6GST
1 2 3 4

Figure 13. Tom1 and Dia2 interact with Cdc6. (A and B) Tom1 Hect domain and Dia2 interact with Cdc6. Hi5 insect cells were co-infected with GST-Cdc6 and FLAG-Hect or Myc-Dia2 baculoviruses. FLAG-Hect, Myc-Dia2 or GST-Cdc6 protein was immunoprecipiated with anti-Flag, -Myc or -GST antibodies and analyzed by immunoblotting. (C) Endogenously expressed Tom1 and Dia2 co-precipitate with Cdc6. Total cell lysates of $Tom1^{FLAG}$ $Dia2^{MYC}$ or $Tom1^{FLAG}$ $Dia2^{MYC}$ $Cdc6^{HA}$ were immunoprecipitated with affinity matrix anti-HA.11and immunoblotted with anti- Flag, -Myc, and - HA antibodies. (D) The leucine rich repeat domain of Dia2 is required for its interaction with Cdc6. Total cell lysates from GST-Cdc6 and MYC-Dia2, FLAG-TPR, or FLAG-ΔN214 baculovirus-infected Hi5 insect cells were immunoprecipitated with anti-GST antibodies and analyzed by immunoblotting with anti-GST, -Myc, or -Flag antibodies.

Figure 14

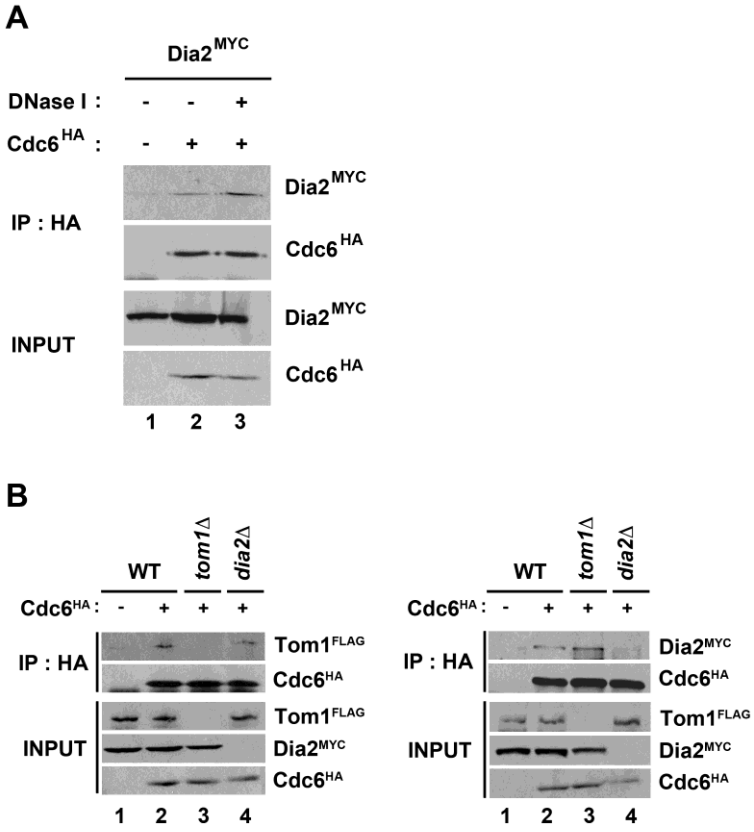
A
Dia2MYC
DNase I : - - +
Cdc6HA : - + +
IP : HA
Dia2MYC
Cdc6HA
INPUT
Dia2MYC
Cdc6HA
1 2 3
B
WT
tom1Δ
dia2Δ
Cdc6HA : - + + +
IP : HA
Tom1FLAG
Cdc6HA
INPUT
Tom1FLAG
Dia2MYC
Cdc6HA
1 2 3 4
WT
tom1Δ
dia2Δ
Cdc6HA : - + + +
IP : HA
Dia2MYC
Cdc6HA
INPUT
Tom1FLAG
Dia2MYC
Cdc6HA
1 2 3 4

Figure 14. Tom1 and Dia2 bind independently to Cdc6. (A) Dia2 binding to Cdc6 is resistant to DNase I treatment. Cell lysate from the Dia2^{MYC} Cdc6^{HA} strain was treated with 20units of DNase I (Promega) for 45 min on ice. Cdc6 was immunoprecipitated with anti-HA antibodies and immunoblotted with anti-HA and -Myc antibodies. (B) Tom1 and Dia2 do not require each other to interact with Cdc6 in S phase. The indicated strains were arrested with 200 mM hydroxyurea for 3 h. Cell lysates were used for immunoprecipitation assays with anti-HA antibodies and analyzed by immunoblotting with anti-HA, -Myc, and –Flag antibodies.

Figure 15

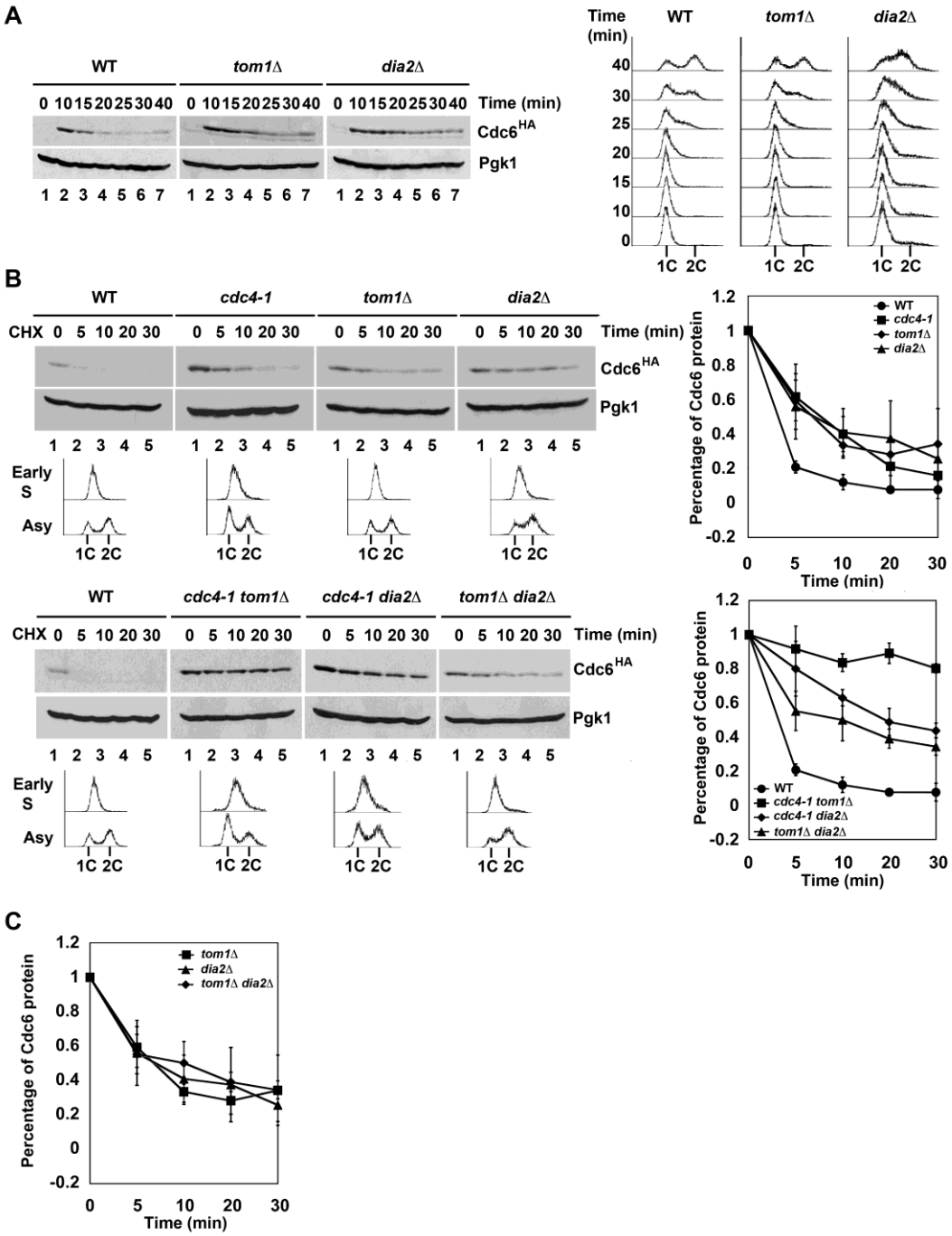
A
WT
tom1Δ
dia2Δ
0 10 15 20 25 30 40
Time (min)
Cdc6HA
Pgk1
1 2 3 4 5 6 7
Time (min)
WT
tom1Δ
dia2Δ
40
30
25
20
15
10
0
1C 2C
B
WT
cdc4-1
tom1Δ
dia2Δ
CHX 0 5 10 20 30
Time (min)
Cdc6HA
Pgk1
1 2 3 4 5
Early S
Asy
1C 2C
Percentage of Cdc6 protein
Time (min)
WT
cdc4-1
tom1Δ
dia2Δ
WT
cdc4-1 tom1Δ
cdc4-1 dia2Δ
tom1Δ dia2Δ
C
tom1Δ
dia2Δ
tom1Δ dia2Δ
Percentage of Cdc6 protein
Time (min)

Figure 15. Tom1 and Dia2 control Cdc6 turnover at the G1/S transition. (A) Cdc6 abundance is increased in *tom1Δ* and *dia2Δ* mutants at the G1/S transition. Wildtype, *tom1Δ*, and *dia2Δ* strains were arrested with αF for 3 h and released into rich medium containing 15 μg/ml nocodazole. Samples were collected at the indicated times and immunoblotted with anti-HA antibodies. Pgk1 was used as a loading control. Flow cytometry analysis was performed to monitor the release from αF arrest. (B) Cdc6 is stabilized in both *tom1Δ* and *dia2Δ* mutants at the G1/S transition and Cdc6 stabilization is significantly increased in *cdc4-1 tom1Δ* and *cdc4-1 dia2Δ* mutants. The indicated strains were arrested with αF for 3 h and released into rich medium containing 200 mM hydroxyurea for 90 min. Cultures were shifted to 37 °C for 30 min and treated with cycloheximide (100 μg/ml). Samples were taken at the indicated times and analyzed by immunoblotting with anti-HA antibodies. Pgk1 was used as a loading control. Three independent experiments were used to quantify the rate of Cdc6 turnover. Error bars indicate standard deviations. (C) Cdc6 turnover rate in *tom1Δ dia2Δ* mutant is indistinguishable from the *tom1Δ* or *dia2Δ* mutant. The results of quantification of the *tom1Δ dia2Δ* mutant and *tom1Δ* and *dia2Δ* mutants are shown in the graph.

Figure 16

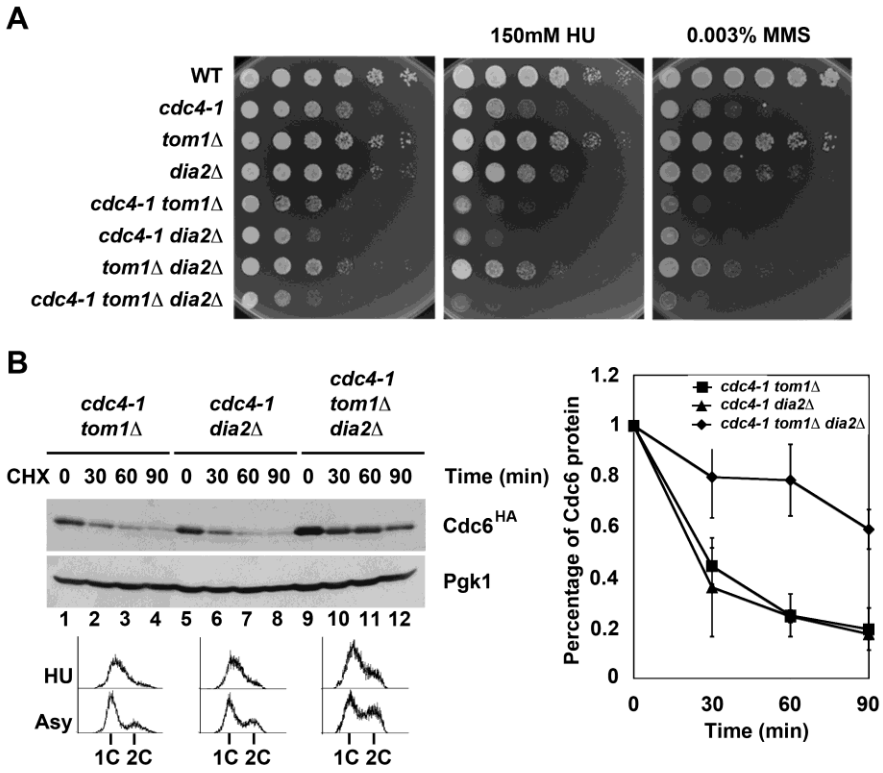
A
150mM HU
0.003% MMS
WT
cdc4-1
tom1Δ
dia2Δ
cdc4-1 tom1Δ
cdc4-1 dia2Δ
tom1Δ dia2Δ
cdc4-1 tom1Δ dia2Δ
B
cdc4-1 tom1Δ
cdc4-1 dia2Δ
cdc4-1 tom1Δ dia2Δ
CHX 0 30 60 90 0 30 60 90 0 30 60 90
Time (min)
Cdc6HA
Pgk1
1 2 3 4 5 6 7 8 9 10 11 12
HU
Asy
1C 2C
1C 2C
1C 2C
Percentage of Cdc6 protein
Time (min)
0
0.2
0.4
0.6
0.8
1
1.2
0
30
60
90

Figure 16. Cdc4, Tom1 and Dia2 all contribute to Cdc6 protein turnover. (A) Hydroxyurea- and MMS-sensitivity is exacerbated in *cdc4-1 tom1Δ*, *cdc4-1 dia2Δ*, and *cdc4-1 tom1Δ dia2Δ* mutants. Five-fold serially diluted cultures of the indicated strains were spotted onto rich medium containing 150 mM hydroxyurea or 0.003% Methyl methanesulfonate (MMS). (B) The *cdc4-1 tom1Δ dia2Δ* triple mutant exhibits highly stabilized Cdc6. The indicated mutants were arrested with 200 mM hydroxyurea for 3h and shifted to 37 ˚C for 30 min. Samples were collected at the indicated times and prepared as in Figure 15. Error bars indicate standard deviations.

Figure 17

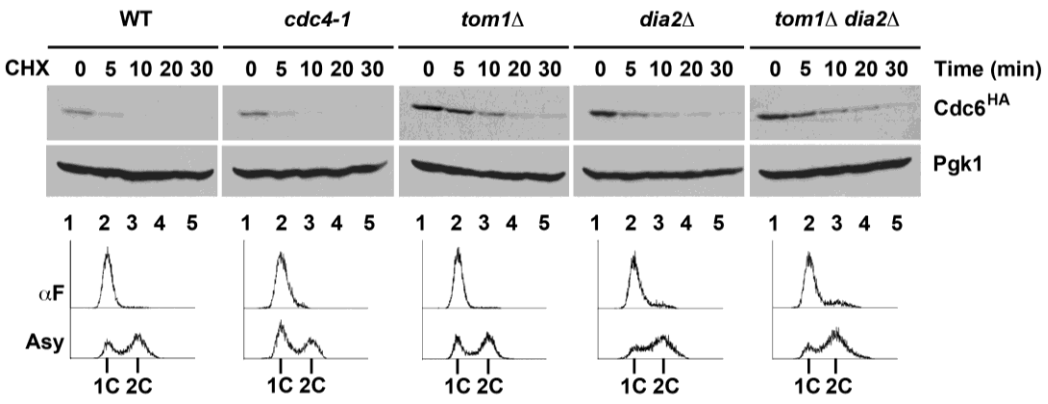
WT
cdc4-1
tom1Δ
dia2Δ
tom1Δ dia2Δ
CHX 0 5 10 20 30
Time (min)
Cdc6HA
Pgk1
1 2 3 4 5
αF
Asy
1C 2C

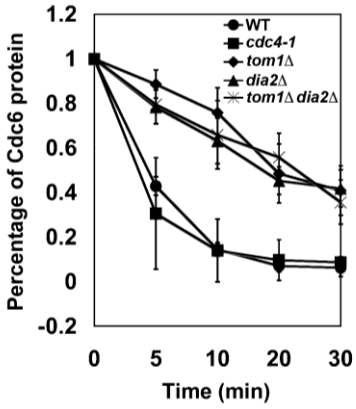
WT
cdc4-1
tom1Δ
dia2Δ
tom1Δ dia2Δ
Percentage of Cdc6 protein
1.2
1
0.8
0.6
0.4
0.2
0
-0.2
0 5 10 20 30
Time (min)

Figure 17. Tom1 and Dia2 control Cdc6 proteolysis in G1. Cdc6 is stabilized in both *tom1Δ* and *dia2Δ* mutants in G1. The indicated strains were arrested with αF for 3 h and shifted to 37°C for 30 min. Samples were prepared for stability assays as in Figure 15. Three independent experiments were used for quantification. Error bars indicate standard deviations.

Figure 18

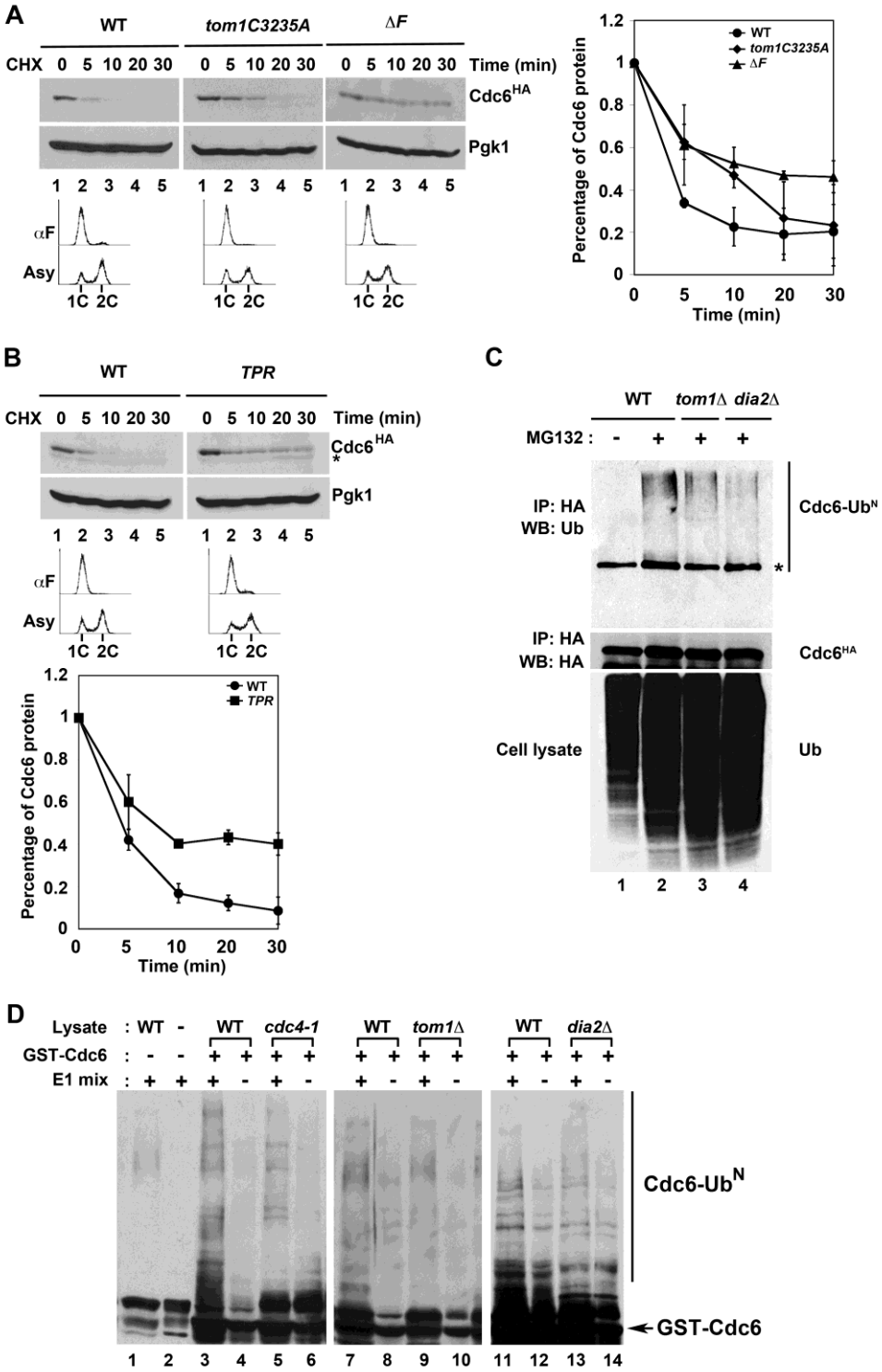
A
WT
tom1C3235A
ΔF
CHX 0 5 10 20 30 0 5 10 20 30 0 5 10 20 30 Time (min)
Cdc6HA
Pgk1
1 2 3 4 5 1 2 3 4 5 1 2 3 4 5
αF
Asy
1C 2C 1C 2C 1C 2C
Percentage of Cdc6 protein
Time (min)
B
WT
TPR
CHX 0 5 10 20 30 0 5 10 20 30 Time (min)
Cdc6HA
*
Pgk1
C
WT tom1Δ dia2Δ
MG132 : - + + +
IP: HA
WB: Ub
Cdc6-UbN
IP: HA
WB: HA
Cdc6HA
Cell lysate
Ub
1 2 3 4
D
Lysate : WT - WT cdc4-1 WT tom1Δ WT dia2Δ
GST-Cdc6 : - - + + + + + + + + + + + +
E1 mix : + + + - + - + - + - + - + -
Cdc6-UbN
GST-Cdc6
1 2 3 4 5 6 7 8 9 10 11 12 13 14

Figure 18. Tom1 and Dia2 target Cdc6 for ubiquitin-dependent degradation. (A) The catalytic activity of Tom1 Hect domain and the F-box domain of Dia2 are required for Cdc6 turnover. Wildtype, *tom1C3235A*, *dia2ΔF* strains arrested with αF were used in protein stability assays. Samples were collected at indicated times after cycloheximide addition. Pgk1 was used as a loading control. Three independent experiments were used for quantification. (B) The *TPR* mutant stabilizes Cdc6. Samples from wildtype and *TPR* strains were prepared as in (A). The asterisk indicates a non-specific band. Error bars indicate standard deviations. (C) Cdc6 ubiquitination is dependent on Tom1 and Dia2. Wildtype, *tom1Δ*, and *dia2Δ* strains were cultured to mid-log phase and treated with DMSO or 50 μM MG132 for 2h. Cdc6 protein was immunoprecipitated with anti-HA antibodies and visualized by immunoblot assays with anti-ubiquitin antibodies. The asterisk indicates a non-specific band. (D) In vitro ubiquitination of Cdc6. GST-Cdc6 protein expressed from baculovirus-infected insect cells was purified using glutathione-sepharose 4B beads. GST-Cdc6 protein was incubated with ubiquitin, E1, E2, ATP, an ATP regeneration system, and fractionated yeast extracts purified from wildtype, *cdc4-1*, *tom1Δ*, or *dia2Δ* strains at 30 °C for 45min. Samples were run on 6% SDS-PAGE and immunoblotted with anti-GST antibodies.

Figure 19

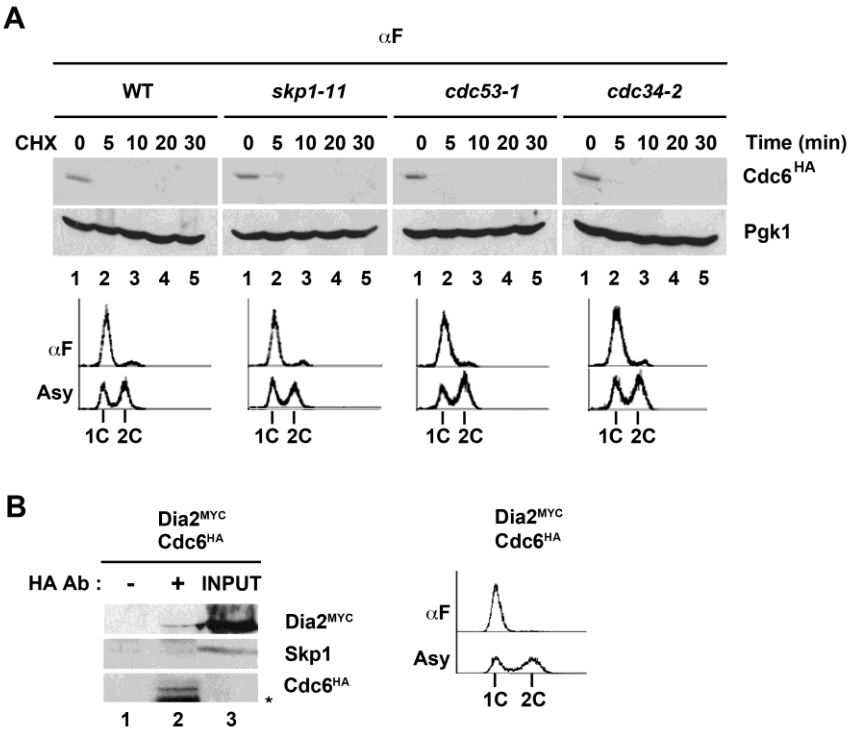
A
αF
WT
skp1-11
cdc53-1
cdc34-2
CHX 0 5 10 20 30 0 5 10 20 30 0 5 10 20 30 0 5 10 20 30
Time (min)
Cdc6HA
Pgk1
1 2 3 4 5 1 2 3 4 5 1 2 3 4 5 1 2 3 4 5
αF
Asy
1C 2C 1C 2C 1C 2C 1C 2C
B
Dia2MYC
Cdc6HA
HA Ab : - + INPUT
Dia2MYC
Skp1
Cdc6HA
*
1 2 3
Dia2MYC
Cdc6HA
αF
Asy
1C 2C

Figure 19. Cdc6 degradation in G1 is not dependent on SCF. (A) Cdc6 is not stabilized in *scf* mutants in G1 phase. Wildtype, *skp1-11*, *cdc53-1*, and *cdc34-2* cells were arrested with αF for 3h and stability assays were performed as in Figure 17. (B) Cdc6 does not bind to Skp1 in G1 phase. Strain DKY559 was arrested with αF for 3h and treated with 50μM MG132 for 2h. Cell lysates were immunoprecipitated with anti-HA antibodies and analyzed by immunoblotting with anti-HA, -Myc, -Skp1 antibodies. Cdc6 input was not detected in cell extract with a short exposure. Asterisk indicates the IgG heavy chain.

Figure 20

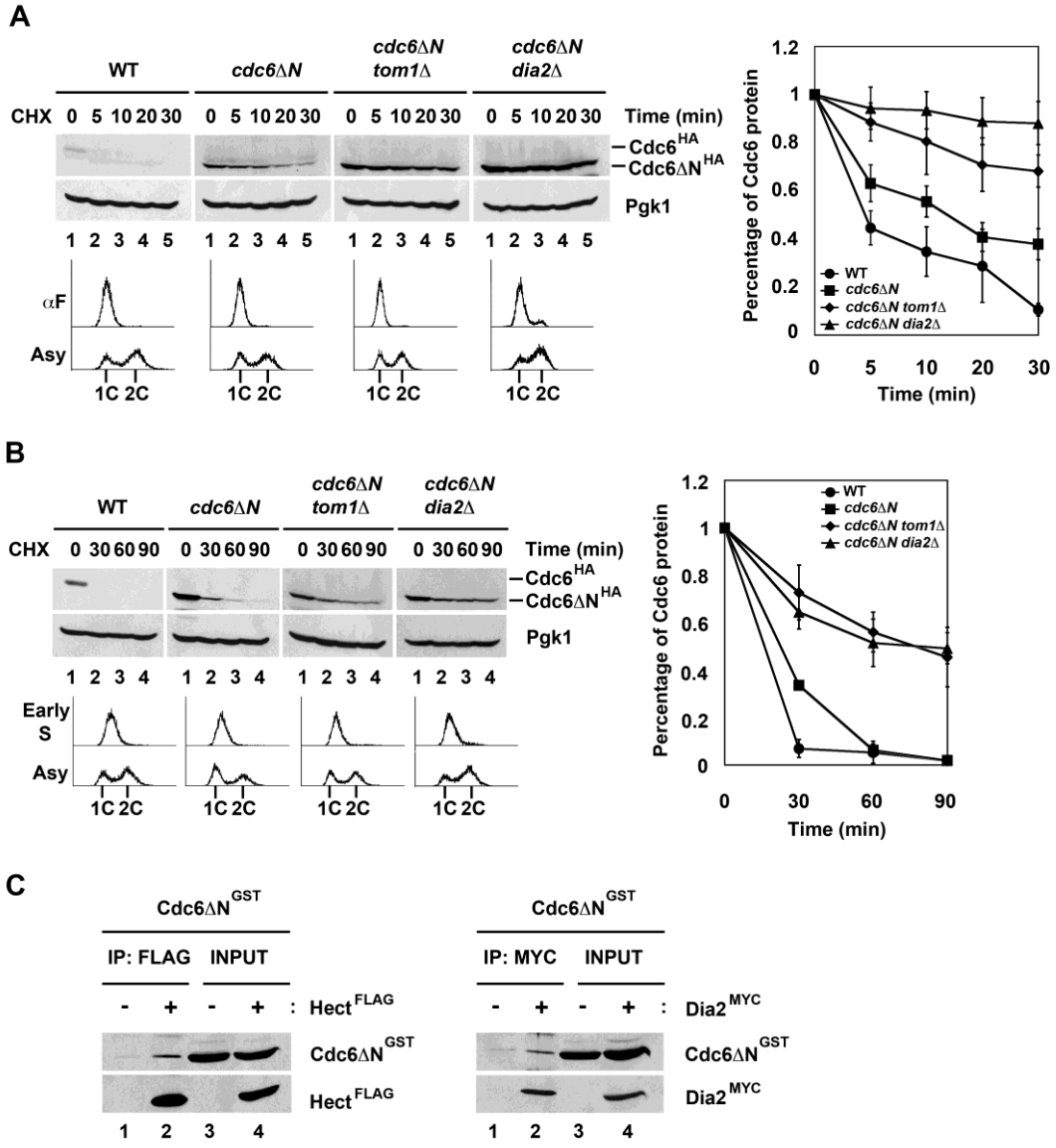
A
WT
cdc6ΔN
cdc6ΔN tom1Δ
cdc6ΔN dia2Δ
CHX 0 5 10 20 30 0 5 10 20 30 0 5 10 20 30 0 5 10 20 30 Time (min)
Cdc6HA
Cdc6ΔNHA
Pgk1
1 2 3 4 5 1 2 3 4 5 1 2 3 4 5 1 2 3 4 5
αF
Asy
1C 2C 1C 2C 1C 2C 1C 2C
Percentage of Cdc6 protein
1.2
1
0.8
0.6
0.4
0.2
0
WT
cdc6ΔN
cdc6ΔN tom1Δ
cdc6ΔN dia2Δ
0 5 10 20 30
Time (min)
B
WT
cdc6ΔN
cdc6ΔN tom1Δ
cdc6ΔN dia2Δ
CHX 0 30 60 90 0 30 60 90 0 30 60 90 0 30 60 90 Time (min)
Cdc6HA
Cdc6ΔNHA
Pgk1
1 2 3 4 1 2 3 4 1 2 3 4 1 2 3 4
Early S
Asy
1C 2C 1C 2C 1C 2C 1C 2C
Percentage of Cdc6 protein
1.2
1
0.8
0.6
0.4
0.2
0
WT
cdc6ΔN
cdc6ΔN tom1Δ
cdc6ΔN dia2Δ
0 30 60 90
Time (min)
C
Cdc6ΔNGST
IP: FLAG INPUT
- + - + : HectFLAG
Cdc6ΔNGST
HectFLAG
1 2 3 4
Cdc6ΔNGST
IP: MYC INPUT
- + - + : Dia2MYC
Cdc6ΔNGST
Dia2MYC
1 2 3 4

Figure 20. Tom1- or Dia2-mediated Cdc6 proteolysis does not require the N-terminal 47 amino acids of Cdc6. (A) Cdc6ΔN stabilization was increased in *tom1Δ* and *dia2Δ* mutants in G1. Wildtype, *cdc6ΔN*, *cdc6ΔN tom1Δ*, and *cdc6ΔN dia2Δ* strains arrested with αF were used for stability assays. Three independent experiments were used for quantification. (B) Cdc6ΔN was significantly stabilized in *tom1Δ* and *dia2Δ* mutants at G1/S. Wildtype, *cdc6ΔN*, *cdc6ΔN tom1Δ*, and *cdc6ΔN dia2Δ* strains were arrested in early S and stability assays were performed as shown in Figure 15B. The rate of full-length Cdc6 and Cdc6ΔN turnover was measured by quantifying three independent results. (C) Cdc6ΔN binds to Tom1 Hect domain and Dia2. Total lysates isolated from Hi5 insect cells infected with GST- Cdc6ΔN, FLAG-Hect, and Myc-Dia2 baculoviruses were incubated together as shown in the figure. FLAG-Hect or Myc-Dia2 was immunoprecipiated with anti-Flag, or -Myc antibodies and analyzed by immunoblotting.

Figure 21

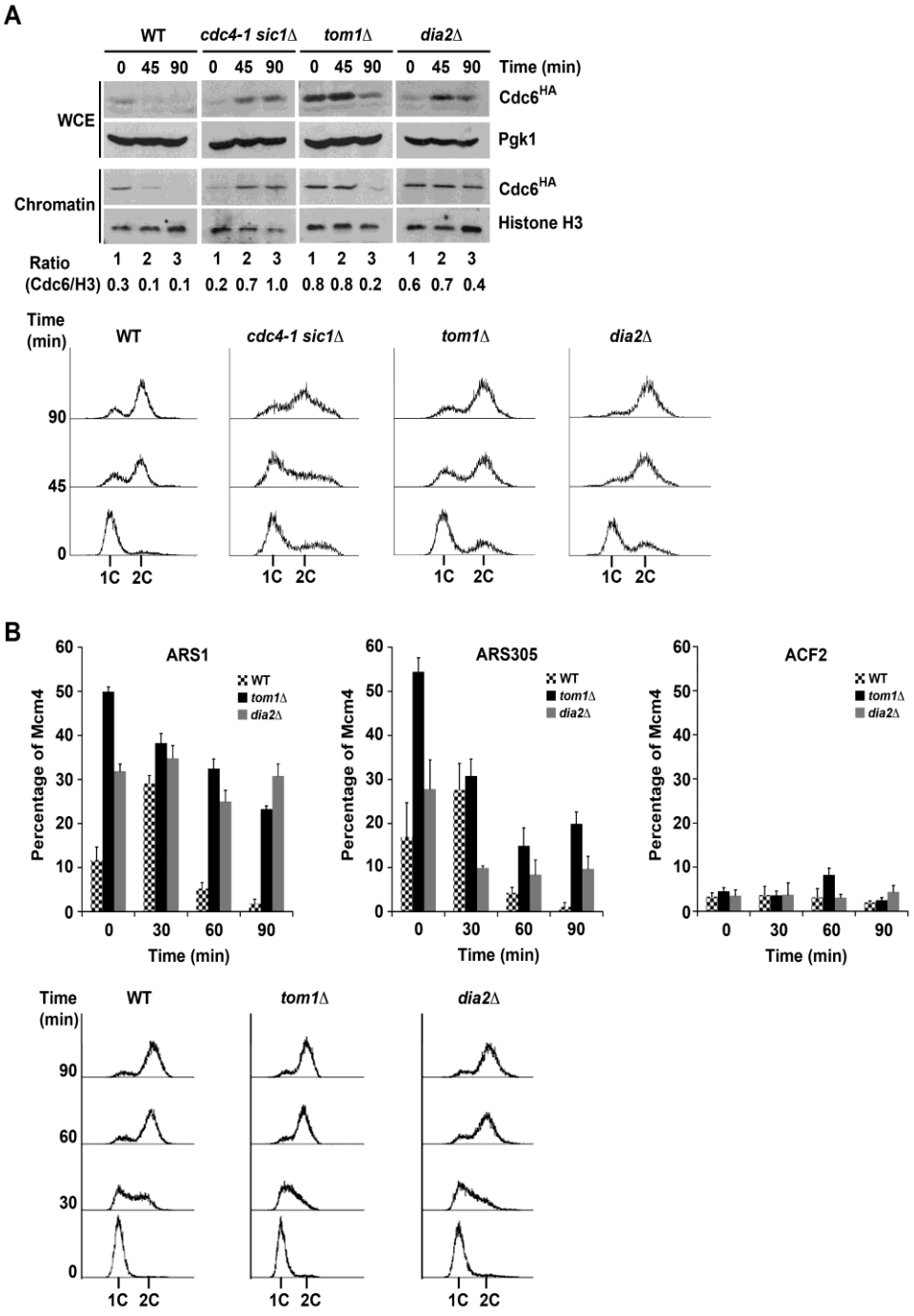
A
WT
cdc4-1 sic1Δ
tom1Δ
dia2Δ
0 45 90 0 45 90 0 45 90 0 45 90 Time (min)
WCE
Cdc6HA
Pgk1
Chromatin
Cdc6HA
Histone H3
Ratio 1 2 3 1 2 3 1 2 3 1 2 3
(Cdc6/H3) 0.3 0.1 0.1 0.2 0.7 1.0 0.8 0.8 0.2 0.6 0.7 0.4
Time (min)
WT
cdc4-1 sic1Δ
tom1Δ
dia2Δ
90
45
0
1C 2C
B
ARS1
ARS305
ACF2
WT
tom1Δ
dia2Δ
Percentage of Mcm4
Time (min)
0 30 60 90
Time (min)
WT
tom1Δ
dia2Δ
90
60
30
0
1C 2C

Figure 21. Failure to degrade chromatin-bound Cdc6 by a Tom1- and Dia2-dependent pathway enhances the association of Mcm4 with early origins. (A) Chromatin-bound Cdc6 is increased in *cdc4-1 sic1Δ, tom1Δ* and *dia2Δ* cells. The indicated strains were arrested with αF at 30°C for 2.5 h and shifted to 37°C for 30 min before release into rich medium containing 15μg/ml nocodazole at 37°C. Samples were taken at the indicated times and prepared for chromatin fractionation. Samples were analyzed by immunoblot assays with anti-HA, -Pgk1, and -Histone H3 antibodies. Flow cytometry was used to monitor cell cycle progression. WCE, whole cell extract. The ratio of chromatin-bound Cdc6 to Histone H3 was measured using Image J software. (B) Mcm4 origin association is increased in *tom1Δ* and *dia2Δ* cells. The indicated strains were arrested and released as in (A). Samples were taken at the indicated times and prepared for chIP assays with HA-tagged Mcm4. *ARS1* and *ARS305* are early firing origins. *ACF2* is non-origin control. Three replicates of each experiment were quantified using Image J. Error bars indicate standard deviations.

Figure 22

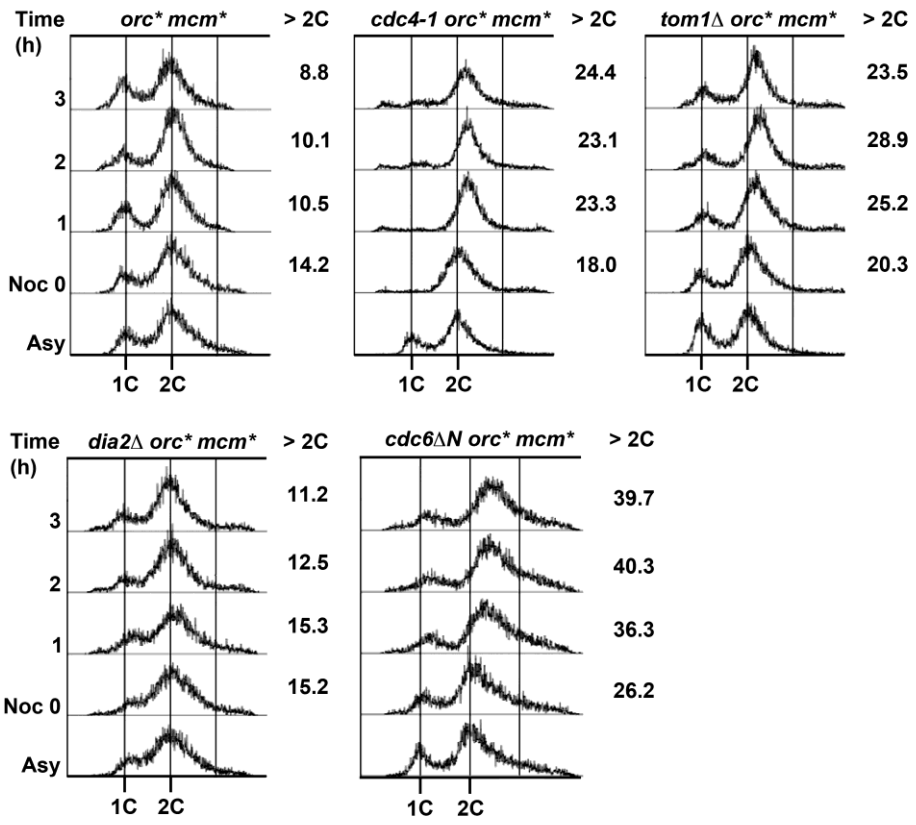
Time (h)
orc* mcm*
> 2C
cdc4-1 orc* mcm*
> 2C
tom1Δ orc* mcm*
> 2C
3
2
1
Noc 0
Asy
8.8
10.1
10.5
14.2
24.4
23.1
23.3
18.0
23.5
28.9
25.2
20.3
1C 2C
dia2Δ orc* mcm*
> 2C
cdc6ΔN orc* mcm*
> 2C
11.2
12.5
15.3
15.2
39.7
40.3
36.3
26.2

Figure 22. Cells lacking Cdc4 and Tom1 exhibit aberrant DNA content. Increased DNA synthesis occurs in *cdc4-1* and *tom1Δ* mutants. *cdc4-1*, *tom1Δ*, *dia2Δ*, and *cdc6ΔN* mutants were generated in the strain with non-phosphorylatable ORC and the constitutive nuclear localization of the Mcm2-7 complex. Cells were arrested with 15μg/ml nocodazole for 3h and shifted to 37°C. Re-replication was analyzed by flow cytometry analysis. *orc* mcm** refers to *orc2 6A orc6 4A MCM7-2NLS*. The percentage of the cells with more than 2C DNA content was measured using Flow Jo software. >2C indicates the percentage of cells containing more than 2C DNA content.

Table I. Yeast Strains used in Chapter II

Strain	Genotype	Source
DKY153	*ade2-1 ura3-1 leu2-3,112 his3-11,15 trp1-1 can1-100 MAT a*	This study
DKY194	*dia2Δ::kanMX ade2-1 ura3-1 leu2-3,112 his3-11,15 trp1-1 can1-100 MAT a*	This study
DKY526	*tom1Δ::kanMX ade2-1 ura3-1 leu2-3,112 his3-11,15 trp1-1 can1-100 MAT a*	This study
DKY546	*CDC6-3HA::TRP1 ade2-1 ura3-1 leu2-3,112 his3-11,15 trp1-1 can1-100 MAT a*	This study
DKY548	*CDC6-3HA::TRP1 tom1Δ::kanMX ade2-1 ura3-1 leu2-3,112 his3-11,15 trp1-1 can1-100 MAT a*	This study
DKY550	*CDC6-3HA::TRP1 dia2Δ::kanMX ade2-1 ura3-1 leu2-3,112 his3-11,15 trp1-1 can1-100 MAT a*	This study
DKY552	*CDC6-3HA::TRP1 TOM1-3XFLAG::kanMX 9MYC-DIA2::URA3 dia2Δ:: kanMX ade2-1 ura3-1 leu2-3,112 his3-11,15 trp1-1 can1-100 MAT a*	This study
DKY540	*TOM1-3XFLAG::kanMX 9MYC-DIA2::URA3 dia2Δ:: kanMX ade2-1 ura3-1 leu2-3,112 his3-11,15 trp1-1 can1-100 MAT a*	This study
DKY559	*CDC6-3HA::TRP1 TOM1-3XFLAG::kanMX MYC-DIA2::URA3 dia2Δ:: kanMX rpn4Δ::HIS3 pdr5Δ::LEU2 ade2-1 ura3-1 leu2-3,112 his3-11,15 trp1-1 can1-100 MAT a*	This study
DKY562	*CDC6-3HA::TRP1 tom1Δ::kanMX MYC-DIA2::URA3 dia2Δ:: kanMX rpn4Δ::HIS3 pdr5Δ::LEU2 ade2-1 ura3-1 leu2-3,112 his3-11,15 trp1-1 can1-100 MAT a*	This study
DKY565	*CDC6-3HA::TRP1 dia2Δ:: kanMX rpn4Δ::HIS3 pdr5Δ::LEU2 ade2-1 ura3-1 leu2-3,112 his3-11,15 trp1-1 can1-100 MAT a*	This study
DKY173	*cdc4-1 ade2-1 ura3-1 leu2-3,112 his3-11,15 trp1-1 can1-100 MAT a carries pRS316 (CEN URA3)*	This study
DKY584	*cdc4-1 tom1Δ::kanMX CDC6-3HA::TRP1 ade2-1 ura3-1 leu2-3,112 his3-11,15 trp1-1 can1-100 MAT a*	This study
DKY587	*cdc4-1 CDC6-3HA::TRP1 ade2-1 ura3-1 leu2-3,112 his3-11,15 trp1-1 can1-100 MAT a*	This study
DKY585	*cdc4-1 dia2Δ::kanMX CDC6-3HA::TRP1 ade2-1 ura3-1 leu2-3,112 his3-11,15 trp1-1 can1-100 MAT a*	This study
DKY600	*CDC6-3HA::TRP1 tom1Δ::kanMX dia2Δ::kanMX TRP1 ade2-1 ura3-1 leu2-3,112 his3-11,15 trp1-1 can1-100 MAT a*	This study
DKY671	*CDC6-3HA::TRP1 tom1C3235A::URA3 ade2-1 ura3-1*	This study

	leu2-3,112 his3-11,15 trp1-1 can1-100 MAT a	
DKY580	*CDC6-3HA::TRP1 dia2Δ::kanMX::9MYC-ΔF-DIA2:URA3 ade2-1 ura3-1 leu2-3,112 his3-11,15 trp1-1 can1-100 MAT a*	This study
DKY568	*9MYC-DIA2::URA3 dia2Δ::kanMX ade2-1 ura3-1 leu2-3,112 his3-11,15 trp1-1 can1-100 MAT a*	This study
DKY588	*dia2Δ::kanMX::9MYC-TPR-DIA2:URA3 CDC6-3HA::TRP1 ade2-1 ura3-1 leu2-3,112 his3-11,15 trp1-1 can1-100 MAT a*	This study
DKY617	*cdc4-1 CDC6-3HA::TRP1 sic1Δ::TRP1 ade2-1 ura3-1 leu2-3,112 his3-11,15 trp1-1 can1-100 MAT a*	This study
DKY875	*CDC6ΔN-3HA::TRP1, ura3 leu2 his3 trp1 ade2, Mat a*	This study
DKY893	*CDC6ΔN-3HA::TRP1 tom1Δ::KanMX ura3 leu2 his3 trp1 ade2, Mat a*	This study
DKY894	*CDC6ΔN-3HA::TRP1 dia2Δ::KanMX ura3 leu2 his3 trp1 ade2, Mat a*	This study
DKY935	*MCM4-3HA::TRP1 ura3 leu2 his3 trp1 ade2, Mat a*	This study
DKY936	*tom1Δ::KanMX MCM4-3HA::TRP1 ura3 leu2 his3 trp1 ade2, Mat a*	This study
AKY145	*dia2Δ::KanMX MCM4-3HA::TRP1 ura3 leu2 his3 trp1 ade2, Mat a*	This study
YJL2068	*orc2 6A orc6 4A MCM7-2NLS leu2 ura3-52 trp1-289 ade2 ade3 bar1::LEU2 his7 sap3 CAN1 Mat a*	Nguyen et al. (2001)
DKY891	*cdc4-1 orc2 6A orc6 4A MCM7-2NLS leu2 ura3-52 trp1-289 ade2 ade3 bar1::LEU2 his7 sap3 CAN1 Mat a*	This study
DKY876	*tom1Δ::KanMX orc2 6A orc6 4A MCM7-2NLS leu2 ura3-52 trp1-289 ade2 ade3 bar1::LEU2 his7 sap3 CAN1 Mat a*	This study
DKY878	*dia2Δ::KanMX orc2 6A orc6 4A MCM7-2NLS leu2 ura3-52 trp1-289 ade2 ade3 bar1::LEU2 his7 sap3 CAN1 Mat a*	This study
DKY896	*CDC6ΔN-3HA::TRP1 orc2 6A orc6 4A MCM7-2NLS leu2 ura3-52 trp1-289 ade2 ade3 bar1::LEU2 his7 sap3 CAN1 Mat a*	This study
DKY869	*CDC6-3HA::TRP1 skp1-11 ura3 leu2 his3 trp1 ade2, Mat a*	This study
DKY870	*CDC6-3HA::TRP1 cdc53-1 ura3 leu2 his3 trp1 ade2, Mat a*	This study
DKY871	*CDC6-3HA::TRP1 cdc34-2 ura3 leu2 his3 trp1 ade2, Mat a*	This study
DKY955	*orc2 6A orc6 4A MCM7-2NLS rho^0 leu2 ura3-52 trp1-289 ade2 ade3 bar1::LEU2 his7 sap3 CAN1 Mat a*	This study
DKY957	*cdc4-1 orc2 6A orc6 4A MCM7-2NLS rho^0 leu2 ura3-52 trp1-289 ade2 ade3 bar1::LEU2 his7 sap3 CAN1 Mat a*	This study

DKY959	*tom1Δ::KanMX orc2 6A orc6 4A MCM7-2NLS rho^{0} leu2 ura3-52 trp1-289 ade2 ade3 bar1::LEU2 his7 sap3 CAN1 Mat a*	This study
DKY961	*dia2Δ::KanMX orc2 6A orc6 4A MCM7-2NLS rho^{0} leu2 ura3-52 trp1-289 ade2 ade3 bar1::LEU2 his7 sap3 CAN1 Mat a*	This study
DKY963	*CDC6ΔN-3HA::TRP1 orc2 6A orc6 4A MCM7-2NLS rho^{0} leu2 ura3-52 trp1-289 ade2 ade3 bar1::LEU2 his7 sap3 CAN1 Mat a*	This study

Table II. Oligonucleotides used in Chapter II

Oligonucleotide	Sequence (5’ - 3’)
DHK6	CCGTCGACATGTACCCATACGATGTTCCAGATTACGCTATG TCAGCTATACCAATA
DHK7	CGGGATCCCTAGTGAAGGAAAGGTTTCAA
DHK9	GCGAGAATTTTATGATGAGATGACCAAAATTTCAATTTTGA AACCTTTCCTTCACCGGATCCCCGGGTTAATTAA
DHK10	GGGATGCAAGTGGAACTGTAAAAAAAAAAGAAAAAATAAA TCTATTAGCTGAGAATTCGAGCTCGTTTAAAC
DHK11	CGTTTGTGGTTGTGTTGGAC
DHK12	TTGCGGTAACAACCCTCTGT
ACT1-5	ACAACGAATTGAGAGTTGCCCCAG
ACT1-3	AATGGCGTGAGGTAGAGAGAAACC
DHK25	GGAATTCCATATGTCAGCTATACCAATAACTCCAACTAAGC G
DHK26	CGGGATCCCTAGTGAAGGAAAGGTTTCAAAATTG
DHK46	C CTAGAGGCTTTCTCGAGGCAAAAATTTTTCCAATCACTTAC C
DHK48	A AGGAAAAAAGCGGCCGCGTGGTAATGGGCAAACCGTTAGT ACCT GCTTCG
DHK81	TCATCAATAGTACCATATACGTTCATGCAGTTTGGCTCACA GTCTATT TTTTTG
DHK82	CAAAAAAATAGACTGTGAGCCAAACTGCATGAACGTATAT GGTACTAT TGATGA
DHK84	CCTAGAGGCTTTCTCGAGGAATGACAAACGATGAAATCAA GAATTCT AAATTA
DHK85	CGCGGATCCTCAGGCAAGACCAAACCCTTCATGCC
DHK88	CGCGGATCCCGCTTGTATATCTTGTGAGAGAAAGGC
DHK89	ATA AGA ATGCGGCCGCTCATGGTATTATAGTTGTCCTCGTTAGACC
DHK90	AGAAAATAGTGCATATTTAGTTTACTTTTTGCCTTTGATTGA AAATATATA TTCGTTTAGCTTGCCTCGTCCCCG
DHK91	AAGACGTTCTAAAATACTTGGTTACATGGCGCTATAAATTT ACACGAA AAATGATTAAGGGTTCTCGAGAGCTCG
DHK92	AAATGATTAGCCATGTCGTATAAATTTATTACCAAGAACAA AAAATAC ACCCCGGTTTAGCTTGCCTCGTCCCCG
DHK93	AATATTCTAAGAATTTTCCGAAGGATACTGCATTATCATCA

	GTGATTT ATTAATTTAAGGGTTCTCGAGAGCTCG
DHK104	GCAATCCGCTCGAGGAATGCAGTTTGGCTCACAGTCTATTT TTTTG
DHK105	CGCGGATCCCTAGTGAAGGAAAGGTTTCAAAATTGA
ZHW57	TTATTCATATGCTACCTATCATATTCCAAAG
ZHW54	TTATTGTCGACCTATGAGTATGAATATGA
ZHW58	TTATTCATATGATGTCTTCCCCAGGGAATTC
AK43	CCGGATCCCTAATTGCCAACTAAATC
ARS1-1	GGTGAAATGGTAAAAGTCAACCCCCTGCG
ARS1-2	GCTGGTGGACTGACGCCAGAAAATGTT
ARS305-1	CTCCGTTTTTAGCCCCCCGTG
ARS305-2	GATTGAGGCCACAGCAAGACCG
ACF2-1	ATGTGTTACAGTAGGCAAGCC
ACF2-2	GTCACTATTCACCTGGCTGTC

CHAPTER III

The Hect E3 ubiquitin ligase Tom1 controls Dia2 degradation during the cell cycle

The ubiquitin proteasome system plays a pivotal role in controlling the cell cycle. The budding yeast F-box protein Dia2 is required for genomic stability and is targeted for ubiquitin-dependent degradation in a cell cycle-dependent manner, but the identity of the ubiquitination pathway is unknown. I demonstrate that the Hect domain E3 ubiquitin ligase Tom1 is required for Dia2 protein degradation. Deletion of *DIA2* partially suppresses the temperature-sensitive phenotype of *tom1* mutants. Tom1 is required for Dia2 ubiquitination and degradation during G1 and G2/M phases of the cell cycle, whereas during S phase, the Dia2 protein is stabilized. I find that Tom1 binding to Dia2 is enhanced in G1 and reduced in S phase, suggesting a mechanism for this proteolytic switch. Tom1 recognizes specific positively charged residues in a Dia2 degradation/NLS domain. Loss of these residues blocks Tom1-mediated turnover of Dia2 and causes a delay in G1 to S-phase progression. Deletion of *DIA2* rescues a delay in the G1 to S-phase transition in the *tom1Δ* mutant. Together, these results suggest that Tom1 targets Dia2 for degradation during the cell cycle by recognizing positively charged residues in the Dia2 degradation/NLS domain and that Dia2 protein degradation contributes to G1 to S-phase progression.

Introduction

The highly conserved ubiquitin proteasome system (UPS) plays a role in a number of cellular processes including cell cycle control, DNA replication, and DNA damage response (50, 65, 85). In budding yeast, the F-box protein Dia2 serves as an adaptor for a multicomponent SCF (Skp1/Cdc53/F-box protein) E3 ubiquitin ligase complex and functions to maintain genomic stability (5, 47, 71). Dia2 assembles with the components of the replisome complex and regulates the progression of the DNA replication fork (60, 62), suggesting a role in controlling the S-phase progression.

Dia2 itself is an unstable protein targeted for degradation by the UPS (45, 60). There are conflicting reports about the pathway responsible for Dia2 protein turnover. One study suggests that Dia2 degradation is the result of an autoubiquitination pathway (60), similar to other F-box proteins (52, 101). By contrast, our lab previously indicates that an SCF-independent pathway targets Dia2 for degradation, as deletion of the F-box domain required for binding the core SCF complex does not stabilize the protein. Rather, a 20-amino acid motif that overlaps with a nuclear localization sequence (NLS)-containing domain was found to be required for Dia2 protein turnover (45). However, the identity of the ubiquitin ligase responsible for targeting Dia2 for degradation via this domain was not determined.

The Dia2 protein turnover rate varies throughout the cell cycle. Dia2 is at its most unstable during G1 phase, is moderately unstable during G2/M and is substantially stabilized in S phase. Dia2 protein stabilization is dependent on the activation of the S-phase checkpoint pathway (45). One model that explains these observations is that Dia2

is stabilized after checkpoint activation so that the SCF^{Dia2} complex may assemble to target S-phase specific proteins for degradation. Two identified targets include replication proteins Mrc1 and Ctf4, although no physiological role for their degradation has yet been established (60).

In this chapter, I identify the E3 ubiquitin ligase that targets Dia2 for ubiquitin-mediated degradation and describe how Dia2 is recruited to the degradation pathway. Moreover, I show that failure to degrade Dia2 leads to a cell cycle progression defect.

Tom1 targets Dia2 for ubiquitin-dependent degradation

To identify the E3 ubiquitin ligase that targets Dia2 for degradation, I carried out a candidate approach. Based on the literature, the Hect-domain E3 ubiquitin ligase Tom1 was a promising candidate, as it has been shown to interact with Yra1 (40), a protein required for Dia2 association with chromatin (90), and Rad53, a S-phase checkpoint kinase (40). I first asked whether there was a genetic relationship between Tom1 and Dia2 by examining the growth of wildtype, *tom1Δ*, *dia2Δ*, and *tom1Δ dia2Δ* strains at 30°C and 37°C. Interestingly, the temperature-sensitive phenotype of *tom1Δ* mutant was partially suppressed by deletion of *DIA2* at 37°C (Figure 23A). The *dia2Δ* mutant also partially rescued the temperature-sensitive phenotype of the *tom1C3235A* mutant in which the catalytic cysteine is replaced with alanine. These results suggest that the temperature-sensitive phenotype of *tom1Δ* and *tom1C3235A* mutants may be due in part to aberrant accumulation of the Dia2 protein. If this were the case, I would expect that overexpression of *DIA2* in *tom1Δ* cells would also lead to a growth defect more

significant than the mild defect observed when *DIA2* is overexpressed in wildtype cells. To test this, *DIA2* was overexpressed in wildtype, *tom1Δ*, and *tom1C3235A* mutants using the *GAL1,10* galactose-inducible promoter. Under these conditions, overexpression of *DIA2* caused a stronger growth defect in *tom1Δ* and *tom1C3235A* mutants than in wildtype cells (Figure 23B).

To determine whether Tom1 and Dia2 physically interact, I performed an *in vitro* binding assay using the Flag-tagged Hect domain of Tom1 and Myc-tagged Dia2 expressed from insect cells. When the Flag-tagged Hect domain of Tom1 was purified, Myc-tagged Dia2 co-precipitated. Reciprocal co-purification of the Flag-tagged Hect domain of Tom1 was observed when Myc-tagged Dia2 was immunoprecipitated (Figure 23C).

The most straightforward explanation for these results is that Tom1 targets Dia2 for ubiquitin-dependent degradation. To ask whether Tom1 is a required for Dia2 protein degradation, I first assessed the turnover of the Dia2 protein in *tom1* mutants using a cycloheximide stability assay. Wildtype, *tom1Δ*, and *tom1C3235A* cells were grown to mid-log phase and Dia2 protein abundance was measured over time. I observed that Dia2 was partially stabilized in both *tom1Δ* and *tom1C3235A* mutants compared to wildtype (Figure 24A). Notably, Dia2 mRNA abundance was not changed in the *tom1Δ* mutant (Figure 24B), indicating that the change in Dia2 protein levels was not the result of transcriptional regulation. To examine Dia2 ubiquitination, I developed an *in vitro* ubiquitination assay using fractionated yeast extracts and GST-Dia2 purified from insect cells. When extracts from wildtype cells were incubated with GST-Dia2 in the presence

of E1, an ATP regeneration system, and ubiquitin, Dia2 ubiquitin conjugates were observed (Figure 24C, lane 3). However, Dia2 ubiquitin conjugates were significantly reduced when extracts from the *tom1Δ* strain were used (Figure 24C, lane 5), indicating that Dia2 ubiquitination is dependent on Tom1. Together, these results suggest that Tom1 targets Dia2 for ubiquitin-mediated degradation.

Tom1 controls Dia2 proteolysis during G1 and G2/M

Dia2 is unstable during G1 and G2/M phases of the cell cycle but is stabilized during S phase or in response to activation of the S-phase checkpoint (45). I investigated when during the cell cycle Tom1 controls Dia2 turnover by performing stability assays in cells synchronized in G1 by alpha factor (αF), early S phase by hydroxyurea (HU), which also activates the S-phase checkpoint, or at metaphase with nocodazole. As shown in Figure 25A, Dia2 was turned over in wildtype but stabilized in *tom1Δ* and *tom1C3235A* mutants in G1. By contrast, no significant turnover of Dia2 was observed in *tom1Δ* and *tom1C3235A* mutants in cells arrested with HU (Figure 25B). However, I found that Dia2 was partially stabilized in *tom1Δ* and *tom1C3235A* mutants in cells arrested by nocodazole (Figure 25C), suggesting that Tom1 is required for Dia2 proteolysis during G2/M. I conclude that degradation of Dia2 during G1 and G2/M phases of the cell cycle is dependent on Tom1.

The mechanistic basis for how Dia2 is stabilized in response to initiation of S-phase or S-phase checkpoint activation is not known. With the identification of Tom1 as the E3 ubiquitin ligase that targets Dia2 for degradation, one possible explanation is that Tom1

and Dia2 no longer interact during S phase or in response to S-phase checkpoint activation. To test this idea, I conducted co-immunoprecipitation assays in synchronized cells (Figure 25D). Cells expressing Myc-tagged Dia2 and Flag-tagged Tom1 from their endogenous loci were arrested in late G1 with αF, early S phase with HU, and G2/M phase with nocodazole. When Flag-tagged Tom1 was immunoprecipitated from αF-arrested cells, I observed significant co-precipitation of Myc-tagged Dia2. However, this co-precipitation was almost completely absent in HU-arrested cells. By contrast, I observed a modest interaction between Tom1 and Dia2 in nocodazole-arrested cells. Thus, inhibition of the interaction between Tom1 and Dia2 may explain the proteolytic switch observed as cells enter S phase or when the S-phase checkpoint is activated.

Tom1 recognizes a stretch of positively charged residues in Dia2

Our lab has previously shown that a domain just upstream of the F-box in Dia2, which also contains two canonical nuclear localization sequences, was required for Dia2 protein turnover. Although nuclear localization is required for Dia2 degradation, this domain is also likely important for recognition by the degradation pathway as the addition of an exogenous NLS to a Dia2 mutant lacking this domain is still stabilized (45). I hypothesized that Tom1 may bind to this domain in Dia2 so I tested whether various truncated Dia2 mutants are able to co-immunoprecipitate Tom1 (Figure 26). I generated strains expressing epitope-tagged Tom1 and the Dia2 mutants expressed from their endogenous loci (Figure 26, upper left panel). As shown, Tom1 and full-length Dia2 co-immunoprecipitate. The Dia2 mutants used include a mutant containing only the

N-terminal TPR region (*TPR)*, a mutant in which the F-box domain was deleted in frame (*ΔF-box)*, a mutant that lacks the first 149 amino acids of the N-terminus (*ΔN149*), and a mutant with the NLS/degradation domain deleted in frame but containing a exogenous SV40 Tag NLS attached to the N-terminus (SVΔNLS). In the co-immunoprecipitation assay, all Dia2 proteins except the SVΔNLS mutant co-purify with Tom1, indicating that the NLS domain of Dia2 is required for its interaction with Tom1.

The domain in Dia2 required for degradation consists of two stretches of lysine residues interrupted by a nine-residue sequence. My co-immunoprecipitation results were unable to determine which sections of this domain were required for recruitment to Tom1. I speculated that there were three possibilities: 1) Tom1 may recognize the lysine residues, perhaps even use them as sites of ubiquitin conjugation, 2) Tom1 may recognize the nine-residue sequence in between the lysines, or 3) Tom1 recognizes positively charged residues. To distinguish between these possibilities, I generated three mutants, one in which the lysines were changed to arginines to conserve charge (Dia2-KR), one in which the lysines were mutated to alanines (Dia2-KA) and one in which the nine-residues middle sequence was deleted in frame (Dia2Δ185-193) (Figure 27A). For the Dia2-KA and Dia2Δ185-193 proteins, I also added the SV40 Tag NLS to the N-terminus to avoid altering the nuclear localization of Dia2 (SVDia2-KA, SVDia2Δ185-193). I then examined the stability of these proteins using the cycloheximide stability assay in G1-arrested cells. As shown in Figure 27B, the turnover rates of wildtype Dia2 and the Dia2-KR mutant were indistinguishable, indicating that exchanging the lysines with arginines has no effect on Dia2 protein turnover. Intriguingly, the SVDia2-KA mutant protein was

significantly stabilized in αF-arrested cells, whereas both the SVDia2 and SVDia2Δ185-193 proteins were turned over with similar rates (Figure 27C). These results indicate that it is not the lysine residues *per se*, but rather the positive charge of these residues in the Dia2 degradation domain that are necessary for protein turnover.

Based on the stability assay results, I predicted that the positively charged residues in the NLS/degradation domain would be required for Tom1 to bind Dia2. To test this, I carried out a co-immunoprecipitation assay using strains expressing epitope-tagged Dia2-KR or SVDia2-KA proteins and Flag-tagged Tom1. I observed that Flag-tagged Tom1 co-precipitated with Dia2-KR but not with the SVDia2-KA protein (Figure 27D). Together, these results suggest that Tom1 specifically recognizes the positive charge on the lysine residues in the Dia2 NLS/degradation domain.

Defects in Dia2 protein turnover lead to a G1 to S phase progression delay

If degradation of Dia2 via Tom1 is the major pathway for Dia2 degradation, I would expect that overexpression of a Dia2 mutant unable to bind Tom1 would produce a stronger overexpression phenotype than full-length Dia2 in wildtype cells. In addition, if Tom1 only recognizes the positively charged residues in the Dia2 degradation/NLS domain, I would also expect that overexpression of the *SV dia2-KA* mutant would be indistinguishable from the *DIA2* overexpression phenotype in *tom1Δ* cells. To test these predictions, I examined the overexpression phenotypes of full-length *DIA2*, *dia2-KR*, *SV dia2-KA*, and *SV dia2-Δ185-193* mutants in wildtype and *tom1Δ* cells (Figure 28A). I observed that both wildtype and *tom1Δ* cells overexpressing the *dia2-KR* mutant behaved

as the parental strains overexpressing full-length *DIA2*. By contrast, overexpression of the *SV dia2-KA* mutant impaired the growth of wildtype cells compared to cells overexpressing full-length *SV DIA2* or *SV dia2-Δ185-193*. Moreover, the growth defect of *tom1Δ* cells caused by *DIA2* overexpression was indistinguishable from overexpression of the *SV dia2-KA* mutant and looked similar to the results when *SV dia2-Δ185-193* is overexpressed (Figure 28A). These results suggest that Tom1 is the primary E3 ubiquitin ligase that controls Dia2 protein turnover, recognizing specific positively charged residues in the degradation/NLS domain.

Our lab has previously reported that the stabilized forms of *dia2* mutants such as *SVΔ214* and *SVΔNLS* modestly increased the percentage of G1 cells in an asynchronous population (45). Therefore, I would expect a similar phenotype to be observed in the *SV dia2-KA* mutant. To test this, wildtype cells carrying overexpression constructs for *SV DIA2* or *SV dia2-KA* were grown to mid-log phase and their cell cycle distributions were measured by flow cytometry (Figure 28B). Consistent with previous results, overexpression of *SV DIA2* showed a modest increase in G1 cells relative to cells carrying an empty vector. Furthermore, cells expressing *SV dia2-KA* exhibited a significant increase in the G1 population. These results suggested that the *dia2-KA* mutant may transit more slowly through G1 phase into S phase than wildtype cells (Figure 28B). To test this possibility, the same strains were arrested with αF and released into medium containing nocodazole to monitor cell cycle progression from late G1 to metaphase (Figure 28B). Cells overexpressing the *SV DIA2* exhibited a mild delay in the G1 to S phase transition as compared to the control cells. In addition, overexpression of

the *SV dia2-KA* mutant prolonged the delay in G1 to S phase progression (Figure 28B), suggesting that Dia2 protein turnover is important for a proper progression from G1 to S. I further asked whether the *tom1Δ* mutant also exhibits the same delay in the G1 to S phase transition as would be expected if Dia2 is a significant target of Tom1. Wildtype, *tom1Δ*, *dia2Δ*, and *tom1Δ dia2Δ* strains arrested with αF were released into rich medium containing nocodazole to monitor cell cycle progression from late G1 to metaphase (Figure 28C). Under these conditions, the *tom1Δ* mutant proceeded into S-phase from G1 phase with a 5-minute delay, compared to wildtype and the *dia2Δ* mutant. Interestingly, the delay in G1 to S-phase progression observed in the *tom1Δ* mutant was rescued by deletion of *DIA2* (Figure 28C). These findings indicate that Tom1-mediated Dia2 turnover in G1 is required for an efficient G1 to S phase transition.

Discussion

Altogether, these results suggest that the Hect-domain E3 ubiquitin ligase Tom1 recruits Dia2 for degradation during G1 and G2/M phases of the cell cycle by recognizing specific positively charged residues just upstream of the F-box domain. Failure to efficiently degrade Dia2 leads to defects in cell cycle dynamics.

These data suggest that the proteolytic inhibition of Dia2 degradation that occurs as cells enter S phase or activate the S-phase checkpoint depends on reduced binding between Dia2 and Tom1. In principle, such an outcome could be the result of a conformational change in Dia2, such as those that accompany post-translational modifications, although there is currently no evidence for S-phase specific modification

of Dia2. Alternatively, Tom1 has additional substrates and interaction partners that may compete for binding to Tom1 more effectively during S phase or in response to activation of the S phase checkpoint. Interestingly, Tom1 targets excess histones for degradation when they are phosphorylated by the S-phase checkpoint kinase Rad53. Moreover, Tom1 physically interacts with Rad53 (86), suggesting that it is possible this role of Tom1 might influence its behavior during checkpoint activation. Future studies will be necessary to distinguish between these possibilities.

How Tom1 binds and recruits target proteins is an open question. My results suggest that a short stretch of positively charged amino acids in Dia2 are required to bind Tom1. This domain may serve as a degron for targeting substrates to Tom1. The two other known targets of Tom1 include histone H3 (86) and Yra1, an mRNA export factor (40). Both proteins contain short stretches of positively charged amino acids, although neither shows a similarly spaced arrangement of residues, with the intervening sequence, as observed in Dia2 (D.H. Kim and D.M. Koepp, unpublished observations). It is possible that a single stretch of 3-4 positively charged residues on either side of the intervening sequence is sufficient for interaction with Tom1 or that the spacing of the positive charges does not play a role in recognition. Indeed, deletion of the intervening sequence does not alter Dia2 degradation kinetics, consistent with the idea that spacing of the residues does not play a role in recognition. I look forward to future studies investigating whether the motif I have identified serves as a recognition domain for other Tom1 targets.

Previous work suggested a role for Dia2 degradation in cell cycle dynamics (45). The results presented here confirm and extend those observations, showing that impaired degradation of Dia2 leads to a delay of the G1/S phase transition. However, the mechanism by which accumulated Dia2 slows down the G1 to S transition is not clear. One explanation might be that Dia2 has an as yet unidentified ubiquitination target that promotes G1 progression or S-phase entry. In this scenario, excess Dia2 would lead to inappropriate degradation of this unknown target. Alternatively, excess Dia2 may simply lead to change in the balance of various SCF complexes by competing for core component proteins. For example, the relative concentration of those SCF complexes that have G1 ubiquitination substrates, such as SCF^{Cdc4}, which targets the Cdk inhibitor Sic1 and the DNA replication protein Cdc6 (20, 88, 95), may be reduced. Regardless of the mechanism, these observations suggest that Dia2 protein levels are modulated throughout the cell cycle to prevent adverse effects on cell cycle progression.

In summary, I have identified a novel degradation pathway for the F-box protein Dia2 involving the Hect domain E3 ligase Tom1. This study establishes a mechanistic basis for recognition of Dia2 by Tom1 and demonstrates a role for Dia2 degradation in cell cycle dynamics.

Future directions

I have shown that the Hect E3 ligase Tom1 targets Dia2 for ubiquitin-dependent degradation during G1 and G2/M. In vitro ubiquitination assay showed that Dia2 ubiquitination is dependent on Tom1. However, I could not identify the E2 responsible

for Dia2 ubiquitination. Since this assay used the fractionated yeast extracts containing multiple E2 proteins, the E2 enzyme required for Dia2 ubiquitination needs to be identified. In order to address this question, Dia2 stability needs to be examined in those E2 mutants. Once the E2 is identified, an in vitro ubiquitination assay using purified E1, E2, Tom1, Dia2, ubiquitin, and ATP needs to be conducted in the future. I also showed that Tom1 binding to Dia2 is reduced as cells enter the S phase or activate the S-phase checkpoint. As suggested in discussion, Tom1 physically interacts with Rad53 in response to replication stress (86), implying that Tom1 binding to Dia2 is decreased because Tom1 might have a high affinity for Rad53 binding in response to activation of the S-phase checkpoint. To test this possibility, a co-immunoprecipitation assay would be required to determine whether binding of Tom1 to Dia2 is increased in *rad53-21* mutant during S phase or in response to activation of the S-phase checkpoint. Likewise, it is also important to examine whether the interaction between Tom1 and Rad53 is reduced by overexpression of Dia2 upon activation of the S-phase checkpoint.

My results suggest that the specific positively charged residues in the degradation/NLS domain of Dia2 are required for the interaction between Tom1 and Dia2. If this domain were critical for Tom1 to recognize its potential substrates, I would expect that this domain might serve as a Tom1 recognition site in other Tom1 substrates. Searching for proteins that contain a domain or motif similar to this would be critical to identify potential substrates of Tom1. Furthermore, identification of Tom1 targets involved in cell cycle progression will help better understand how cell cycle dynamics are regulated by Tom-mediated proteolysis.

I also observed that excess Dia2 in G1 causes a delay in the G1 to S-phase progression. If excess Dia2 alters the balance of SCF complexes in G1, the abundance of Sic1 which is targeted by the SCF^{Cdc4} complex for degradation might be increased by overexpression of Dia2 or in *tom1Δ* mutant during G1. To address this question, Sic1 abundance or stability needs to be observed when Dia2 is overexpressed or in *tom1Δ* mutant in G1.

What role Dia2 plays in during S phase or in response to activation of the S-phase checkpoint is an unanswered question. Given that Dia2 is stabilized during S phase or upon replication stress, Dia2 might have a role in stabilizing replication fork or controlling the progression of replication fork in response to replication stress by assembling the SCF^{Dia2} complex and targeting replication or S-phase proteins for degradation. Therefore, identification of Dia2 substrates during S phase or in the presence of replication stress will help us better understand the mechanistic role of Dia2 in DNA replication or activation of the S-phase checkpoint.

Figure 23

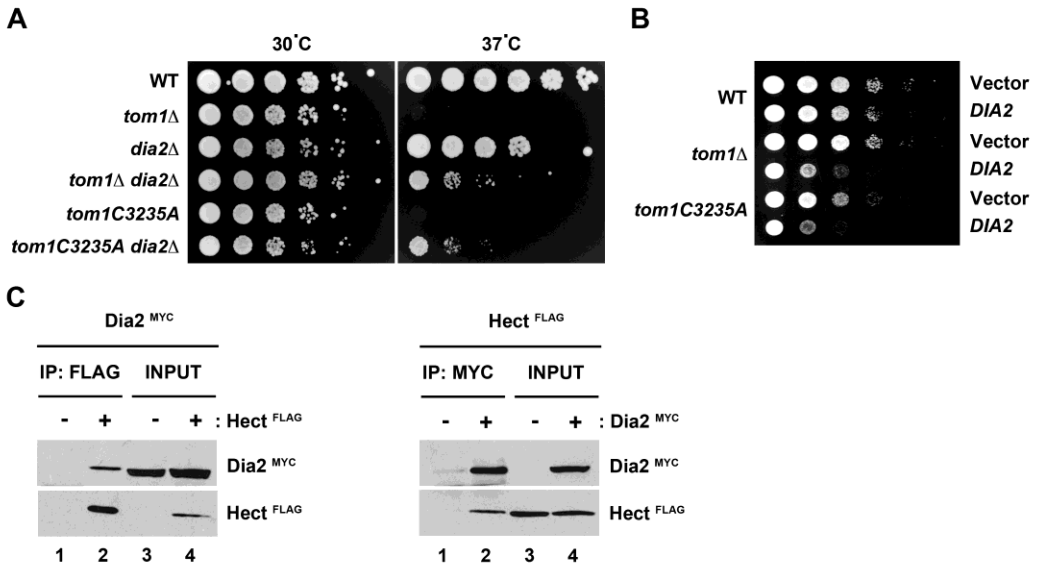
A
30˚C
37˚C
WT
tom1Δ
dia2Δ
tom1Δ dia2Δ
tom1C3235A
tom1C3235A dia2Δ
B
WT
tom1Δ
tom1C3235A
Vector
DIA2
Vector
DIA2
Vector
DIA2
C
Dia2 MYC
IP: FLAG
INPUT
- + - + : Hect FLAG
Dia2 MYC
Hect FLAG
1 2 3 4
Hect FLAG
IP: MYC
INPUT
- + - + : Dia2 MYC
Dia2 MYC
Hect FLAG
1 2 3 4

Figure 23. Tom1 genetically and physically interacts with Dia2. (A) The temperature-sensitive phenotype of *tom1Δ* and *tom1C3235A* mutants is partially suppressed by deletion of *DIA2*. The indicated strains were grown to mid-log phase and spotted in 10-fold serial dilutions onto rich medium plates. The plates were incubated at 30°C and 37°C for 2 days. (B) Overexpression of *DIA2* results in a growth defect in *tom1Δ* and *tom1C3235A* mutants. The 10-fold serial dilutions of wild-type, *tom1Δ*, and *tom1C3235A* cells carrying empty vector or *DIA2* under the control of *GAL1,10* promoter were spotted onto minimal plates with 2% galactose. Plates were incubated at 30°C for 2-3 days. (C) The Hect domain of Tom1 binds to Dia2. Hi5 insect cells were co-infected with Flag-Tom1 Hect domain and Myc-Dia2 baculoviruses. Flag-Tom1 Hect domain or Myc-Dia2 protein was immunoprecipiated with anti-Flag or -Myc antibodies and analyzed by immunoblotting. (-) and (+) represent uninfected and infected with the indicated baculoviruses. Anti-Flag or –Myc antibodies were added to the indicated immunoprecipitation assays.

Figure 24

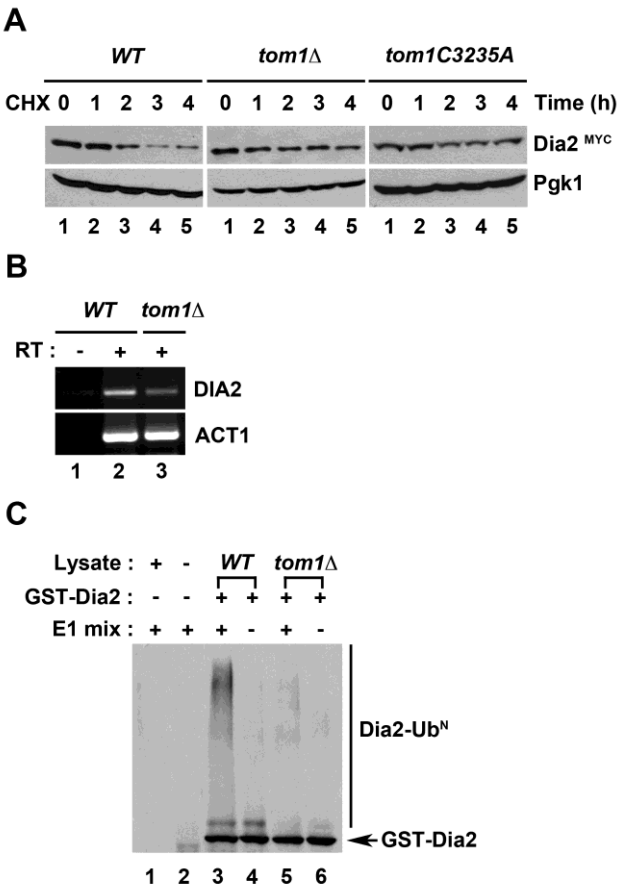
A
WT
tom1Δ
tom1C3235A
CHX 0 1 2 3 4 0 1 2 3 4 0 1 2 3 4 Time (h)
Dia2 MYC
Pgk1
1 2 3 4 5 1 2 3 4 5 1 2 3 4 5
B
WT
tom1Δ
RT : - + +
DIA2
ACT1
1 2 3
C
Lysate : + - WT tom1Δ
GST-Dia2 : - - + + + +
E1 mix : + + + - + -
Dia2-UbN
GST-Dia2
1 2 3 4 5 6

Figure 24. Tom1 is required for ubiquitin-dependent Dia2 degradation. (A) Dia2 is partially stabilized in *tom1Δ* and *tom1C3235A* mutants. Wildtype, *tom1Δ* and *tom1C3235A* cells were grown to mid-log phase and treated with cycloheximide (100 μg/ml). Samples were taken at the indicated times and processed for stability assay. Immunoblotting was performed with anti-Myc and -Pgk1 antibodies. Pgk1 was used as a loading control. (B) Dia2 mRNA levels are not changed in the *tom1Δ* mutant. RT-PCR was conducted to examine the level of Dia2 transcript in wildtype and *tom1Δ* strains. *ACT1* was used as a loading control. RT, reverse transcriptase. (C) *In vitro* ubiquitination of Dia2. GST-Dia2 protein expressed from baculovirus-infected insect cells was purified using glutathione-sepharose 4B beads. GST-Dia2 protein was incubated with ubiquitin, E1, ATP, an ATP regeneration system, and fractionated yeast extracts purified from wildtype or *tom1Δ* strains at 30°C for 45min. Samples were run on 6% SDS-PAGE and immunoblotted with anti-GST antibodies.

Figure 25

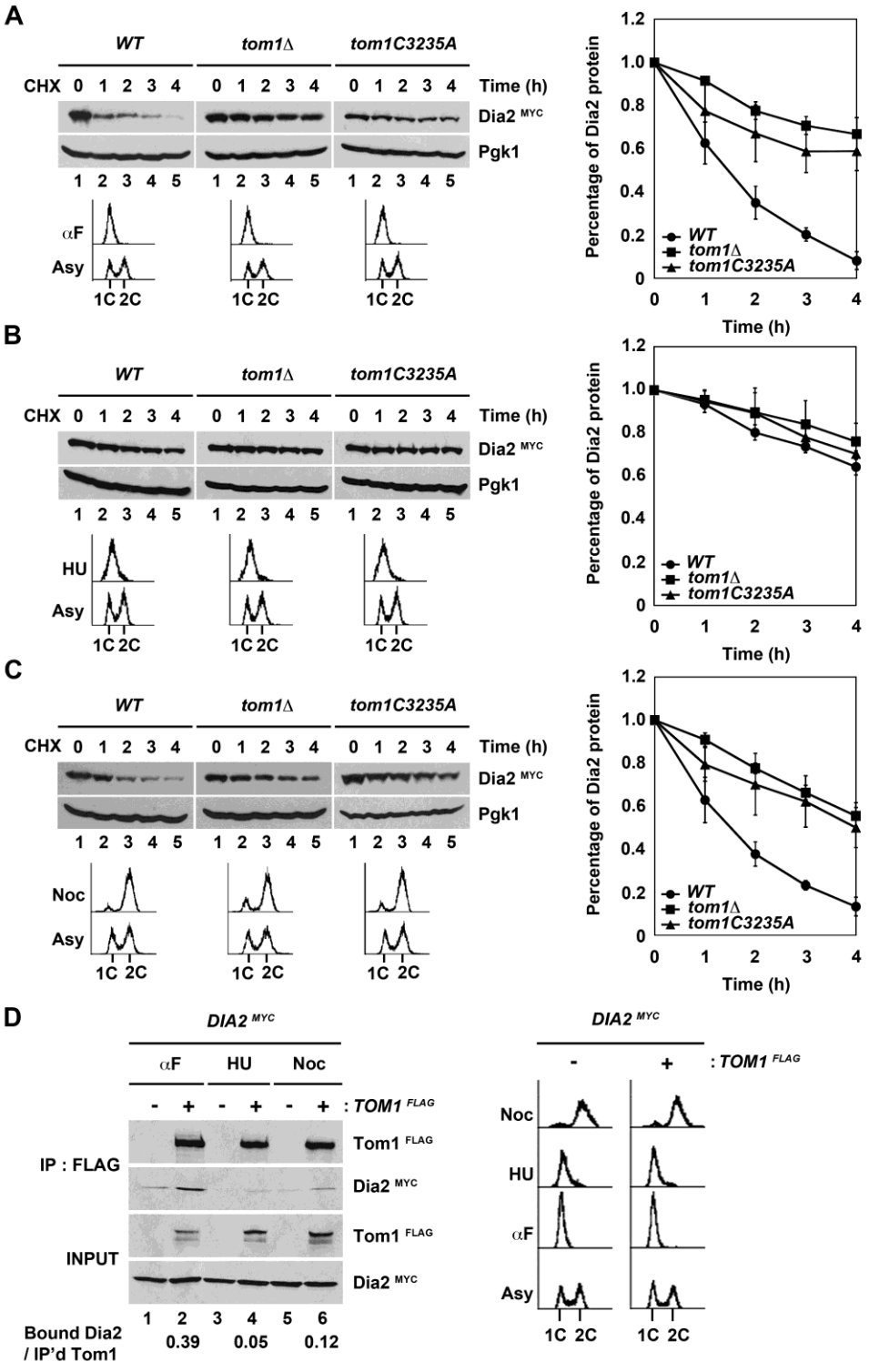
A
WT
tom1Δ
tom1C3235A
CHX 0 1 2 3 4 0 1 2 3 4 0 1 2 3 4 Time (h)
Dia2 MYC
Pgk1
1 2 3 4 5 1 2 3 4 5 1 2 3 4 5
αF
Asy
1C 2C 1C 2C 1C 2C
Percentage of Dia2 protein
WT
tom1Δ
tom1C3235A
Time (h)
B
WT
tom1Δ
tom1C3235A
CHX 0 1 2 3 4 0 1 2 3 4 0 1 2 3 4 Time (h)
Dia2 MYC
Pgk1
1 2 3 4 5 1 2 3 4 5 1 2 3 4 5
HU
Asy
1C 2C 1C 2C 1C 2C
Percentage of Dia2 protein
WT
tom1Δ
tom1C3235A
Time (h)
C
WT
tom1Δ
tom1C3235A
CHX 0 1 2 3 4 0 1 2 3 4 0 1 2 3 4 Time (h)
Dia2 MYC
Pgk1
1 2 3 4 5 1 2 3 4 5 1 2 3 4 5
Noc
Asy
1C 2C 1C 2C 1C 2C
Percentage of Dia2 protein
WT
tom1Δ
tom1C3235A
Time (h)
D
DIA2 MYC
αF HU Noc
- + - + - + : TOM1 FLAG
IP : FLAG
Tom1 FLAG
Dia2 MYC
INPUT
Tom1 FLAG
Dia2 MYC
1 2 3 4 5 6
Bound Dia2 / IP'd Tom1
0.39 0.05 0.12
DIA2 MYC
- + : TOM1 FLAG
Noc
HU
αF
Asy
1C 2C 1C 2C

Figure 25. Tom1 regulates Dia2 turnover in G1 and G2/M. (A) Dia2 stabilization in *tom1Δ* and *tom1C3235A* mutants in G1 phase. Wildtype, *tom1Δ* and *tom1C3235A* strains were arrested with αF for 3 h. After cycloheximide treatment (100 μg/ml), samples were collected at the indicated times and immunoblotted with anti-Myc antibodies. Pgk1 was used as a loading control. Flow cytometry analysis was performed to monitor the αF arrest. Dia2 protein turnover was quantified with three independent experiments. Error bars indicate standard deviations. (B) Dia2 is stable in S phase. The indicated strains were arrested with 200 mM hydroxyurea for 3 h. Samples were taken at the indicated times after cycloheximide treatment (100 μg/ml) and analyzed by immunoblotting with anti-Myc antibodies. Pgk1 was used as a loading control. Three independent results were used to quantify the rate of Dia2 turnover. Error bars indicate standard deviations. The HU arrest was monitored by flow cytometry. (C) Dia2 is stabilized in *tom1Δ* and *tom1C3235A* mutants in G2/M phase. Wildtype, *tom1Δ* and *tom1C3235A* cells were arrested with nocodazole (15μg/ml) for 3 h. Stability assays were performed as in (A and B). The results of quantification of Dia2 turnover in wildtype, *tom1Δ* and *tom1C3235A* strains are shown in the graph. Error bars indicate standard deviations. Flow cytometry was used to examine the nocodazole arrest. (D) Dia2 binding to Tom1 is regulated during the cell cycle. $Dia2^{MYC}$ and $Tom1^{FLAG}$ $Dia2^{MYC}$ cells were arrested with αF, hydroxyurea, and nocodazole for 3 h as in (A, B, and C), respectively. Total cell lysates (2mg) of the indicated strains were immunoprecipitated with anti-Flag antibodies and immunoblotted with anti-Flag and -Myc antibodies. The ratio of bound Dia2 to immunoprecipitated

Tom1 was measured using Image J software. Flow cytometry was conducted to monitor the arrests in G1, S, and G2/M.

Figure 26

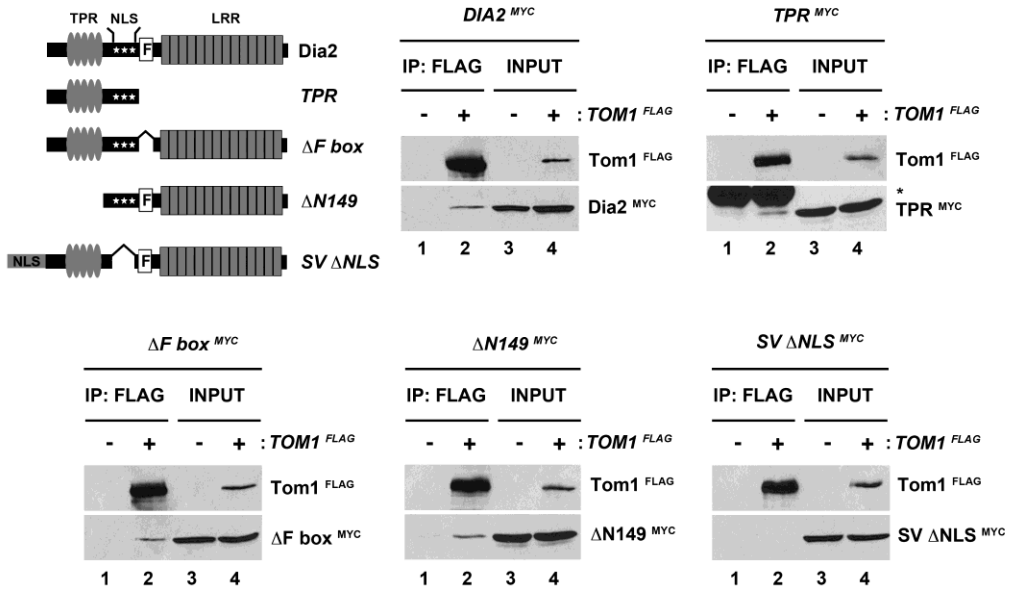
TPR
NLS
LRR
F
Dia2
TPR
ΔF box
ΔN149
SV ΔNLS
NLS
DIA2 MYC
IP: FLAG
INPUT
- + - + : TOM1 FLAG
Tom1 FLAG
Dia2 MYC
1 2 3 4
TPR MYC
*
ΔF box MYC
ΔN149 MYC
SV ΔNLS MYC

Figure 26. Tom1 binds to Dia2 through the degradation/NLS domain of Dia2. Endogenously expressed Tom1 and Dia2 co-precipitate each other via the degradation/NLS domain of Dia2. The indicated strains were grown to mid-log phase. 2 mg of total cell lysates were immunoprecipitated with anti-Flag antibodies and immunoblotted with anti-Flag and -Myc antibodies.

Figure 27

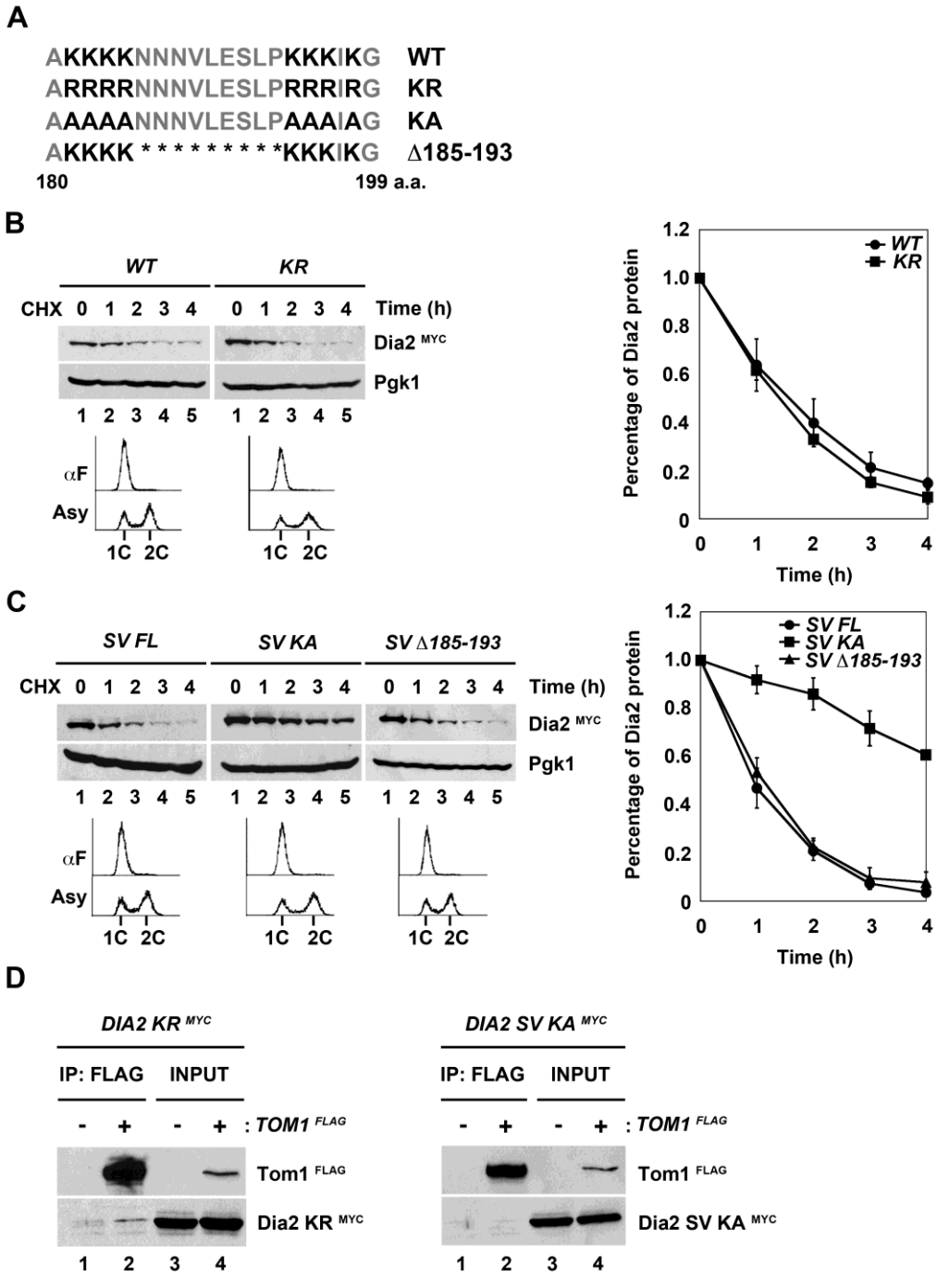
A
AKKKKNNNVLESLPKKKIKG WT
ARRRRNNNVLESLPRRRIRG KR
AAAAANNNVLESLPAAAIAG KA
AKKKK * * * * * * * * *KKKIKG Δ185-193
180
199 a.a.
B
WT
KR
CHX 0 1 2 3 4 0 1 2 3 4 Time (h)
Dia2 MYC
Pgk1
1 2 3 4 5 1 2 3 4 5
αF
Asy
1C 2C 1C 2C
Percentage of Dia2 protein
Time (h)
C
SV FL
SV KA
SV Δ185-193
CHX 0 1 2 3 4 0 1 2 3 4 0 1 2 3 4 Time (h)
Dia2 MYC
Pgk1
1 2 3 4 5 1 2 3 4 5 1 2 3 4 5
αF
Asy
1C 2C 1C 2C 1C 2C
Percentage of Dia2 protein
Time (h)
D
DIA2 KR MYC
DIA2 SV KA MYC
IP: FLAG INPUT
- + - + : TOM1 FLAG
Tom1 FLAG
Dia2 KR MYC
Dia2 SV KA MYC
1 2 3 4

Figure 27. Tom1-mediated Dia2 proteolysis requires positively charged residues in the degradation domain of Dia2. (A) Domain containing the degradation/NLS region of Dia2. (B) Substitution of lysine for arginine does not stabilize Dia2 in G1. Wildtype and *dia2-KR* strains were arrested with αF for 3 h. Samples were taken at the indicated times and prepared for stability assay as described in Figure 3A. Three independent results were used for quantification. Error bars indicate standard deviations. (C) The SVDia2-KA mutant protein is stabilized in G1 phase. The indicated strains were arrested with αF for 3 h. Stability assay was performed as in (Figure 25A and 27B). SV indicates the SV40 Tag NLS. Quantification shows the rates of Dia2 turnover in the indicated strains. Error bars indicate standard deviations. (D) The SVDia2-KA mutant protein does not bind to Tom1. The indicated strains were grown to mid-log phase and used for a co-immunoprecipitation assay. Flag-tagged Tom1 was immunoprecipitated with anti-Flag antibodies. Immunoblot assay was conducted with anti-Flag and –Myc antibodies. See also Figure 26.

Figure 28

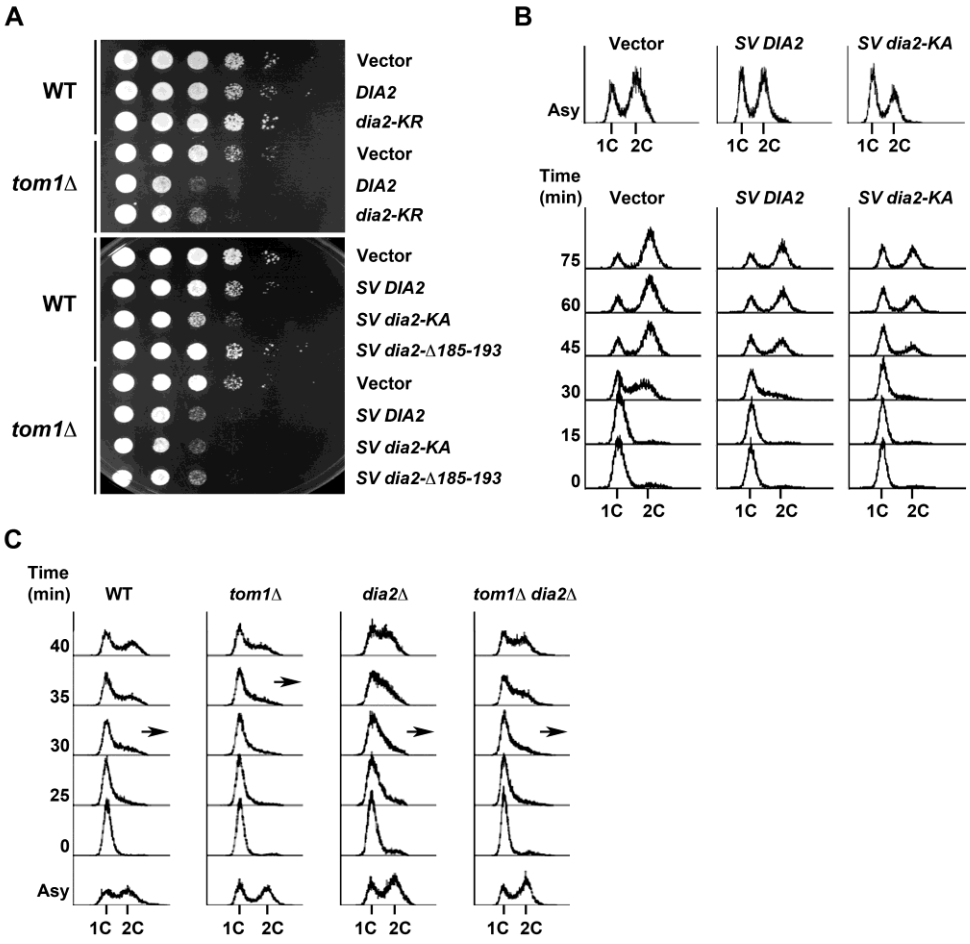
A
WT
tom1Δ
WT
tom1Δ
Vector
DIA2
dia2-KR
Vector
DIA2
dia2-KR
Vector
SV DIA2
SV dia2-KA
SV dia2-Δ185-193
Vector
SV DIA2
SV dia2-KA
SV dia2-Δ185-193
B
Vector
SV DIA2
SV dia2-KA
Asy
Time (min)
75
60
45
30
15
0
1C 2C
C
Time (min)
WT
tom1Δ
dia2Δ
tom1Δ dia2Δ
40
35
30
25
0
Asy
1C 2C

Figure 28. Tom1-mediated Dia2 turnover is required for efficient G1 to S phase progression. (A) Overexpression of the *SVdia2-KA* mutant leads to a growth defect in wildtype cells. Wildtype and *tom1Δ* strains carrying the indicated galactose-inducible vectors were spotted in 10-fold dilutions onto minimal media containing 2% galactose. Plates were incubated at 30°C for 2-3 days. SV indicates the SV40 Tag NLS. (B) Overexpression of the *SVdia2-KA* mutant causes a delay in G1 to S-phase progression. Wildtype cells carrying the indicated galactose-inducible plasmids were grown to mid-log phase in minimal media containing 2% galactose. Samples were processed for flow cytometry. Separately, cells were also arrested with αF for 3 h and released into minimal media containing 2% galactose and 15μg/ml nocodazole. Samples were taken at the indicated times and prepared for flow cytometry. (C) Suppression of G1 to S phase progression delay of *tom1Δ* mutant by deletion of *DIA2*. Wildtype, *tom1Δ*, *dia2Δ*, and *tom1Δ dia2Δ* cells were arrested with αF for 3 h and released into rich medium containing 15μg/ml nocodazole. Samples taken at the indicated times were processed for flow cytometry. Arrows indicate start of S-phase.

Table III. Yeast Strains used in Chapter III

Strain	Genotype	Source
DKY153	*ade2-1 ura3-1 leu2-3,112 his3-11,15 trp1-1 can1-100 MAT a*	This study
DKY194	*dia2Δ::kanMX ade2-1 ura3-1 leu2-3,112 his3-11,15 trp1-1 can1-100 MAT a*	This study
DKY526	*tom1Δ::kanMX ade2-1 ura3-1 leu2-3,112 his3-11,15 trp1-1 can1-100 MAT a*	This study
DKY527	*tom1Δ::kanMX dia2Δ::kanMX ade2-1 ura3-1 leu2-3,112 his3-11,15 trp1-1 can1-100 MAT a*	This study
DKY534	*tom1C3235A::URA3 ade2-1 ura3-1 leu2-3,112 his3-11,15 trp1-1 can1-100 MAT a*	This study
DKY536	*tom1C3235A::URA3 dia2Δ::kanMX ade2-1 ura3-1 leu2-3,112 his3-11,15 trp1-1 can1-100 MAT a*	This study
AKY149	*9MYC-DIA2::URA3 dia2Δ::kanMX ade2-1 ura3-1 leu2-3,112 his3-11,15 trp1-1 can1-100 MAT a*	(45)
DKY538	*TOM1-3XFLAG::kanMX ade2-1 ura3-1 leu2-3,112 his3-11,15 trp1-1 can1-100 MAT a*	This study
DKY533	*tom1Δ::kanMX 9MYC-DIA2::URA3 dia2Δ::kanMX ade2-1 ura3-1 leu2-3,112 his3-11,15 trp1-1 can1-100 MAT a*	This study
DKY558	*tom1C3235A::URA3 9MYC-DIA2::URA3 dia2Δ::kanMX ade2-1 ura3-1 leu2-3,112 his3-11,15 trp1-1 can1-100 MAT a*	This study
DKY540	*TOM1-3XFLAG::kanMX 9MYC-DIA2::URA3 dia2Δ::kanMX ade2-1 ura3-1 leu2-3,112 his3-11,15 trp1-1 can1-100 MAT a*	This study
AKY192	*9MYC-dia2-TPR::URA3 dia2Δ::kanMX ade2-1 ura3-1 leu2-3,112 his3-11,15 trp1-1 can1-100 MAT a*	(45)
DKY596	*TOM1-3XFLAG::kanMX 9MYC-dia2-TPR::URA3 dia2Δ::kanMX ade2-1 ura3-1 leu2-3,112 his3-11,15 trp1-1 can1-100 MAT a*	This study
AKY188	*9MYC-dia2-ΔF::URA3 dia2Δ::kanMX ade2-1 ura3-1 leu2-3,112 his3-11,15 trp1-1 can1-100 MAT a*	(45)
DKY904	*TOM1-3XFLAG 9MYC-dia2-ΔF::URA3 dia2Δ::kanMX ade2-1 ura3-1 leu2-3,112 his3-11,15 trp1-1 can1-100 MAT a*	This study
AKY199	*9MYC-dia2-ΔN149::URA3 dia2Δ::kanMX ade2-1 ura3-1 leu2-3,112 his3-11,15 trp1-1 can1-100 MAT a*	(45)
DKY592	*TOM1-3XFLAG 9MYC-dia2-ΔN149::URA3 dia2Δ::kanMX ade2-1 ura3-1 leu2-3,112 his3-11,15 trp1-1 can1-100 MAT a*	This study

AKY240	*9MYC-SV40NLS-dia2-ΔNLS::URA3 dia2Δ::kanMX ade2-1 ura3-1 leu2-3,112 his3-11,15 trp1-1 can1-100 MAT a*	(45)
DKY595	*TOM1-3XFLAG 9MYC-SV40NLS-dia2-ΔNLS::URA3 dia2Δ::kanMX ade2-1 ura3-1 leu2-3,112 his3-11,15 trp1-1 can1-100 MAT a*	This study
DKY952	*9MYC-dia2-KR::URA3 dia2Δ::kanMX ade2-1 ura3-1 leu2-3,112 his3-11,15 trp1-1 can1-100 MAT a*	This study
DKY976	*TOM1-3XFLAG::kanMX 9MYC-dia2-KR::URA3 dia2Δ::kanMX ade2-1 ura3-1 leu2-3,112 his3-11,15 trp1-1 can1-100 MAT a*	This study
AKY238	*9MYC-SV40NLS-DIA2::URA3 dia2Δ::kanMX ade2-1 ura3-1 leu2-3,112 his3-11,15 trp1-1 can1-100 MAT a*	(45)
DKY968	*9MYC-SV40NLS-dia2-KA::URA3 dia2Δ::kanMX ade2-1 ura3-1 leu2-3,112 his3-11,15 trp1-1 can1-100 MAT a*	This study
DKY979	*TOM1-3XFLAG::kanMX 9MYC-SV40NLS-dia2-KA::URA3 dia2Δ::kanMX ade2-1 ura3-1 leu2-3,112 his3-11,15 trp1-1 can1-100 MAT a*	This study
DKY969	*9MYC-SV40NLS-dia2-Δ185-193::URA3 dia2Δ::kanMX ade2-1 ura3-1 leu2-3,112 his3-11,15 trp1-1 can1-100 MAT a*	This study

Table IV. Plasmids used in Chapter III

Plasmid	Features	Source
p1219	*GAL1,10* promoter, *CEN TRP1 Amp^r*	(55)
pACK135	*GAL1,10* promoter, *9MYC-DIA2 CEN TRP1 Amp^r*	(45)
pACK176	*GAL1,10* promoter, *9MYC-SV40NLS-DIA2 CEN TRP1 Amp^r*	(45)
pDHK9	*GAL1,10* promoter, *9MYC-dia2-KR CEN TRP1 Amp^r*	This study
pDHK10	*GAL1,10* promoter, *9MYC-SV40NLS-dia2-KA CEN TRP1 Amp^r*	This study
pDHK11	*GAL1,10* promoter, *9MYC-SV40NLS-dia2-Δ185-193 CEN TRP1 Amp^r*	This study
pDHK12	pRS406 1-kb *5'DIA2 UTR 9 9MYC-dia2-KR URA3 Amp^r*	This study
pDHK13	pRS406 1-kb *5'DIA2 UTR 9 9MYC-SV40NLS-dia2-KA URA3 Amp^r*	This study
pDHK14	pRS406 1-kb *5'DIA2 UTR 9 9MYC-SV40NLS-dia2-Δ185-193 URA3 Amp^r*	This study

Table V. Oligonucleotides used in Chapter III

Oligonucleotide	Sequence (5’ - 3’)
DHK3	GTTCACTATTATTGGCAATCAATGAAGGGCATGAAGGGTTTGGTCTTGCCAGGGAACAAAAGCTGGAGCTC
DHK4	CGTTCTAAAATACTTGGTTACATGGCGCTATAAATTTACACGAAAAATGACTATAGGGCGAATTGGGTACC
DHK16	GGGAATAGTAGAAGAAAAGG
DHK17	CAATTGGATATAGCTTGTTC
ACT1-5	ACAACGAATTGAGAGTTGCCCCAG
ACT1-3	AATGGCGTGAGGTAGAGAGAAACC
DHK106	GGAATTCCATATGTCTTCCCCAGGGAATTC
DHK107	GAGGAGACCAAAATAGCAAGAAGAAGAAGGAATAATAATGTTCTAGAA
DHK108	TTCTAGAACATTATTATTCCTTCTTCTTCTTGCTATTTTGGTCTCCTC
DHK109	TCGTTACCAAGGAGGAGGATTAGAGGTAGTACC
DHK110	GGTACTACCTCTAATCCTCCTCCTTGGTAACGA
DHK111	GCAGAACCACTTATCGATGTCCCCATTAGATCCAAC
DHK112	GAGGAGACCAAAATAGCAGCAGCAGCAGCGAATAATAATGTTCTAGAA
DHK113	TTCTAGAACATTATTATTCGCTGCTGCTGCTGCTATTTTGGTCTCCTC
DHK114	TCGTTACCAGCGGCGGCGATTGCAGGTAGTACC
DHK115	GGTACTACCTGCAATCGCCGCCGCTGGTAACGA
DHK116	GAGGAGACCAAAATAGCAAAAAAAAAAAAGAAGAAGAAGATTAAAGGTAGTACCAAGAAA
DHK117	TTTCTTGGTACTACCTTTAATCTTCTTCTTCTTTTTTTTTTTTGCTATTTTGGTCTCCTC

CHAPTER IV

Summary and Discussion

Cdc6 degradation by a Tom1 and Dia2-dependent pathway regulates pre-RC assembly during the cell cycle

I have identified that the Hect E3 ligase Tom1 and the F-box protein Dia2 are required for Cdc6 degradation during G1 and at the G1 to S phase transition. Tom1 and Dia2 act in the same pathway or co-operatively but function independently of the SCF^{Cdc4} complex. Consistent with this, *cdc4-1 tom1Δ* and *cdc4-1 dia2Δ* mutants exhibit greater Cdc6 stabilization than single mutants at the G1 to S phase transition. In addition, *tom1Δ dia2Δ* double mutant shows equivalent Cdc6 turnover to *tom1Δ* or *dia2Δ* single mutants in G1 and at the G1 to S phase transition. Tom1 and Dia2 recognize a Cdc6 N-terminal mutant which lacks amino acids 2-47. Defects in Tom1- or Dia2-mediated Cdc6 proteolysis lead to aberrant Cdc6 chromatin association and Mcm4 binding to early origins. More importantly, increased DNA content is observed in *tom1Δ* mutant when ORC phosphorylation and Mcm2-7 export to the cytoplasm are compromised, suggesting that Cdc6 degradation by a Tom1-mediated pathway may control re-replication along with other inhibitory mechanisms.

It is surprising that Cdc6 is stabilized in *dia2 ΔF-box* mutant but not in *scf* mutants during the G1 phase of the cell cycle because previous work showed that SCF complexes are not responsible for Cdc6 degradation in G1 (21). Although a non-SCF role of Dia2 has not been previously identified, Dia2 might play a role in Cdc6 degradation independently of a traditional SCF complex since other F-box proteins have been shown

to function outside of SCF complexes (24, 29, 91, 99). Identifying Dia2 interacting proteins in G1 will help to elucidate the non-SCF role of Dia2 in Cdc6 degradation during G1. For example, Dia2 might assemble a Cullin-based complex with Rtt101, also known as Cul8, to regulate Cdc6 degradation during G1. Future experiments will be necessary to test these possibilities. In addition, I cannot rule out the possibility that other pathways may also contribute to Cdc6 degradation during G1 phase. This possibility is supported by the observation that the Cdc6ΔN mutant is stabilized in G1 and its stability is significantly enhanced in *tom1Δ* and *dia2Δ* mutants during G1 phase. Thus, identification of another E3 ligase responsible for this pathway will provide insight into the mechanism of Cdc6 degradation during G1.

The biological significance of Tom1- or Dia2-mediated Cdc6 proteolysis in G1 still remains elusive. The Tom1- and Dia2-mediated pathway may be important to regulate the assembly of the pre-RC complex during G1. In support of this idea, I observed that Cdc6 chromatin association and Mcm4 binding to early origins are increased in *tom1Δ* and *dia2Δ* mutants during G1. Given that Cdc6 synthesis is increased in late G1 and only an individual Cdc6 protein is required for pre-RC assembly at a single origin, excess Cdc6 proteins may need to be targeted for degradation by the Tom1- and Dia2-mediated pathway. Future studies will be required to unravel the biological significance of Cdc6 degradation during G1.

My data suggest that multiple E3 ligases are required for Cdc6 degradation at the G1 to S phase transition. This raises a question about how specificity of these E3s is regulated. The SCF^{Cdc4} complex requires Cdk-mediated phosphorylation for recognition

and degradation of Cdc6 (73). However, it is not clear whether Tom1 and Dia2 recognize phosphorylated Cdc6. The requirement of Cdk-dependent phosphorylation for Tom1- or Dia2-mediated Cdc6 degradation needs to be examined. If Tom1 and Dia2 bind phosphorylated Cdc6 for degradation, it is likely that they recognize Cdk consensus sites located in a domain in Cdc6 C-terminal to amino acid 47 since I have shown that Tom1 and Dia2 bind the Cdc6 N-terminal mutant. Among four consensus sites (T135, S354, T368, and S372) located in the domain described above, two sites T368 and S372 have been shown to be recognized by the SCF^{Cdc4} complex for degradation during G2/M (73). If Cdk-mediated phosphorylation is important for Tom1 and Dia2 to target Cdc6 for degradation, phosphorylation at the other two consensus sites T135 and S354 might be required for Tom1 and Dia2 to recognize Cdc6, as a Tom1- and Dia2-mediated pathway is distinct from the SCF^{Cdc4} complex. However, it is unlikely that the Tom1- and Dia2-mediated pathway requires Cdk-dependent phosphorylation for Cdc6 degradation, as Tom1 and Dia2 control Cdc6 degradation in G1 when Cdk activity is low.

I have suggested that Tom1-mediated Cdc6 degradation may be important to control re-replication in a strain sensitized to re-replication. Although flow cytometry analysis shows that DNA content above 2C is increased in *tom1Δ* mutant in a background sensitized to re-replication, I do not know what fraction of early origins are re-fired in that strain within a single cell cycle. Alternatively, flow cytometry assay might not be sensitive to detect a subset of origins that have been re-fired within a single cell cycle. Thus, microarray comparative genomic hybridization (CGH) assay will be needed to further analyze and answer this question.

Loss of re-replication control may contribute to tumorigenesis. Recent work in budding yeast has demonstrated that the absence of re-replication control is a potent inducer of gene amplifications (31), which are hallmarks of cancer cells. Intriguingly, the human homolog of Tom1, HUWE1/ARF-BP/Mule, has been proposed to contribute to tumorigenesis, but the mechanism by which this occurs is unclear. HUWE1/ARF-BP/Mule has multiple ubiquitination targets, several of which act in antagonistic pathways (1, 12, 100), making it difficult to sort out the contribution of HUWE1/ARF-BP/Mule to cancer development. No link to re-replication has yet been investigated, although increased Cdc6 abundance has been observed in HUWE1-depleted cells in the presence of DNA damage (32). This suggests that the role of HUWE1 in Cdc6 degradation may be to promote growth arrest in response to DNA damage, implying that HUWE1-mediated Cdc6 degradation may help to impede the growth of cancer cells. In this case, the loss of HUWE1 may contribute to tumorigenesis. However, future studies will be needed to determine the significance of this observation.

The Hect E3 ubiquitin ligase Tom1 controls Dia2 degradation during the cell cycle

I have found that the Hect-domain E3 ligase Tom1 targets Dia2 for ubiquitin-dependent degradation during G1 and G2/M phases by recognizing the specific positively charged residues in the degradation/NLS domain of Dia2. Deletion of *DIA2* partially suppresses the temperature-sensitive growth phenotype of *tom1Δ* and *tom1C3235A* mutants. Moreover, overexpression of Dia2 in *tom1*mutants causes a growth defect, suggesting that Tom1 controls Dia2 degradation. Tom1-mediated Dia2 proteolysis during

the cell cycle is regulated by a proteolytic switch mechanism. Tom1 binding to Dia2 is enhanced in G1 and reduced during S phase or in response to activation of the S-phase checkpoint. The positively charged residues in the degradation/NLS domain are required for Tom1 to recognize and target Dia2 for degradation. Defects in Dia2 degradation caused by loss of the positively charged residues or deletion of *TOM1* result in a delay in G1 to S phase progression. In support of this, deletion of *DIA2* rescues a delay in G1 to S phase progression of *tom1Δ* mutant.

I showed that Dia2 ubiquitination is dependent on Tom1. However, I do not know the identity of E2 enzyme for Dia2 ubiquitination since the fractionated yeast extract used in the *in vitro* assay contains multiple E2 proteins. Identifying the E2 protein responsible for this will be needed in the future.

Although I have identified a domain, also known as degron, required for Dia2 to bind Tom1, the sites of ubiquitination in Dia2 are still not known. When the lysines located in the degradation domain were replaced with arginines, Dia2-KR was still turned over as fast as wildtype Dia2, indicating that those lysines do not serve as ubiquitination sites. However, it is possible that the TPR domain of Dia2 may contain the ubiquitination sites. One model that supports this idea is that the TPR Dia2 binding to Tom1 is weaker than full-length or ΔN149 Dia2, implying that the TPR domain may be quickly degraded as soon as Tom1 binds and ubiquitinates it. We look forward to identifying the ubiquitination sites on Dia2 in the future.

The biological significance of Tom1 in cellular processes remains to be further understood, although several reports have shown that Tom1 functions in DNA damage,

transcriptional activation, and mRNA export (32, 40, 82, 86). Thus, identifying Tom1 targets will be important to clarify the biological role of Tom1 in various cellular processes including DNA replication and DNA damage response. I have found that the specific positively charged residues in the degradation/NLS domain in Dia2 are required for Dia2 binding to Tom1. I was also able to identify a list of proteins that contain a stretch of positively charged residues similar to this using a BLAST search. If this domain serves as a degron for potential Tom1 targets, it will be important to test whether those candidate proteins are *bona fide* Tom1 substrates. One of those candidates I found using the BLAST search is Dpb11 which assembles the pre-LC complex with Sld2, GINS, and Polymerase ε. Given that abundance of Dpb11 is low and it is likely an unstable protein, it is tempting to speculate that Dpb11 may be a novel substrate of Tom1. Identifying Tom1 substrates that are involved in DNA replication or cell cycle will help us better understand the mechanistic role of Tom1 in these processes. In addition to the BLAST search, screening potential suppressors of the temperature-sensitive phenotype of *tom1* mutants may be a good alternative to identify Tom1 substrates.

Dia2 has been shown to play a role in DNA replication and activation of the S-phase checkpoint (5, 45, 47, 60, 62). However, the mechanistic role of Dia2 in these processes is not clear. Dia2 has two potential substrates, Mrc1 and Ctf4, but the biological significance of their ubiquitination is not known (60). Identification of Dia2 substrates involved in cell cycle, DNA replication, and activation of the S-phase checkpoint will be necessary to elucidate the functional significance and mechanistic role of Dia2 in those

cellular processes. In addition to its role in activation of the S-phase checkpoint or DNA replication, I also showed that Tom1-mediated Dia2 turnover in G1 contributes to G1 to S phase progression, suggesting that Dia2 may have an additional role in controlling the G1 to S phase transition or have a potential target that promotes the entry into S phase from G1 phase. For example, defects in Dia2 turnover in G1 may alter the balance of SCF complexes such that the abundance of Cdk inhibitor Sic1, which is targeted by the SCF^{Cdc4} complex for degradation in late G1, might be increased, leading to a defect in G1 to S-phase progression. Alternatively, Cdc6 could be that potential substrate of Dia2 in G1 as overexpression of Dia2 in G1 leads to a delay in G1 to S phase progression.

Altogether, I have found that Tom1 and Dia2 control Cdc6 degradation during G1 and at the G1 to S-phase transition and that Tom1 also targets Dia2 for degradation during G1 and G2/M. This raises an important question about the relationship among Tom1, Dia2, and Cdc6. How does Tom1-mediated Dia2 proteolysis affect the role of Dia2 in Cdc6 degradation? Given that *tom1Δ* mutant exhibits more severe defects or phenotypes such as Cdc6 ubiquitination, aberrant Cdc6 chromatin association, and enhanced Mcm4 binding to early origins than *dia2Δ* mutant, it is likely that Tom1-mediated Dia2 degradation may account for the difference of these defects or phenotypes. Why do Tom1 and Dia2 function in the same pathway to control Cdc6 degradation? How does Tom1-mediated Dia2 degradation contribute to regulating Cdc6 proteolysis during G1? One possible explanation is that if Tom1 did not control Dia2 degradation in G1, both Tom1 and stabilized Dia2 may function redundantly to target Cdc6 for degradation. As a result, Cdc6 levels may be too low in G1 by these two redundant pathways. This

may result in inhibition of pre-RC assembly at some origins in G1, leading to insufficient DNA replication initiation. In support of this idea, when the *SV dia2 KA* mutant which is not targeted for degradation by Tom1 was over-expressed in wildtype cells, it caused a significant delay in G1 to S phase progression, implying that the regulation of Cdc6 degradation in G1 may be important for a proper G1 to S phase progression. Future studies will be needed to clarify this relationship.

CHAPTER V

Materials and Methods

Plasmids and strains

Yeast strains and oligonucleotides used in the Chapter II are described in Tables I and II. To generate the *CDC6-3HA* strain (DKY546), the *3HA-TRP1* fragment containing the 3' end of *CDC6* open reading frame and the 3' UTR of *CDC6* was amplified with primers DHK9 and 10 using pFA6a-3HA-TRP1 as a template (56) and integrated into strain DKY153 via homologous recombination. The centromeric HA-CDC6 TRP1 plasmid using a *GAL1,10* promoter (pDHK1) was constructed via PCR amplification of *CDC6* from genomic DNA with primers DHK6 and 7 and then inserted into *SalI* and *BamHI* sites of the p1216 plasmid. To generate the GST-*CDC6* baculovirus construct (pZHW073), the *CDC6* open reading frame was amplified with primers DHK25 and 26 using yeast genomic DNA and cloned into the pUNI-10 vector with *NdeI* and *BamHI* sites (pZHW072). Plasmid pZHW072 was then recombined with p1212 (55) using cre-lox recombination to generate plasmid pZHW073. To generate the FLAG-*TOM1 HECT* baculovirus construct (pDHK5), the *HECT* domain was amplified using yeast genomic DNA with primers DHK84 and 85 and cloned into the pUNI-10 vector with *XhoI* and *BamHI* sites to construct the plasmid pDHK4. Plasmid pDHK4 was then recombined with p1214 (55) using cre-lox recombination to generate the FLAG-*TOM1 HECT* baculovirus construct (pDHK5). The pUNI-10-*CDC6ΔN*, - *DIA2 TPR*, and - *DIA2-ΔN214* plasmids (pDHK7, pZHW094, pZHW079) were constructed by amplifying the

CDC6ΔN, DIA2 TPR, and *DIA2-ΔN214* fragments using the plasmids pDHK6, pACK140, and pACK137 as a template with primers DHK104, 105, ZHW57, 54, 58, and AK43. The amplified fragments were then cloned into the *XhoI* and *NotI*, the *NdeI* and *SalI*, and the *NdeI* and *BamHI* sites of the pUNI-10 plasmid, respectively. The GST-*CDC6ΔN,* FLAG-*DIA2 TPR* and FLAG-*DIA2-ΔN214* baculovirus constructs (pDHK8, pZHW095 and pZHW080) were also generated via cre-lox recombination using p1212 and p1214 (55). To construct the *CDC6ΔN-3HA* strain (DKY875), the *CDC6-3HA-TRP1* fragment was cloned into pBluescript SK+ plasmid with *XhoI* and *NotI* sites to generate plasmid (pDHK2). The N-terminal 2-47 amino acid was then deleted by amplifying the *CDC6ΔN* fragment using the plasmid pDHK2 as a template with primers DHK46, 82, 81, and 48 and cloned into the *XhoI* and *NotI* sites of the plasmid pDHK2 to construct the plasmid *CDC6ΔN*-3HA (pDHK6). The *CDC6ΔN*-3HA fragment cut with the *XhoI* and *NotI* restriction enzymes was integrated into strain DKY 153 via homologous recombination. For generating the strains used in re-replication assay (Figure 21), the *cdc4-1* allele was amplified using yeast genomic DNA isolated from the *cdc4-1* strain (DKY173) with primers DHK88 and 89 and then inserted into pRS406 URA3 plasmid (pDHK3). Plasmid pDHK3 was linearized with the *BpU10I* restriction enzyme and transformed into YJL2068 (*orc2 6A orc6 4A MCM7-2NLS* from J. Li, UCSF, Nguyen *et al.*, 2001). A loop-in/out gene replacement method was used to generate strain DKY891. The open reading frames of *TOM1* and *DIA2* were replaced with *KanMX* via homologous recombination in strains YJL2068 and DKY891 to construct strains DKY876 and 878, respectively. The *CDC6ΔN*-3HA fragment cut with *XhoI* and *NotI* restriction enzymes

was also integrated into strain YJL 2068 via homologous recombination to generate strain DKY896. For generating the mitochondrial DNA deficient rho^0 strains (DKY955, 957, 959, 961, and 963), strains YJL2068, DKY891, 876, 878, and 896 were grown on rich medium plates containing 10μg/ml ethidium bromide. The loss of mitochondrial DNA was confirmed by testing individual colonies on YP plates containing 3% glycerol.

Yeast strains, plasmids, and oligonucleotides used in the Chapter III are described in Tables III, IV, and V. To generate the *tom1Δ* strain (DKY526), the open reading frame of *TOM1* was replaced with *KanMX* via homologous recombination in strain DKY153. The *TOM1-3FLAG* strain (DKY538) was generated using the previously described method (30). The centromeric *9MYC-DIA2 KR*, *9MYC-SV40-DIA2-KA*, and *9MYC-SV40-Δ185-193* plasmids using a *GAL1,10* promoter (pDHK9, 10, and 11, respectively) were constructed via the generation of the KR or KA substitution and the deletion of 185-193 fragment (Δ185-193) by the PCR stitching method using the plasmids pACK135 or pACK176 with primers DHK107, 108, 109, 110 and 112, 113, 114, 115, 116, 117 and followed by the amplification of the *KR*, *KA*, and *Δ185-193* fragments with primers DHK106 and 111. Then, these fragments were inserted into *MluI* and *HpaI* sites of the pACK135 or pACK176 plasmids. To construct the 9MYC-*KR*, 9MYC-*SV40-KA*, and 9MYC-*SV40-Δ185-193* strains (DKY952, 968, and 969), the 9MYC-*KR*, 9MYC-*SV40-KA*, and 9MYC-*SV40-Δ185-193* fragments were cloned into the plasmids pACK142 and pACK181 with *MluI* and *HpaI* sites to generate plasmids (pDHK12, 13, and 14,

respectively). The plasmids (pDHK12, pDHK13, and pDHK14) linearized with the *BclI* restriction enzyme were integrated into strain DKY194 via homologous recombination.

Reverse transcription PCR (RT-PCR)

Cultures were grown to mid-log phase (2 x 10^7 cells/ml) at 30°C and total RNA was isolated with PURE LINK micro- to midi-Kit (Invitrogen) using the manufacturer's protocol. After DNase I treatment, 3 μg of total RNA was reverse transcribed using Superscript II (Invitrogen) with oligo $(dT)_{50}$ primer. The cDNA was amplified with primers DHK11, 12 16, and 17 or ACT1-5 and ACT1-3.

In vitro binding assays

1mg of total cell lysate isolated from baculovirus-infected Hi5 insect cells was immunoprecipitated with anti-Flag M2 monoclonal (Sigma), anti-Myc 9E10 monoclonal (Covance) or anti-GST polyclonal (Santa Cruz) antibodies and immunoblotted with anti-Flag M2, anti-Myc 9E10 and anti-GST (Santa Cruz) antibodies.

Stability assays

Cells at 1 x 10^7 cells/ml were arrested with 40μg/ml αF, 200 mM hydroxyurea or 15μg/ml nocodazole for 3 h. To arrest cells in early S, cells were released from αF arrest into rich medium containing 200 mM hydroxyurea for 90 min. Cycloheximide was added at 100 μg/ml. Cell pellets were washed and lysed by vortexing with glass beads in 20% trichloroacetic acid (TCA) for 3 min. Lysed cell pellets were centrifuged at 3,000 rpm for

10 min and resuspended in Laemmli buffer. Precipitated proteins were neutralized with 1M Tris and boiled for 5 min. Protein concentration was quantified using the RC/DC protein assay kit (BioRad). 20 μg of proteins were run on 8% SDS-PAGE. Protein abundance was measured using the Image J software and normalized against a loading control.

Immunoprecipitation

Cells were cultured to mid-log phase (2 x 10^7 cells/ml) and collected by centrifuging at 4,000 rpm for 2 min. For Cdc6 co-immunoprecipitation analysis, total cell lysate was isolated by vortexing the cells with glass beads in RIPA buffer (1% Triton X-100, 0.1% SDS, 0.5% deoxycholic acid, 20 mM Tris pH 7.5, 10% Glycerol) with protease inhibitor cocktail (Roche) for 40 min at 4°C. Protein concentration was determined using Bio-Rad protein assay (Bio-Rad). 1 mg of total lysate was incubated with affinity matrix anti-HA.11 (Covance) and Protein A/G agarose (Santa Cruz) for 3 h at 4°C. Samples were washed with RIPA buffer 4 times and boiled in Laemmli buffer for 5 min.

To perform Tom1 co-immunoprecipitation assays, cells were cultured to mid-log phase (2 x 10^7 cells/ml) and collected by centrifuging at 4,000 rpm for 2 min. Total cell lysate was isolated by vortexing the cells with glass beads in 0.3% CHAPS buffer (0.3% CHAPS, 40 mM HEPES pH 7.4, 120 mM NaCl, 1mM EDTA, 50mM NaF, 10mM Glycerol 2-β) with protease inhibitor cocktail (Roche) for 40 min at 4°C. Protein concentration was determined using Bio-Rad protein assay (Bio-Rad). 2 mg of total lysate was incubated with anti-Flag M2 monoclonal (Sigma) antibodies and Protein A/G

agarose (Santa Cruz) for 3 h at 4°C. Samples were washed with CHAPS buffer 4 times and boiled in Laemmli buffer for 5 min.

In vivo and *In vitro* Ubiquitination assays

For *in vivo* Cdc6 ubiquitination, cells were grown to mid-log phase and treated with DMSO or 50 μM MG132 for 2h. 2mg of total protein was used for immunoprecipitation with anti-HA.11 monoclonal antibodies (Covance). Proteins were analyzed by 8% SDS-PAGE followed by an immunoblot assay with anti-P4D1 monoclonal ubiquitin and -HA.11 antibodies (Covance).

For *in vitro* Cdc6 ubiquitination, 50 μg of fractionated yeast extracts were incubated with 50 μg ubiquitin, 50 nM E1, 1.5 μg Cdc34 (E2), 10 mM ATP, 60 mM creatine phosphate, 1 mM magnesium acetate, 150 μg/ml creatine kinase, and 40 μg GST-Cdc6 protein bound to the Glutathione Sepharose 4B beads (GE Health care) at 30°C for 45 min. Samples were run on 6% SDS-PAGE and immunoblotted with anti-GST polyclonal antibodies (Santa Cruz).

To perform *in vitro* Dia2 ubiquitination assay, 50 μg of fractionated yeast extracts were incubated with 50 μg ubiquitin, 50 nM E1, 10 mM ATP, 60 mM creatine phosphate, 1 mM magnesium acetate, 150 μg/ml creatine kinase, and 40 μg GST-Dia2 protein bound to the Glutathione Sepharose 4B beads (GE Health care) at 30°C for 45 min. Samples were run on 6% SDS-PAGE and immunoblotted with anti-GST polyclonal antibodies (Santa Cruz).

Chromatin fractionation

Chromatin fractionation assay was performed as described (53). Protein concentration was quantified using the RC/DC protein assay kit (BioRad). 30 μg of whole cell extract and crude chromatin fraction were resolved on 8% and 15% SDS-PAGE, respectively and analyzed by immunoblotting with anti-HA.11 (Covance), anti-3-phosphoglycerate kinase 22C5 (anti-Pgk1, Invitrogen), and anti-Histone H3 (Abcam) antibodies. The ratio of chromatin-bound Cdc6 to Histone H3 was measured using the Image J software.

Chromatin immunoprecipitation

Total yeast cell lysates were prepared for chromatin immunoprecipitations as previously described (89). PCR was performed using primers for early-firing origins *ARS1* and *ARS305* and non-origin region *ACF2*.

Flow cytometry

For re-replication assays, cells were arrested with 15 μg/ml nocodazole for 3h and shifted to 37°C. When cells were shifted to 37°C, nocodazole was also added to prevent cells from breaking through the nocodazole arrest. Samples were fixed at the indicated times and stained with propidium iodide. DNA re-replication was analyzed using FACS Calibur 501 (University of Minnesota flow cytometry facility). Flow Jo software was used to measure the populations of the cells with more than 2C DNA content.

BIBLIOGRAPHY

1. **Adhikary, S., F. Marinoni, A. Hock, E. Hulleman, N. Popov, R. Beier, S. Bernard, M. Quarto, M. Capra, S. Goettig, U. Kogel, M. Scheffner, K. Helin, and M. Eilers. 2005. The ubiquitin ligase HectH9 regulates transcriptional activation by Myc and is essential for tumor cell proliferation. Cell 123:409-21.**
2. **Araki, H. 2010. Cyclin-dependent kinase-dependent initiation of chromosomal DNA replication. Curr Opin Cell Biol 22:766-71.**
3. **Arias, E. E., and J. C. Walter. 2007. Strength in numbers: preventing rereplication via multiple mechanisms in eukaryotic cells. Genes Dev 21:497-518.**
4. **Ayyagari, R., X. V. Gomes, D. A. Gordenin, and P. M. Burgers. 2003. Okazaki fragment maturation in yeast. I. Distribution of functions between FEN1 AND DNA2. J Biol Chem 278:1618-25.**
5. **Blake, D., B. Luke, P. Kanellis, P. Jorgensen, T. Goh, S. Penfold, B. J. Breitkreutz, D. Durocher, M. Peter, and M. Tyers. 2006. The F-box protein Dia2 overcomes replication impedance to promote genome stability in Saccharomyces cerevisiae. Genetics.**
6. **Bloom, J., and F. R. Cross. 2007. Multiple levels of cyclin specificity in cell-cycle control. Nat Rev Mol Cell Biol 8:149-60.**
7. **Blow, J. J., and A. Dutta. 2005. Preventing re-replication of chromosomal DNA. Nat Rev Mol Cell Biol 6:476-86.**
8. **Borlado, L. R., and J. Mendez. 2008. CDC6: from DNA replication to cell cycle checkpoints and oncogenesis. Carcinogenesis 29:237-43.**
9. **Bueno, A., and P. Russell. 1992. Dual functions of CDC6: a yeast protein required for DNA replication also inhibits nuclear division. Embo J 11:2167-76.**
10. **Carrano, A. C., E. Eytan, A. Hershko, and M. Pagano. 1999. SKP2 is required for ubiquitin-mediated degradation of the CDK inhibitor p27. Nat Cell Biol 1:193-9.**
11. **Cenciarelli, C., D. S. Chiaur, D. Guardavaccaro, W. Parks, M. Vidal, and M. Pagano. 1999. Identification of a family of human F-box proteins. Curr Biol 9:1177-9.**
12. **Chen, D., N. Kon, M. Li, W. Zhang, J. Qin, and W. Gu. 2005. ARF-BP1/Mule is a critical mediator of the ARF tumor suppressor. Cell 121:1071-83.**
13. **Chen, S., and S. P. Bell. 2011. CDK prevents Mcm2-7 helicase loading by inhibiting Cdt1 interaction with Orc6. Genes Dev 25:363-72.**
14. **Cocker, J. H., S. Piatti, C. Santocanale, K. Nasmyth, and J. F. Diffley. 1996. An essential role for the Cdc6 protein in forming the pre-replicative complexes of budding yeast. Nature 379:180-2.**
15. **Cohen-Fix, O., J. M. Peters, M. W. Kirschner, and D. Koshland. 1996. Anaphase initiation in Saccharomyces cerevisiae is controlled by the APC-**

dependent degradation of the anaphase inhibitor Pds1p. Genes Dev 10:3081-93.

16. **Deshaies, R. J., and C. A. Joazeiro. 2009. RING domain E3 ubiquitin ligases. Annu Rev Biochem 78:399-434.**
17. **Devault, A., E. A. Vallen, T. Yuan, S. Green, A. Bensimon, and E. Schwob. 2002. Identification of Tah11/Sid2 as the ortholog of the replication licensing factor Cdt1 in Saccharomyces cerevisiae. Curr Biol 12:689-94.**
18. **Donovan, S., J. Harwood, L. S. Drury, and J. F. Diffley. 1997. Cdc6p-dependent loading of Mcm proteins onto pre-replicative chromatin in budding yeast. Proc Natl Acad Sci U S A 94:5611-6.**
19. **Drury, L. S., and J. F. Diffley. 2009. Factors affecting the diversity of DNA replication licensing control in eukaryotes. Curr Biol 19:530-5.**
20. **Drury, L. S., G. Perkins, and J. F. Diffley. 1997. The Cdc4/34/53 pathway targets Cdc6p for proteolysis in budding yeast. Embo J 16:5966-76.**
21. **Drury, L. S., G. Perkins, and J. F. X. Diffley. 2000. The cyclin-dependent kinase Cdc28p regulates distinct modes of Cdc6p proteolysis during the budding yeast cell cycle. Current Biology 10:231-240.**
22. **Elsasser, S., Y. Chi, P. Yang, and J. L. Campbell. 1999. Phosphorylation controls timing of Cdc6p destruction: A biochemical analysis. Mol Biol Cell 10:3263-77.**
23. **Elsasser, S., F. Lou, B. Wang, J. L. Campbell, and A. Jong. 1996. Interaction between yeast Cdc6 protein and B-type cyclin/Cdc28 kinases. Mol Biol Cell 7:1723-35.**
24. **Escobar-Henriques, M., B. Westermann, and T. Langer. 2006. Regulation of mitochondrial fusion by the F-box protein Mdm30 involves proteasome-independent turnover of Fzo1. J Cell Biol 173:645-50.**
25. **Feldman, R. M., C. C. Correll, K. B. Kaplan, and R. J. Deshaies. 1997. A complex of Cdc4p, Skp1p, and Cdc53p/cullin catalyzes ubiquitination of the phosphorylated CDK inhibitor Sic1p. Cell 91:221-30.**
26. **Friedel, A. M., B. L. Pike, and S. M. Gasser. 2009. ATR/Mec1: coordinating fork stability and repair. Curr Opin Cell Biol 21:237-44.**
27. **Galan, J. M., and M. Peter. 1999. Ubiquitin-dependent degradation of multiple F-box proteins by an autocatalytic mechanism. Proc Natl Acad Sci U S A 96:9124-9.**
28. **Garcia, V., K. Furuya, and A. M. Carr. 2005. Identification and functional analysis of TopBP1 and its homologs. DNA Repair (Amst) 4:1227-39.**
29. **Gearhart, M. D., C. M. Corcoran, J. A. Wamstad, and V. J. Bardwell. 2006. Polycomb group and SCF ubiquitin ligases are found in a novel BCOR complex that is recruited to BCL6 targets. Mol Cell Biol 26:6880-9.**
30. **Gelbart, M. E., T. Rechsteiner, T. J. Richmond, and T. Tsukiyama. 2001. Interactions of Isw2 chromatin remodeling complex with nucleosomal arrays: analyses using recombinant yeast histones and immobilized templates. Mol Cell Biol 21:2098-106.**

31. Green, B. M., K. J. Finn, and J. J. Li. 2010. Loss of DNA Replication Control Is a Potent Inducer of Gene Amplification. Science 329:943-946.
32. Hall, J. R., E. Kow, K. R. Nevis, C. K. Lu, K. S. Luce, Q. Zhong, and J. G. Cook. 2007. Cdc6 stability is regulated by the Huwe1 ubiquitin ligase after DNA damage. Mol Biol Cell 18:3340-50.
33. Hall, J. R., H. O. Lee, B. D. Bunker, E. S. Dorn, G. C. Rogers, R. J. Duronio, and J. G. Cook. 2008. Cdt1 and Cdc6 are destabilized by rereplication-induced DNA damage. J Biol Chem 283:25356-63.
34. Harper, J. W., and S. J. Elledge. 2007. The DNA damage response: ten years after. Mol Cell 28:739-45.
35. Heller, R. C., S. Kang, W. M. Lam, S. Chen, C. S. Chan, and S. P. Bell. 2011. Eukaryotic origin-dependent DNA replication in vitro reveals sequential action of DDK and S-CDK kinases. Cell 146:80-91.
36. Ho, Y., A. Gruhler, A. Heilbut, G. D. Bader, L. Moore, S. L. Adams, A. Millar, P. Taylor, K. Bennett, K. Boutilier, L. Yang, C. Wolting, I. Donaldson, S. Schandorff, J. Shewnarane, M. Vo, J. Taggart, M. Goudreault, B. Muskat, C. Alfarano, D. Dewar, Z. Lin, K. Michalickova, A. R. Willems, H. Sassi, P. A. Nielsen, K. J. Rasmussen, J. R. Andersen, L. E. Johansen, L. H. Hansen, H. Jespersen, A. Podtelejnikov, E. Nielsen, J. Crawford, V. Poulsen, B. D. Sorensen, J. Matthiesen, R. C. Hendrickson, F. Gleeson, T. Pawson, M. F. Moran, D. Durocher, M. Mann, C. W. Hogue, D. Figeys, and M. Tyers. 2002. Systematic identification of protein complexes in Saccharomyces cerevisiae by mass spectrometry. Nature 415:180-3.
37. Honey, S., and B. Futcher. 2007. Roles of the CDK phosphorylation sites of yeast Cdc6 in chromatin binding and rereplication. Mol Biol Cell 18:1324-36.
38. Huang, T. T., and A. D. D'Andrea. 2006. Regulation of DNA repair by ubiquitylation. Nat Rev Mol Cell Biol 7:323-34.
39. Hurley, J. H., and H. Stenmark. 2011. Molecular mechanisms of ubiquitin-dependent membrane traffic. Annu Rev Biophys 40:119-42.
40. Iglesias, N., E. Tutucci, C. Gwizdek, P. Vinciguerra, E. Von Dach, A. H. Corbett, C. Dargemont, and F. Stutz. 2010. Ubiquitin-mediated mRNP dynamics and surveillance prior to budding yeast mRNA export. Genes Dev 24:1927-38.
41. Iovine, B., M. L. Iannella, and M. A. Bevilacqua. 2011. Damage-specific DNA binding protein 1 (DDB1): a protein with a wide range of functions. Int J Biochem Cell Biol 43:1664-7.
42. Jin, Y., E. K. Blue, S. Dixon, L. Hou, R. B. Wysolmerski, and P. J. Gallagher. 2001. Identification of a new form of death-associated protein kinase that promotes cell survival. J Biol Chem 276:39667-78.
43. Kawakami, H., and T. Katayama. 2010. DnaA, ORC, and Cdc6: similarity beyond the domains of life and diversity. Biochem Cell Biol 88:49-62.
44. Kelly, T. J., and G. W. Brown. 2000. Regulation of chromosome replication. Annu Rev Biochem 69:829-80.

45. Kile, A. C., and D. M. Koepp. 2010. Activation of the S-phase checkpoint inhibits degradation of the F-box protein Dia2. Mol Cell Biol 30:160-71.
46. Kim, H. M., Y. Yu, and Y. Cheng. 2011. Structure characterization of the 26S proteasome. Biochim Biophys Acta 1809:67-79.
47. Koepp, D. M., A. C. Kile, S. Swaminathan, and V. Rodriguez-Rivera. 2006. The F-box protein Dia2 regulates DNA replication. Mol Biol Cell 17:1540-8.
48. Koepp, D. M., L. K. Schaefer, X. Ye, K. Keyomarsi, C. Chu, J. W. Harper, and S. J. Elledge. 2001. Phosphorylation-dependent ubiquitination of cyclin E by the SCFFbw7 ubiquitin ligase. Science 294:173-7.
49. Komander, D., and M. Rape. 2012. The ubiquitin code. Annu Rev Biochem 81:203-29.
50. Kouranti, I., and A. Peyroche. 2012. Protein degradation in DNA damage response. Semin Cell Dev Biol 23:538-45.
51. Kunkel, T. A., and P. M. Burgers. 2008. Dividing the workload at a eukaryotic replication fork. Trends Cell Biol 18:521-7.
52. Kus, B. M., C. E. Caldon, R. Andorn-Broza, and A. M. Edwards. 2004. Functional interaction of 13 yeast SCF complexes with a set of yeast E2 enzymes in vitro. Proteins 54:455-67.
53. Liang, C., and B. Stillman. 1997. Persistent initiation of DNA replication and chromatin-bound MCM proteins during the cell cycle in cdc6 mutants. Genes Dev 11:3375-86.
54. Liang, C., M. Weinreich, and B. Stillman. 1995. ORC and Cdc6p interact and determine the frequency of initiation of DNA replication in the genome. Cell 81:667-76.
55. Liu, Q., M. Z. Li, D. Leibham, D. Cortez, and S. J. Elledge. 1998. The univector plasmid-fusion system, a method for rapid construction of recombinant DNA without restriction enzymes. Curr Biol 8:1300-9.
56. Longtine, M. S., A. McKenzie, 3rd, D. J. Demarini, N. G. Shah, A. Wach, A. Brachat, P. Philippsen, and J. R. Pringle. 1998. Additional modules for versatile and economical PCR-based gene deletion and modification in Saccharomyces cerevisiae. Yeast 14:953-61.
57. Maiorano, D., J. Moreau, and M. Mechali. 2000. XCDT1 is required for the assembly of pre-replicative complexes in Xenopus laevis. Nature 404:622-5.
58. Melo, J., and D. Toczyski. 2002. A unified view of the DNA-damage checkpoint. Curr Opin Cell Biol 14:237-45.
59. Michel, J. J., J. F. McCarville, and Y. Xiong. 2003. A role for Saccharomyces cerevisiae Cul8 ubiquitin ligase in proper anaphase progression. J Biol Chem 278:22828-37.
60. Mimura, S., M. Komata, T. Kishi, K. Shirahige, and T. Kamura. 2009. SCF(Dia2) regulates DNA replication forks during S-phase in budding yeast. Embo J 28:3693-705.
61. Mimura, S., T. Seki, S. Tanaka, and J. F. Diffley. 2004. Phosphorylation-dependent binding of mitotic cyclins to Cdc6 contributes to DNA replication control. Nature 431:1118-23.

62. Morohashi, H., T. Maculins, and K. Labib. 2009. The amino-terminal TPR domain of Dia2 tethers SCF(Dia2) to the replisome progression complex. Curr Biol 19:1943-9.
63. Murata, S., H. Yashiroda, and K. Tanaka. 2009. Molecular mechanisms of proteasome assembly. Nat Rev Mol Cell Biol 10:104-15.
64. Musacchio, A., and E. D. Salmon. 2007. The spindle-assembly checkpoint in space and time. Nat Rev Mol Cell Biol 8:379-93.
65. Nakayama, K. I., and K. Nakayama. 2006. Ubiquitin ligases: cell-cycle control and cancer. Nat Rev Cancer 6:369-81.
66. Navadgi-Patil, V. M., S. Kumar, and P. M. Burgers. 2011. The unstructured C-terminal tail of yeast Dpb11 (human TopBP1) protein is dispensable for DNA replication and the S phase checkpoint but required for the G2/M checkpoint. J Biol Chem 286:40999-1007.
67. Nguyen, V. Q., C. Co, K. Irie, and J. J. Li. 2000. Clb/Cdc28 kinases promote nuclear export of the replication initiator proteins Mcm2-7. Curr Biol 10:195-205.
68. Nguyen, V. Q., C. Co, and J. J. Li. 2001. Cyclin-dependent kinases prevent DNA re-replication through multiple mechanisms. Nature 411:1068-1073.
69. Nishitani, H., Z. Lygerou, T. Nishimoto, and P. Nurse. 2000. The Cdt1 protein is required to license DNA for replication in fission yeast. Nature 404:625-8.
70. Nishitani, H., and P. Nurse. 1995. p65cdc18 plays a major role controlling the initiation of DNA replication in fission yeast. Cell 83:397-405.
71. Pan, X., P. Ye, D. S. Yuan, X. Wang, J. S. Bader, and J. D. Boeke. 2006. A DNA integrity network in the yeast Saccharomyces cerevisiae. Cell 124:1069-81.
72. Perkins, G., and J. F. Diffley. 1998. Nucleotide-dependent prereplicative complex assembly by Cdc6p, a homolog of eukaryotic and prokaryotic clamp-loaders. Mol Cell 2:23-32.
73. Perkins, G., L. S. Drury, and J. F. Diffley. 2001. Separate SCF(CDC4) recognition elements target Cdc6 for proteolysis in S phase and mitosis. Embo J 20:4836-45.
74. Peters, J. M. 1998. SCF and APC: the Yin and Yang of cell cycle regulated proteolysis. Curr Opin Cell Biol 10:759-68.
75. Piatti, S., C. Lengauer, and K. Nasmyth. 1995. Cdc6 Is an Unstable Protein Whose De-Novo Synthesis in G(1) Is Important for the Onset of S-Phase and for Preventing a Reductional Anaphase in the Budding Yeast Saccharomyces-Cerevisiae. Embo Journal 14:3788-3799.
76. Pichler, S., S. Piatti, and K. Nasmyth. 1997. Is the yeast anaphase promoting complex needed to prevent re-replication during G2 and M phases? Embo J 16:5988-97.
77. Pickart, C. M. 2004. Back to the future with ubiquitin. Cell 116:181-90.
78. Pickart, C. M. 2001. Mechanisms underlying ubiquitination. Annu Rev Biochem 70:503-33.

79. Randell, J. C., J. L. Bowers, H. K. Rodriguez, and S. P. Bell. 2006. Sequential ATP hydrolysis by Cdc6 and ORC directs loading of the Mcm2-7 helicase. Mol Cell 21:29-39.
80. Ribar, B., L. Prakash, and S. Prakash. 2007. ELA1 and CUL3 are required along with ELC1 for RNA polymerase II polyubiquitylation and degradation in DNA-damaged yeast cells. Mol Cell Biol 27:3211-6.
81. Rotin, D., and S. Kumar. 2009. Physiological functions of the HECT family of ubiquitin ligases. Nature Reviews Molecular Cell Biology 10:398-409.
82. Saleh, A., M. Collart, J. A. Martens, J. Genereaux, S. Allard, J. Cote, and C. J. Brandl. 1998. TOM1p, a yeast hect-domain protein which mediates transcriptional regulation through the ADA/SAGA coactivator complexes. Journal of Molecular Biology 282:933-946.
83. Sanchez, M., A. Calzada, and A. Bueno. 1999. The Cdc6 protein is ubiquitinated in vivo for proteolysis in Saccharomyces cerevisiae. J Biol Chem 274:9092-7.
84. Sclafani, R. A., and T. M. Holzen. 2007. Cell cycle regulation of DNA replication. Annu Rev Genet 41:237-80.
85. Silverman, J. S., J. R. Skaar, and M. Pagano. 2012. SCF ubiquitin ligases in the maintenance of genome stability. Trends Biochem Sci 37:66-73.
86. Singh, R. K., M. H. Kabbaj, J. Paik, and A. Gunjan. 2009. Histone levels are regulated by phosphorylation and ubiquitylation-dependent proteolysis. Nat Cell Biol 11:925-33.
87. Skaug, B., X. Jiang, and Z. J. Chen. 2009. The role of ubiquitin in NF-kappaB regulatory pathways. Annu Rev Biochem 78:769-96.
88. Skowyra, D., K. L. Craig, M. Tyers, S. J. Elledge, and J. W. Harper. 1997. F-box proteins are receptors that recruit phosphorylated substrates to the SCF ubiquitin-ligase complex. Cell 91:209-19.
89. Strahl-Bolsinger, S., A. Hecht, K. Luo, and M. Grunstein. 1997. SIR2 and SIR4 interactions differ in core and extended telomeric heterochromatin in yeast. Genes Dev 11:83-93.
90. Swaminathan, S., A. C. Kile, E. M. MacDonald, and D. M. Koepp. 2007. Yra1 is required for S phase entry and affects Dia2 binding to replication origins. Mol Cell Biol 27:4674-84.
91. Tafforeau, L., S. Le Blastier, S. Bamps, M. Dewez, J. Vandenhaute, and D. Hermand. 2006. Repression of ergosterol level during oxidative stress by fission yeast F-box protein Pof14 independently of SCF. Embo J 25:4547-56.
92. Tanaka, T., D. Knapp, and K. Nasmyth. 1997. Loading of an Mcm protein onto DNA replication origins is regulated by Cdc6p and CDKs. Cell 90:649-60.
93. Tinker-Kulberg, R. L., and D. O. Morgan. 1999. Pds1 and Esp1 control both anaphase and mitotic exit in normal cells and after DNA damage. Genes Dev 13:1936-49.
94. Tsakraklides, V., and S. P. Bell. 2010. Dynamics of pre-replicative complex assembly. J Biol Chem 285:9437-43.

95. Verma, R., R. M. Feldman, and R. J. Deshaies. 1997. SIC1 is ubiquitinated in vitro by a pathway that requires CDC4, CDC34, and cyclin/CDK activities. Mol Biol Cell 8:1427-37.
96. Wasch, R., and F. R. Cross. 2002. APC-dependent proteolysis of the mitotic cyclin Clb2 is essential for mitotic exit. Nature 418:556-62.
97. Weinreich, M., C. Liang, and B. Stillman. 1999. The Cdc6p nucleotide-binding motif is required for loading mcm proteins onto chromatin. Proc Natl Acad Sci U S A 96:441-6.
98. Willems, A. R., M. Schwab, and M. Tyers. 2004. A hitchhiker's guide to the cullin ubiquitin ligases: SCF and its kin. Biochim Biophys Acta 1695:133-70.
99. Yoshida, Y., A. Murakami, K. Iwai, and K. Tanaka. 2007. A neural-specific F-box protein Fbs1 functions as a chaperone suppressing glycoprotein aggregation. J Biol Chem 282:7137-44.
100. Zhong, Q., W. Gao, F. Du, and X. Wang. 2005. Mule/ARF-BP1, a BH3-only E3 ubiquitin ligase, catalyzes the polyubiquitination of Mcl-1 and regulates apoptosis. Cell 121:1085-95.
101. Zhou, P., and P. M. Howley. 1998. Ubiquitination and degradation of the substrate recognition subunits of SCF ubiquitin-protein ligases. Mol Cell 2:571-80.

APPENDIX

LICENSE AND PUBLISHING AGREEMENT

Molecular Biology of the Cell

MANUSCRIPT NO.: E12-07-0548 **DATE:** August 17, 2012

MANUSCRIPT TITLE - The Hect E3 ubiquitin ligase Tom1 controls Dia2 degradation during the cell cycle

AUTHOR(S) - Dong-Hwan Kim and Deanna Koepp

1. I (we) ("Author[s]"), on consideration of the acceptance of the work cited above along with all associated supplemental data, video files, and/or cover images ("Manuscript") for publication, do hereby grant to the American Society for Cell Biology ("ASCB") a license to publish the Manuscript in accordance with the following terms and conditions:
(a) Retention of Rights. The Authors retain the copyright and the right to reprint the Manuscript in any publication of which Authors serve as an author or editor, subject to proper citation of the Manuscript in *Molecular Biology of the Cell* ("*MBoC*") and where feasible the presence of a link to the original publication of the Manuscript in *MBoC*. Also, Authors are permitted to post the *MBoC* PDF of their articles (and/or supplemental material) on their personal websites or in an online institutional repository provided there appears always the proper citation of the Manuscript in *MBoC* and a link to the original publication of the Manuscript in *MBoC*. (Authors agree not to post the unedited accepted Manuscript as it appears in *MBoC In Press*.) Authors further retain the right to revise, adapt, prepare derivative works, present, or distribute the Manuscript provided that all such distribution is for noncommercial benefit and there appears always the proper citation of the Manuscript in *MBoC* and where feasible a link to the original publication of the Manuscript in *MBoC*.
(b) Licensing of Rights to ASCB. The Authors hereby grant to ASCB a perpetual, irrevocable, paid-up, world-wide license with the right to publish, distribute, reproduce, display, translate, sublicense for commercial purposes, and store the Manuscript in all forms now known or hereafter devised and to authorize others to do so. Such license shall be exclusive until the effective date of the licensing of rights to the public as set forth in subsection (c) below.
(c) Licensing of Rights to the Public. The Authors hereby grant to the general public, effective two months after publication of (i.e., the appearance of) the edited Manuscript in an online issue of *MBoC* the nonexclusive right to copy, distribute, or display the Manuscript subject to the terms of the Creative Commons-Noncommercial-Share Alike 3.0 Unported licensed (http://creativecommons.org/licenses/by-nc-sa/3.0), by which the public: (1) Is permitted to copy, distribute, transmit, and adapt the Manuscript;(2) Is **not** permitted to make commercial use of, or license or sublicense the Manuscript for commercial use; and, (3) Is required: a. To attribute the work to the author (in a way that

does not suggest that the authors endorse the users or any user's use); b. To include the terms of this license so that they apply to any subsequent use or distribution; and, c. To respect the fair use rights, moral rights, and rights that the Authors and any others have in the Manuscript.

2. Authors warrant that the Manuscript is an original work of the Authors; that it does not infringe or violate any copyright, proprietary right, or any other right of any third party; and Authors agree to indemnify and hold the ASCB harmless against any claim to the contrary. Authors further warrant that they have the right to convey these rights to the ASCB and that no portion of the copyright to the Manuscript has been previously assigned.

3. Authors understand that the ASCB assesses publication charges that are based upon the total number of pages published in PDF format. Also, Authors are responsible for reprint charges for any number of reprints ordered and alteration charges for any changes deemed as author alterations made to page proofs of the Manuscript. Publication charges are billed to the senior or corresponding author within one month of publication at rates established by the ASCB Council. ***The current rate is $145 per page and is applied based on the length, in full-page increments only, of the published article.*** ASCB members receive a discount of 20% on page charges. Publication charges may be waived, by prior agreement, for some types of solicited articles.

4. Authors agree to be responsible for the payment of all appropriate and relevant publication charges associated with the production of the above named article. ***All publication and reprint charges are due upon receipt of invoice.*** Unpaid balances more than 30 days past due are subject to a finance charge of 1.5% per month (18% per annum). Authors with unpaid balances of more than 90 days will lose their right to publish with the ASCB until the outstanding balance is settled.

5. Authors have obtained written permission to use any quotation or excerpt from another work or from another's property not in the public domain or covered by fair use provision of the U.S. Copyright law. Proper acknowledgment has been given in the article for the use of such material.

6. Authors authorize the editor to modify the Manuscript as necessary to prepare the article for publication - including changes in title, style, and format to conform to editorial usage, journal format, and ASCB editorial style. Minor stylistic changes may be made immediately before publication to meet ASCB editorial requirements. Authors may be asked to update material that appears in the Manuscript before publication.

7. Authors understand that since the January 2008 issue *Molecular Biology of the Cell* has been published only online and that the online publication is the journal of record.

8. Authors will receive a PDF page proof of the Manuscript that will show figures in position.

9. Authors agree to review and return the page proof within 48 hours of receipt of it and to mark on the page proof or an attached file or email message any corrections that need to be made to the Manuscript. Authors can be held responsible for payment of extra charges for changes that are not a result of a printer or editor error or query.

10. Authors confirm that the material presented in the Manuscript has not been published previously, is not currently being considered for publication elsewhere, that all authors listed on the Manuscript have seen and agreed to all information contained in the Manuscript, and that the information contained in the Manuscript is available for general dissemination.

11. Authors confirm that when reporting research that involves recombinant DNA, humans, and animals, they have carried out all of the experiments in accordance with the recommendations of the Declaration of Helsinki and the appropriate National Institutes of Health guidelines and that the research protocols have been approved where necessary by the appropriate institutional committees.

12. Authors understand that publication of the Manuscript in *Molecular Biology of the Cell* implies that Authors agree to make available all propagative materials such as mutant organisms, cell lines, recombinant plasmids, vectors, viruses, and monoclonal antibodies that were used to obtain results presented in the article. Prior to obtaining these materials, interested scientists will provide Authors with a written statement that they will be used for noncommercial research purposes only. Authors are not required to make such material available to others when the terms under which the Authors originally obtained that material prohibit them from doing so. If there is more than one author, the Author(s) identified below also certifies that he/she/they is/are the duly authorized agent(s) for any or all other Authors stated on the Manuscript and hereby give(s) authorization for his/her colleagues by signing on the "Agent" line.

Agent: Deanna Koepp
Date: 8/17/12
REV. December 28, 2011br />MBoC pub license STANDARD 1-20-12 AGENT
local_p_id: 51546
time: 1345239128
ip address: 128.101.217.232